University of Padova

Department of Pharmaceutical and Pharmacological Sciences

DOCTORAL COURSE IN PHARMACOLOGICAL SCIENCES

CRRRICULUM MOLECULAR AND CELLULAR PHARMACOLOGY

CYCLE XXIX

EXOSOMAL DOXORUBICIN AND THE TREATMENT OF BREAST AND OVARIAN CANCERS

COORDINATOR: Prof. Piero Maestrelli

SUPERVISOR: Prof. Pietro Giusti

EXTERNAL SUPERVISOR: Dr. Giuseppe Toffoli

Ph.D. STUDENT: Mohamad Hadla

Università Degli Studi di Padova

Dipartimento di Scienze del Farmaco

CORSO DI DOTTORATO DI RICERCA IN SCIENZE FARMACOLOGICHE

CURRICULUM IN FARMACOLOGIA MOLECOLARE E CELLULARE

CICLO XXIX

EXOSOMAL DOXORUBICIN AND THE TREATMENT OF BREAST AND OVARIAN CANCERS

COORDINATORE: Ch.mo Prof. Piero Maestrelli

SUPERVISORE: Ch.mo Prof. Pietro Giusti

SUPERVISORE ESTERNO: Dr. Giuseppe Toffoli

DOTTORANDO: Mohamad Hadla

This thesis work was done at the Doctoral School of Pharmacological Sciences, following the Molecular and Cellular Pharmacology course at the University of Padova, directed by Prof. Pietro Giusti in collaboration with the Division of Experimental and Clinical Pharamcology in the National Cancer Institute (CRO-IRCCS) – Aviano, directed by Dr. Giuseppe Toffoli.

INDEX Page

ABSTRACT

Background

The application of nanotechnology in the medical field is called nanomedicine. This novel sector have got a lot of interest from many investigators nowadays due to the important development that happened in the last decades, in particular in cancer treatment. Cancer nanomedicine has been applied in different domains such as drug delivery, nanopharmaceuticals and nanodevices. The application of nanotechnology to pharmaceutical science allowed to build up system based on at least two stage vectors (drug/nanomaterial). New formulations based on that platform show often an improvement in drug pharmacokinetics (PK), bioavailability and biodistribution owing enhanced permeability and retention (EPR) effect to passively target tumor both decreasing side effect of free drug [1]. Among natural nanovectors, exosomes (exo) were first described in 1981 as extracellular nanovesicles with a size range of 50-200 nm [2]. Exosomes are produced by cells embedded of cellular information and represent a formidable natural cargo for long distance communication. The name "fedexosome" denotes the general idea that exosomes could deliver cargo that conveniently manipulated could be of help for patients therapy [3].

Aims

- To develop exosomes loaded with doxorubicin (DOX)
- To test the cytotoxic effect of exoDOX (exosomal doxorubincin) *in vitro* using cell lines models compared to the parental drug (DOX)
- To test the antitumor activity and the toxic side effects of exoDOX compared to the parental DOX in *in vivo* experimental models
- To test tissue biodistribution and pharmacokinetics (PK) of exoDOX compared to DOX *in vivo* experimental models
- To define the maximum tolerated dose (MTD) of exoDOX and DOX in *in vivo* experimental models

Materials and Methods

Purified exosomes from cell lines were loaded with DOX and characterized by nanoparticle tracking analysis (NTA), Scanning/Transmission electron microscopy (SEM/TEM) and western blot. The anti-tumoral effects of exoDOX were tested *in vitro* (MDA-MB-231 breast, HCT-116, LoVo and DLD1 colon and STOSE ovarian cancer cell lines) and *in vivo* using nude and FVB/N mice as breast and ovarian cancer models. The antitumor effect was assessed by measuring the tumor volumes. The toxic effects were evaluated by following the body weight and through histopathological analyses of mice organs. The biodistribution and PK of exoDOX and DOX were assessed by mass spectrometry (LC-MS).

Results

- *In vitro* studies showed no increased cytotoxic effect (cell viability) of exoDOX compared to DOX in all the investigated cell lines .
- Similar results were observed in the *in vivo* models indicating no significant differences in the tumor volume after treating mice with the same concentrations of exoDOX and DOX.
- *In vivo* toxicity analysis showed a significant reduction of cardio-toxic side effects by using exoDOX compared to free DOX. Mass spectrometry studies showed that the accumulation of exoDOX in the heart was reduced by about 40% compared to free DOX when using the same concentration of active drug.
- ExoDOX avoids heart toxicity by partially limiting the crossing of DOX through the myocardial endothelial cells. For this reason, mice can be treated with higher concentration of exoDOX thus increasing the efficacy of DOX as demonstrated in breast and ovarian mouse tumors.

Conclusions

Differently from previously published papers that focused on the efficacy of the doxorubicin encapsulated in exosomes, in this thesis for the first time, we demonstrated that unmodified exosomes loaded with DOX are less toxic than free DOX by altering the biodistribution of the drug, these results were published in Nanomedicine (Lond) Journal in 2015 [4].

ExoDOX is safer and more effective than free DOX using breast cancer model and importantly was confirmed using the first spontaneous transformed syngeneic model of high-grade serous ovarian cancer which open the road for providing a new therapeutic opportunity, which was published recently in *Nanomedicine (Lond)* Jounral in 2016 [5].

Riassunto

Introduzione

L'applicazione delle nanotecnologie in medicina è chiamata nanomedicina. Questo settore è motivo di interesse da parte di molti ricercatori dovuto agli importanti avanzamenti avvenuti negli ultimi decenni, in particolare nel trattamento del cancro. In oncologia la nanomedicina è stata applicata in diversi settori quali la costruzione di nuovi sistemi di veicolazione del farmaco e nano dispositivi per la diagnosi. L'applicazione delle nanotecnologie alle scienze farmaceutiche ha permesso di costruire sistemi basati su almeno due vettori (farmaco/nanomateriali). Le nuove formulazioni spesso mostrano un miglioramento del profilo di farmacocinetica (PK), la biodisponibilità e biodistribuzione dimostrando una migliorata permeabilità e ritenzione passiva nel tumore (EPR effect) diminuendo gli effetti collaterali del farmaco libero [1]. Tra i nanovettori naturali, gli esosomi (exo) sono stati descritti nel 1981 come nanovescicole extracellulari con una gamma di dimensioni da 50-200 nm [2]. Gli esosomi sono prodotti dall'invaginazione dalla conseguente gemmazione della membrana cellulare consentendo il caricamento di acidi nucleici e di componenti citoplasmatiche rappresentando formidabile mezzo naturale per la comunicazione a lunga distanza. Il nome "fedexosome" denota l'idea generale che exosomes potevano consegnare contenuti che adeguatamente ingegnerizzato potrebbe essere di aiuto per la terapia di pazienti [3].

Scopo

- Sviluppare esosomi caricati con doxorubicina (DOX)
- Verificare l'effetto citotossico dell' exoDOX (exosomal doxorubincin) *in vitro* rispetto al farmaco libero (DOX), utilizzando modelli cellulari.
- Testare l'attività antitumorale e la tossicità dell'exoDOX rispetto alla DOX libera in modelli sperimentali *in vivo.*
- Valutare la biodistribuzione nei tessuti e la farmacocinetica (PK) dell' exoDOX rispetto al DOX in modelli sperimentali *in vivo*.
- Definire la dose massima tollerata (MTD) dell' exoDOX e DOX in modelli sperimentali *in vivo.*

Materiali e metodi

Gli esosomi purificati da linee cellulari sono stati caricati con DOX e caratterizzati tramite nanoparticle tracking analysis (NTA), microscopia a scansione/ trasmissione elettronica (SEM/TEM) e western blot. Gli effetti anti-tumorali dell'exoDOX sono stati valutati *in vitro* in linee cellulari di tumore alla mammella (MDA-MB-231), colon (HCT-116, LoVo e DLD1) e ovaio (STOSE) e *in vivo* utilizzando topi nudi e FVB/N come modelli di tumore della mammella e dell' ovaio.

L'effetto antitumorale è stato valutato misurando il volume del tumore. Gli effetti tossici sono stati determinati monitorando il peso corporeo e attraverso analisi istopatologiche degli organi dei topi. La biodistribuzione e la PK dell'exoDOX e DOX sono state definite mediante spettrometria di massa (LC-MS).

Risultati

• Studi *in vitro* hanno dimostrato un aumento dell'effetto citotossico (vitalità cellulare) dell'exoDOX rispetto alla DOX in tutte le linee cellulari esaminate.
• Risultati simili sono stati ottenuti nei modelli *in vivo* e indicano differenze significative nel volume del tumore dopo aver trattato i topi con le stesse concentrazioni dell'exoDOX e DOX.
• Le analisi della tossicità *in vivo* hanno mostrato una riduzione significativa degli effetti collaterali cardio-tossici dell' exoDOX rispetto alla DOX libera. Dalle analisi di spettrometria di massa è emerso un minore accumulo dell'exoDOX a livello del cuore di circa il 40% rispetto alla DOX libera a parità di concentrazione di farmaco attivo.
• La minore tossicità cardiaca della exoDOX è dovuta ad un ridotto passaggio della DOX attraverso le cellule endoteliali del miocardio. Pertanto, come dimostrato in tumori alla mammella e all'ovaio, l'efficacia terapeutica della DOX può essere ottimizzata trattando i topi con una maggiore concentrazione dell' exoDOX.

Conclusioni

A differenza di quanto riportato in letteratura circa l'efficacia della doxorubicina incapsulata negli esosomi, dal nostro studio, pubblicato nel 2015 nella rivista *Nanomedicine* [4], emerge che:

- la tossicità della DOX veicolata dagli esosomi è minore rispetto al farmaco libero;
-la biodistribuzione della DOX veicolata dagli esosomi è diversa da quella del farmaco libero.

In conclusione, lo studio effettuato dimostra che l'exoDOX è più biocompatibile ed efficace della DOX libera in modelli di tumore alla mammella. Inoltre, come da noi pubblicato di recente sulla rivista *Nanomedicine* [5], tale risultato è stato confermato con studi su un modello singenico di carcinoma ovarico sieroso, aprendo così la strada ad un nuovo approccio terapeutico per il cancro all'ovaio.

1. INTRODUCTION

1.1. NANOPARTICLES AND NANOMEDICINE

Nanoparticles (NPs) for pharmaceutical purposes are defined by the Encyclopedia of Pharmaceutical Technology as solid colloidal particles ranging in size from 1 to 1000 nm (1 μm). They consist of macromolecular materials and can be used therapeutically as drug carriers, in which the active principle (drug or biologically active material) is dissolved, entrapped, or encapsulated. Based on their chemical constitution can be classified in inorganic nanoparticle builded essentially by metal, metal oxides or carbon and organic NPs when composed by organic compounds mainly lipids or polymers.

The term NPs in the pharmaceutical field was in use much early than the 2000 when the current nanotechnology revolution began. The development and the use of organic NPs as drug delivery system (DDS) originate in fact during the period of 1950s and the 1960s considered the gold age for the progress and the development of bio-pharmaceutics and pharmacokinetics controlled release drugs formulations. One of the pioneers in this field was Professor Peter Paul Speiser and its research group at the ETH (Swiss Federal Institute of Technology) in Zurich where they first attempt, by using a micelles polymerization process, to incorporate immunoglobulin G (IgG) and virus to acrylamide or methylmethaacrilaet based polymeric nano structure to create an alternative delivery system for more efficient tetanus and diphtheria vaccines [6], [7]. Independently to the Speiser's group at the department of radiological science of the Johns Hopkins Medical Institution in Baltimore Mariland USA was developed another type of organic NPs obtained by denaturating a water solution of albumin emulsioned in cottonseed oil at high temperature. Such NPs with dimension ranged from 300 to 1000 nm were labeled with 99mTc and studied the interaction with the reticuloendothelial system (RES) [8]. Few years later in Japan Sugibayashy et al using a similar process conjugated 5-fluorouracil to albumin nanoparticles to improve the PK profile of this anticancer drug [9].

Most of the NPs have taken advantage of the stealth and biodistribution features conferred by the PEGylation even those composed by lipids as organic compound. The historical development of this latter class of NPs mainly represented by liposome structure appear particularly significant in view of their clinical success. The first observation that lipids, particularly phospholipids derivatives, can - without any chemical intervention - generate physical micro-nanostructures was observed in the middle of 60's by Alec Bangham and colleagues with the introduction of the electron microscope. They were able to give the first description of swollen phospholipid systems that established the basis for model membrane systems [10].

Within a few years, a variety of enclosed phospholipid bilayer structures consisting of single bilayers, initially termed 'bangosomes' and then 'liposomes' were described. Through crucial experiments was demonstrated that the lipid bilayers of the vesicles could maintain concentration gradient and the early pioneers such as Gregory Gregoriadis, established the concept that liposomes could entrap drugs and be used as DDS [11]. The first liposome generation had numerous problems as DDS such as the reduced retention of the drug and their rapid clearance form blood circulation. A period of "disillusionment" mainly from industry was followed by a consolidation interlude than most of the original problem of the liposome as DDS were overcome by different chemical approaches and development such as the introduction of cholesterol as stabilizing agent of the bilayer structure and the adoption of the surface phospholipids PEGylation as well as the developed of techniques for high yield drug entrapment.

Lipid micelles are colloidal particles, formed by amphiphilic molecules (e.g. block copolymers or surfactants) that self-assemble to form nanocapsules in aqueous solutions. Micelles have a hydrophilic (polar) heads to form the outer shell, and hydrophobic (nonpolar) tails to form the interior part. This relatively simple lipid nanostructure was first postulate by Professor James William McBain in early 1900's to explain the electrolytic conductivity of sodium palmitate solutions trough "colloid ione". The hydrophobic/hydrophilic structures features of micelles have early attracted the interest as delivery system especially to improve bioavailability of poor water soluble drugs [12]. However, their application resulted limited by their pour

chemical versatility and by their pour structure stability and in the 90s a more sophisticated version representing by the polymeric micelles has been proposed. Polymeric micelles have been actively studied in the field of polymer chemistry The major advantage over simple surfactant micelles is represented by their large chemical versatility that allow to control and to modulate both chemical and structure features in order to improve drug load capacity as well as drug target specificity [13]. Their applications as drug carriers started from the Ringsdorf's research group that first demonstrated the *in vitro* sustained drug release [14].

Soon after, different *in vivo* studies reported that polymeric micelles may increase the activity of neuroleptic drug physically associated with a polymeric amphiphile (Pluronic_P-85; poly(propylene oxide)–poly(ethylene oxide) block copolymer) as well as that of anticancer drugs that incorporate into polymeric micelles have showed selective delivery to solid tumor [15], [16].

In spite their potential as drug nano-carriers polymeric micelles are still under intensive development to improve their *in vivo* efficient drug targeting mainly by control physico-chemical properties such as size, drug retain and release as well as their *in vivo* stability. A significant challenge facing the research for efficient drug nano-carriers is the development of structure-controlled methodologies that will enable cost-effective, controlled assembly of nanostructures in a very routine manner. Polymeric micelles can be considered just as one of the primitive attempt of "Bottom-up" synthetic strategy to produce size-mono dispersed, chemically defined organic nanostructures with dimensions ranging between 1 and 100 nm. The polymeric dendritic synthetic strategies instead represent a sophisticated approach that have allow the systematic construction of nanoscale structures and devices with precise atom-by-atom control as a function of size, shape, and surface chemistry. Dendrimer polymers are highly branched, star-shaped macromolecules with nanometer-scale dimensions. They have symmetrical three dimensions structure with a central core, a inner shell constituted by radial branches molecular moieties, and an outer shell with functional surface groups. The synthetic approach of dendritic polymeric structure was first conceptualized in the early '40s but the first success synthesis of these original polymer structure was first realized by Fritz

Vogtle group in 1978 and mainly by Donald Tomalia and co-workers operating at the Dow Chemical Co in the early 1980s [17]–[19].

From those early days a great variety of dendrimers exist, and each has biological properties such as poly-valency, self-assembling, electrostatic interactions. Dendrimers as DDS are of great interest due to their highly controllable structure and size and the presence of terminal functional groups of dendrimers confer an higher chemical reactivity and versatility compared with other polymers. The polyamidoamine dendrimers, commonly known as PAMAM originally developed by the Tomalia 'group have been extensively investigated as oral drug delivery because they are a family of water-soluble polymers characterized by unique tree-like branching architecture and a compact spherical shape in solution [20], [21]. Moreover, the great potential of dendrimer PAMAM as drug carrier arises from the large number of arms and surface amine groups that can be utilized to immobilize drugs, enzymes, antibodies, or other bioactive agents [22].

Another polymer nanoscale structures that have received great attention also as nano drug delivery carrier are those obtained by the guided folding of nucleic acid strands to create non-arbitrary two- and three-dimensional shapes. Although the chemical versatility of such nano structures are relatively lower being limited by the use of the limited chemistry of the monomer such as the DNA bases, their structure versatility appear instead unlimited and called "DNA origami" [23]. The evidence that junction structures could be generated from DNA strands and that individual structures could be combined using simple sticky end base pairing to assemble complex, multi-dimensional objects was first proposed by Nadrian Seeman in the early '80. However, the early attempts to use DNA molecules to construct specific architectures from single branch points were unsuccessful due to the high flexibility of DNA building blocks and the use of a single junction point that did not facilitate the creation of higher order stable structures. The introduction in the early '90 of multiple-crossover motifs have overcame the original flexibility limitation providing the necessary rigidity for the assembly of larger nucleic acid polymer objects. The introduction of such double crossover motif remains the central motif in DNA nanotechnology and has been used for the construction of many discrete and periodic assemblies [24], [25].

NANOMEDICINE

In 2004, the European science foundation define Nanomedicine as "the science and technology of diagnosing, treating and preventing diseases and traumatic injuries, of relieving pain, of preserving and improving human health, using molecular tools and molecular knowledge of the human body" [26]. Another definition of nanomedicine that explains better the working field of that discipline is the application of nanoscale material in medicine that takes advantages of the nanomaterial's unique properties [27]. Accordingly to the federal US research and development program agency, the National Nanotechnology Initiative (NNI), nanotechnology involves the development of carriers devices or systems sized from 1 to 100 nm range although this limit can be extended up to 1000 nm [28]. In the last two decades, nanotechnology was rapidly developed allowing the incorporation of multiple therapeutics, sensing and targeting agents into NPs in order to set up new nanodevices able to detect, prevent and treat complex disease as cancer. It is well known that chemotherapeutic agents present severe side effects including bone marrow suppression, cardiac and kidney toxicity, hair loss and mucositis. In addition, these drugs are poorly soluble in biological fluids, quickly recognized by the mononuclear phagocyte system (MPS) and cleared from the body [29]. The binding or the encapsulation of a drug to NPs can also modify the chemical and physical properties such as poor water solubility, drug circulation half-life, escaping the immune system, biodistribution and pharmacokinetic [30]. The application of nanotechnology to drug delivery has an enormous potential concerning the improvement of selectivity in targeting neoplastic cells by allowing the preferential delivery of drugs to tumours owing the enhanced permeability and retention (EPR) effect of leaky vasculature in tumors and inflamed tissue [31]. Poorly aligned endothelial cells in the fast growing tumor vasculature with fenestration larger than 100 nm in size and reduced lymphatic drainage in tumor tissue result in preferred accumulation of nanocarriers in these tissues over healthy tissues, reducing volume distribution while improving pharmacokinetic profile, and consequently, the efficacy of the anticancer drug [32], [33].

Drug delivery systems and more generally nanovectors can be divided into three generations of compounds, accordingly to whether or not they were developed to

target specific cells, which is expressed on the tumor cells or the microenvironment. First generation nanovectors are the simplest way to build a carrier nanoparticle able to accumulate by passive mechanisms exploiting the EPR effect, or more specifically they extravasate through gaps in tumor neovasculature. Among the "first generation" vectors, liposomes based drug delivery is the most successfully used in the clinic, as demonstrated by liposomal doxorubicin for breast, ovarian and Kaposi's sarcoma. The "second generation" of therapeutic nanovectors represents the natural evolution of the first generation, constructed with additional function including: surface modification with ligand able to bind specific biological molecules of the tumor cell [34]. The aim is to deliver higher drug concentrations to pathological tissues, sparing the normal ones in order to enhance the effect on the tumor, thereby reducing systemic toxicity. Moreover, they can possess advanced features including the possibility to co-deliver drugs and imaging agents, or they can be modify in order to have a controlled or triggered release. The so-called "third generation" of nanovectors has been developed and is based on a multi-stage strategy in order to overcome the numerous obstacles that are encountered on their way to reach the tumor. These carriers are made by different nanoparticles nested into a single vector to build a system that can avoid the biological barrier and at the same time possess tumor cytotoxicity and targeting activity [35]. An example is represented by biodegradable silicon nanoparticles [36], [37].

The particles possess the ability to recognize specifically the pathological endothelium through a surface with physical-chemical and geometrical well defined features (first stage). The second stage nanoparticles are loaded into the first one and released inside tumor. The size of these particles is smaller than 20 nm, so they can easily cross the inter-endothelial junctions and extravasate in the tumor to deliver the drugs.

The above mentioned strategies allowed the developing of more than 200 products that have been approved or are under clinical investigation [38]. In contrast with the large number of DDS successfully at preclinical stages, recent studies demonstrate that the clinical translation is a challenging process with about 10% of success in approval rate for therapeutics entering in phase I trials [39].

The path for a drug, which travels from the lab to the clinic is typically long and every drug takes a unique route. Often, a drug is developed to treat a specific disease

but an important application may also be discovered by accident. An interesting example is Retrovir (zidovudine, also known as AZT) that has been studied firstly as an anti-cancer drug in the 1960s with disappointing results. Later, after twenty years, investigators discovered that the drug could treat HIV infected patients and the U.S. Food and Drug Administration (FDA) approved the drug that was manufactured by GlaxoSmithKline, for that purpose in 1987 [40]. It often takes a long time for an experimental treatment to be approved as a cancer treatment.

1.2. THERAPEUTIC AND DIAGNOSTIC APPLICATIONS IN ONCOLOGY

1.2.1. LIPOSOMES

Decades of such chemistry and clinical development have led, in 1995 to the "first in man" use of doxorubicin liposome drug injectable formulation (Doxyl/Celix) as anticancer treatment, approved by FDA. After almost forty years from their discovery, liposomes represent a well established nano-technology delivery system that together with other lipid nanosized colloidal DDSs such as emulsion and suspension still gaining significant attention. Their formulation protect therapeutic cargo from the *in vivo* environment and increase circulation half-life, permeability, biodistribution and targeting specificity [41]. These principles were the base on which Barenholz developed the formulation of liposomal doxorubicin (Doxil®) [1]. Doxorubicin is an anthracycline antibiotic that intercalates in DNA helix preventing replication [42] and it is used for various type of cancers: breast, lung, gastric, ovarian, sarcoma, myeloma, leukemias and lymphomas [43]. Unfortunately, its poor selectivity toward cancer cell induces severe systemic side effects. In particular, the patients treated with doxorubicin have been experienced severe cardiotoxicity, bone marrow toxicity with consequent myelosuppression [44]. The development of Doxil® and its approval reduces drastically doxorubicin side effects. The first clinical study carried out on Doxil® demonstrated that the new doxorubicin formulation holds a completely different pharmacokinetics profile, which enhances the circulation time of the drug changing the biodistribution and increasing tumoral accumulation due to the EPR effect [45]. Two key changes in the history of Doxil®

were considered real breakthroughs. Firstly, the inclusion of polyethylene glycol (PEG) in liposome surface to create a "stealth" particle, which can escape the recognition by the RES system. The second major improvement was the remote loading driven by ammonium sulfate gradient to increase doxorubicin loading within each liposome [1]. Various pre-clinical and clinical studies (1991-1994) have focused on the use of Doxil® pharmacokinetics compared with free doxorubicin in addition to deep studies using Doxil® in the treatment of AIDS-related Kaposi's sarcoma. Which led in 1995 to the approvement by FDA and European Medicines Agency (EMA) in 1996. Soon later the same drug formulation was approved in 1999 by FDA for the treatment of Ovarian cancer, in 2003 for breast cancer treatment and lastly it was approved in 2007 for multiple myeloma treatment.

Additionally, the ability of liposomes to entrap different water-soluble compounds within the inner aqueous phase and lipophilic agents between liposomal bilayers has made them useful for carrying diagnostic agents in all imaging modalities like gamma-scintigraphy, magnetic resonance imaging (MRI), computed tomography (CT) imaging, and sonography. Liposomal modification with PEG increases their field of usage by enhancing circulation time and attachment of antibodies or different targeting moieties to their surface to target specific affected areas.

1.2.2. POLYMERIC NANOPARTICLES

Polymeric nanoparticles have been widely studied for their physical and chemical properties and used to encapsulate drugs. They are prepared from biocompatible polymers and can transport drugs in a controlled and targeted way through the surface modification [46]. Polymeric NPs can be synthesized from natural polymers, such as albumin [47], hyaluronic acid [48], and chitosan [49], and from synthetic polymers, such as, poly acrylic acid (PAA), poly glycolic acid (PGA), poly(lactide-co-glycolide) (PLGA), poly lactic acid (PLA), dendrimers, and hyperbranched polymers [50]. Different methods of synthesis of polymeric nanoparticles are investigated depending on the application and drug type. These methods include solvent evaporation, nanoprecipitation, emulsion diffusion and salting out method [51]–[54].

Albumin is the most abundant protein in plasma and used widely for the preparation of nanoparticles due to its biodegradability, non-toxicity, availability, hydrophilicity, and easy to prepare [55]. The major advantage of albumin is its high binding capacity for different drugs due to multiple drug binding sites [56]. The drugs can be loaded by electrostatic interaction on the surface of nanoparticles, incorporated into the nanoparticles matrix, or linked covalently to the protein due to the presence of surface reactive groups such as amines, thiols, and carboxylic acids [57], and released through hydrolysis, diffusion, or enzymatic degradation of nanoparticles (Figure 1) [58], [59].

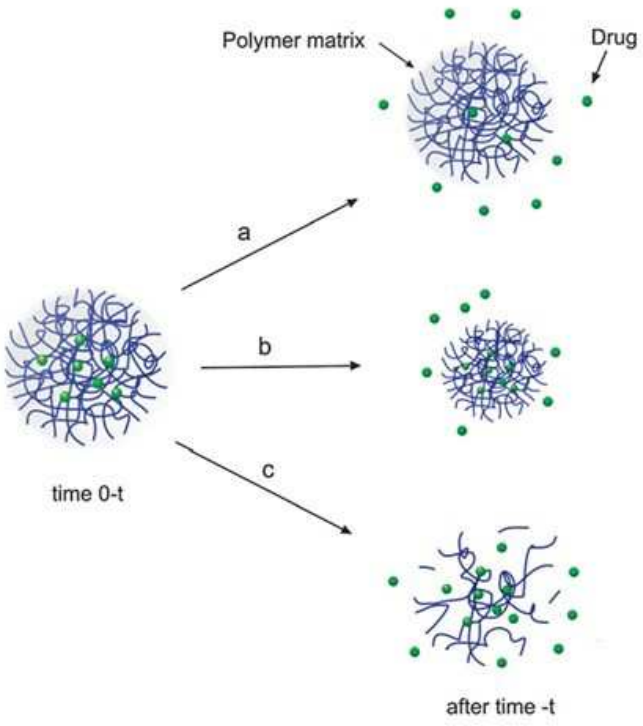

Figure 1. Drug Release Mechanism from polymeric nanoparticles: (**a**) diffusion from polymer matrix, (**b**) degradation of polymer matrix, and (**c**) biodegradation of polymer matrix due to hydrolytic degradation.

Abraxane was the first drug formulation of this category approved by FDA in 2005. Abraxane is an albumin-bound (Nab) paclitaxel formulation. Paclitaxel, discovered in 1962, is a natural compound extracted from the bark of western yew (*Taxus brevifolia*) [60] and is widely used for the treatment of breast, lung and advanced ovarian cancer [61]. The high hydrophobicity of paclitaxel limits its clinical application. To overcome poor water solubility, a formulation of a nonionic surfactant Cremophor EL (polyethoxylated castor oil) and ethanol (1:1, v/v) is used to dissolve paclitaxel for clinical use [62]. However, the presence of Cremophor EL causes allergic, hypersensitivity and anaphylaxis reactions in animals and humans [61]. To overcome these side effects and deliver paclitaxel safely, a new paclitaxel formulation was needed. Paál et al [63] develop a formulation which is Cremophor EL free. This formulation is non-covalent binding of paclitaxel to albumin, known as Abraxane. Albumin is the major component of plasma protein and is a natural carrier of hydrophobic molecules such as vitamins, hormones, and other water-insoluble plasma substances [64], [65]. In addition, albumin is involved in endothelial transcytosis through the binding of a cell surface receptor glycoprotein (gp60) called albondin [66] and is also demonstrated that albumin is recognized by SPARC, a secreted acidic protein rich in cysteine, that appears to be up-regulated in many malignancies (breast, lung and prostate cancer), which can interact with albumin and increase the accumulation of albumin-bound drugs in the tumor [64]. Albumin stabilizes the paclitaxel particles at an average size of 130 nm, which prevents any risk of capillary obstruction and does not necessitate any particular infusion systems or steroid/antihistamine premedication before the infusion [67]. Abraxane possesses a reduced treatment volume and time required for administration. Antitumor activity and mortality were assessed in nude mice bearing human tumor xenografts [lung (H522), breast (MX-1), ovarian (SK-OV-3), prostate (PC-3), and colon (HT29)] treated with Nab or cremophor-based paclitaxel. In tumors, Abraxane had a significantly increased efficacy compared with cremophor-based paclitaxel, the difference was higher in breast (MX-1) and in ovarian (SK-OV-3) xenografts.

Additionally, Abraxane was deeply studied in several clinical trials, in one of the first phase I clinical trials, Abraxane™ was used in the treatment of a group of patient

with solid tumors, which failed standard therapy were treated with [68]. Abraxane™ efficacy was studied in many phase II clinical trial for metastatic breast cancer (MBC) treatment by Ibrahim et al. [69]. In 2005, a phase III randomized controlled trial confirmed the superiority of Abraxane™ compared to Cremophor-EL paclitaxel [70]. Based on the studies and on the consideration above, in 2005 FDA approved Abraxane™ for the treatment of MBC who failed combinatorial chemotherapy. The encouraging results obtained in the application of Abraxane™ encouraged researchers to try these new formulations on metastatic lung cancer and non-small cell lung cancer (NSCLC) since paclitaxel is employed in the treatment often in combination with carboplatin. A phase II clinical trial was conducted by Green et al. to investigate the efficacy of Abraxane™ in the treatment of advanced NSCLC [71].

All the previous mentioned clinical trials have led to and the EMA in 2008 for the treatment of MBC. Soon after it was approved in 2011 by FDA for the treatment of advanced or metastatic non-small cell lung cancer (NSCLC), in combination with carboplatin. Recently the FDA approved the combination of Abraxane™ and gemcitabine as first line therapy for the treatment of advanced pancreatic cancer after getting interesting results from many clinical trials (phase I/II) [72], phase III [73]–[77].

From a diagnostic point of view, polymeric nanoparticles, incorporated with contrast agents, have shown significant benefits in molecular imaging applications [78]. These materials possess the ability to encapsulate different contrast agents within a single matrix enabling multimodal imaging possibilities. The materials can be surface conjugated to target-specific biomolecules for controlling the navigation under *in vivo* conditions. The versatility of this class of nanomaterials makes them an attractive platform for developing highly sensitive molecular imaging agents. The paucity in the data is mainly attributed to challenges associated with poor stability, and rapid release of imaging agent under *in vivo* conditions. The research community's progress in the area of synthesis of polymeric nanomaterials and their *in vivo* imaging applications has been noteworthy, but it is still in the pioneer stage of development. The challenges ahead should focus on the design and fabrication of these materials including burst release of contrasts agents, solubility, and stability issues of polymeric nanomaterials [79].

1.2.3. MICELLES

Regarding micelles, the formation has an essential role in the absorption of fat-soluble vitamins and complex lipids inside the human body. The formation of bile salts in the liver their secretion by the gallbladder allow the formation of fatty acids micelles [80]. Hence, the absorption of complex lipids (e.g., lecithin) and lipophilic vitamins (A, D, E, and K) within the micelles in the small intestine [81]. Micelles can also be used as a template to synthesize gold NPs with controlled sizes using a pH-sensitive triblock copolymer micelle, and have important applications in biological process such as ion transport and targeted drug delivery [82].

Instead polymeric micelles are prepared by a self-assembly process using hydrophilic and hydrophobic block copolymers to form a hydrophilic shell and a hydrophobic core [83], [84]. Detergents are the most common example of this interaction that clean soluble hydrophobic materials (such as oils and lipids). Detergents act also by decreasing the surface tension of water, and it will be easier to remove materials from a surface. The surfactants emulsifying property is also important for the emulsion polymerization [85]. There are two routes to load drug using the amphiphilic micelle structure: drug conjugation and drug encapsulation. Drug conjugation utilizes a non-water soluble drug as a hydrophobic core of the micelle, which is conjugated to the hydrophilic polymer backbone [86]. Drug encapsulation is formed by the encapsulation of hydrophobic drugs into the core of a core-shell nanostructures during the self-assembly process via hydrophobic interactions [87]. PLGA is one of the most popular hydrophobic polymers used as a core for drug encapsulation and break down the ester bonds in the body, resulting in the release of the drug [88]. Other studies used a multi-benzene ring as the hydrophobic core, which can bind to a drug containing many benzene rings through π-π interactions under neutral pH, and acidic conditions could decrease these π-π interactions and cause the release of the drug [89].

Currently, several micellar formulations for cancer therapy are under clinical evaluation, but only Genexol-PM has been approved by FDA in 2007 for the treatment of breast cancer. Genexol-PM is based on the development of polymeric micelles formulation of paclitaxel. The formulation of micelles is based on

biodegradable amphiphilic di-block copolymer comprised of monomethoxy poly(ethylene-glycole)-block-poly (D,L-lactide) (mPEG-PDLLA). Like Abraxane, this formulation avoiding the employment of lipid-based solvent (Cremophor EL). The first preclinical study compared the *in vivo* efficacy, toxicity and biodistribution of Genexol-PM to cremophor-EL based paclitaxel [90]. The increasing of MTD and the lethal dose 50 (LD_{50}) of Genexol-PM compared to classical paclitaxel formulation demonstrated that is a less toxic formulation. Administered in animals at the same dose of lipid-based paclitaxel, Genexol-PM resulted with the same concentration in plasma with an increased accumulation (2-3 fold higher) in heart, lungs, kidneys and spleen. Importantly, Genexol-PM also resulted in 2-fold higher levels of paclitaxel in tumors. Subsequently, favorable results from clinical trials in line with Abraxane, Genexol-PM has been approved for the treatment of metastatic breast cancer (MBC) and non-small cells lung cancer (NSCLC) in South Korea in 2007. Genexol-PM has not been already approved by FDA and phase III and IV clinical trials are ongoing.

Several micellar forms of contrast agents have been established for different medical imaging modalities (e.g., nuclear imaging, MRI, X-ray CT, and ultrasonography) for both purely diagnostic/imaging purposes and for the visual control over the drug delivery by micellar carriers [91]. Micelles with pH-responsive property were designed as cancer-recognizing MRI contrast agents. Moreover, the micelles triggered significant photothermal damage to cancer cells via the destabilization of organelles, leading to successful tumor necrosis upon photoirradiation [92]. CT represents an imaging modality with high spatial and temporal resolution, which uses X-ray absorbing heavy elements, such as iodine, as contrast agents. In addition, single-photon emission computed tomography (SPECT/CT) imaging technique has also been employed to investigate pharmacokinetics and biodistribution of DNA micellar nanoparticles [93].

1.3. EXOSOMES

1.3.1. DISCOVERY, BIOGENESIS AND CLASSIFICATION

The discovery of cell-derived vesicles dates back to 1940, when preliminary studies were performed, addressing the "biological significance of the thromboplastic protein of blood". Clotting times of plasma were determined after centrifugation at different speeds, and prolonged high-speed centrifugation (150 min at 31,000 xg) was shown to significantly extend the clotting time of the supernatant. Furthermore, when the pellet containing "the clotting factor of which the plasma is deprived" was added to plasma, the clotting times shortened, indicating that cell-free plasma contains a subcellular factor that promotes clotting of blood [94]. More than 20 years later, in 1967, this subcellular fraction was identified by electron microscopy and was shown to consist of small vesicles, originating from platelets and termed "platelet dust". These vesicles were reported to have a diameter between 20 and 50 nm and had a density of 1.020 to 1.025 g/ml [95]. One decade later, fetal calf serum was also shown to contain "numerous microvesicles" ranging in diameter from 30 to 60 nm [96].

During 1970s, biological vesicles were discovered. The group of Rose Johnstone described lipid nanoparticles that burped out by the sheep red blood cells called exosomes [97]. In reticulocytes (immature red blood cells), and generally in mammalian cells, parts of the cellular membrane are regularly internalized forming endosomes, 50 - 180% of the plasma membrane is cycled in and out of the cell every one hour [98]. In multicellular organisms, cells communicate via extracellular molecules such as nucleotides, lipids, short peptides and proteins. Released by cells, these molecules can bind to receptors of other cells, inducing intracellular signaling and physiological modification of the recipient cells. Additionally to these single molecules, eukaryotic cells release also biological micro- and nano-structures in their extracellular environment called membrane vesicles, containing several lipids, proteins, and even nucleic acids that affect the encounter cells in a complex way.

Exosomes are equivalent to cytoplasm enclosed in a lipid bilayer with the transmembrane proteins localized in the cellular surface. They are formed inside the cells in compartments known as multi-vesicular bodies (MVBs), which take up bits

of the cytoplasm and its contents into membrane-bound vesicles. Once the MVBs are fused with the plasma membrane, these internal vesicles are secreted. (Figure 2) [99]. The biological function of exosomes is still under study, they can mediate inter-cellular communication, or induce intra- and extracellular signals and it is well know that the exosomes are involved in the exchange of functional genetic information [100], [101]. Exosomes are present in cell culture medium and in different biological fluids. It is known that they are secreted by most cell types in normal and pathological conditions. Furthermore, exosomes have been found to be released by all cells studied such as B-cells, dendritic cells, T-cells, mast cells, epithelial cells, platelets, stem cells and cancer cells and have been found to be present in physiological fluids, such serum, urine, breast milk, cerebrospinal fluid, bronchoalveolar lavage fluid, saliva, and malignant effusions [102]–[109].

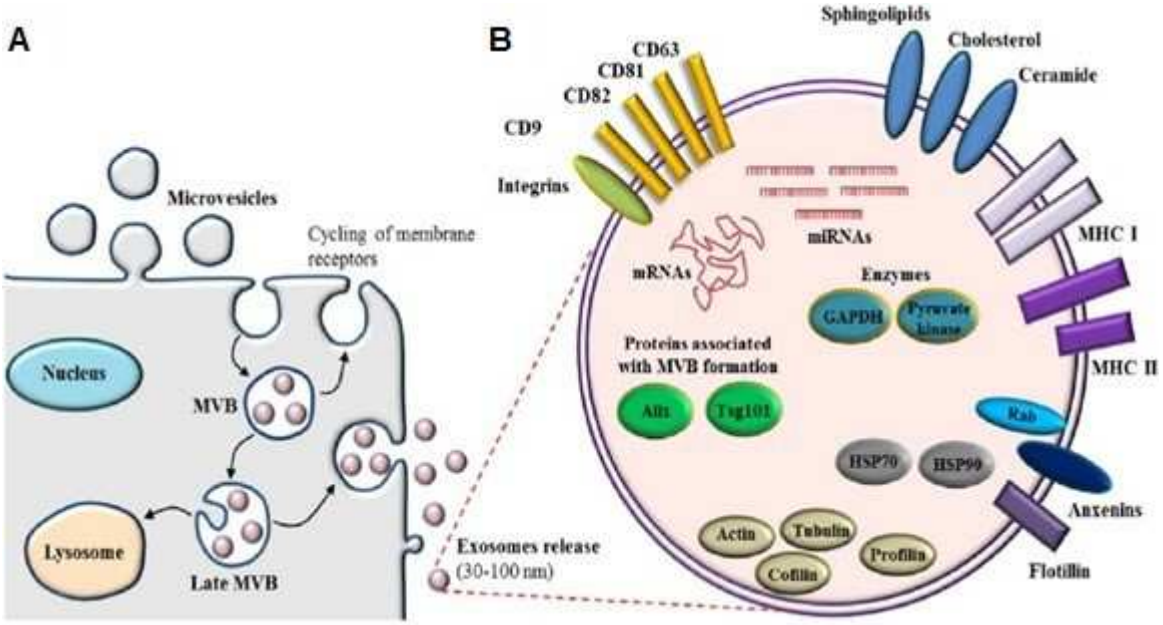

Figure 2. Biogenesis, secretion and molecular composition of exosomes. A) Intracellular machineries of exosome biogenesis and secretion. **B)** Exosomes dimension, structure and the various packed compounds (nucleic acids and proteins).

Extracellular vesicles classification can be based on their cellular origin or biological function; alternatively, extracellular vesicles can be categorized on the basis of their biogenesis pathways [110].

Cellular origin and biological function of extracellular vesicles:

- Ectosomes: vesicles secreted by neutrophils or monocytes
- Microparticles: vesicles shed from platelets in blood or endothelial cells
- Tolerosomes: vesicles purified from serum of antigen-fed mice
- Prostatosomes: vesicles extracted from seminal fluid
- Cardiosomes: vesicles secreted by cardiomyocytes
- Vexosomes: vesicles linked with adeno-associated virus vectors

1.3.2. NOVEL DIAGNOSTIC TOOLS

Due to the selective cargo loading of exosomes and their resemblance to the producer cells, they have high importance in cancer biomarkers discovery. By improving the isolation protocols from cell culture and patient body fluids , and their advanced characterizations [111], scientists are utilizing exosomes to identify molecules for cancer targeting more effectively and apply more personalized techniques for detection, diagnosis, and prognosis [112], [113]. Protein characterization by mass spectrometry [114], as well as immunoprecipitation techniques are also used to identify and quantify peptide and nucleic acid (miRNA, mRNA, etc..) profiles [115].

Tetraspanins, a family of scaffolding membrane proteins, are highly present in exosomes. The exosomal marker CD63 is a member of the tetraspanin family. Logozzi and coworkers reported in 2009 that plasma CD63+ exosomes are significantly increased in patients with melanoma compared with healthy controls [116]. Recently in 2013, Yoshioka et al performed a comparative analysis of exosomal protein markers in different human cancer types and found that CD63 is present at higher levels in exosomes derived from malignant cancer cells than those derived from normal cells, which provides further evidence that exosomal CD63 could be a protein marker for cancer [117]. CD81, is another exosomal marker from

the tetraspanin family, has a role in hepatitis C attachment and/or cell entry. In addition, Welker et al studies in 2012 reported that the level of serum exosomal CD81 is high in patients with chronic hepatitis C and possibly associated with inflammation and fibrosis severity, suggesting that exosomal CD81 may be a potential marker for hepatitis C diagnosis and treatment response [118].

Additionally, various exosomal proteins have been reported to be potentially useful in the diagnosis of central nervous system diseases. In 2008, Skog et al detected glioblastoma-specific epidermal growth factor receptor vIII (EGFRvIII) in serum exosomes extracted from 7 out of 25 glioblastoma patients, indicating that exosomal EGFRvIII may present diagnostic information for glioblastoma [119]. One year later, accordingly with Skog's findings, Graner et al. have found that serum exosomes from patients with brain tumors contain EGFR, EGFRvIII, and TGF-beta [120]. It has also been reported that exosomal amyloid peptides accumulate in the brain plaques of Alzheimer's disease (AD) patients [121]; and tau phosphorylated at Thr-181, an established biomarker for AD, is present at elevated levels in exosomes isolated from cerebrospinal fluid specimens of AD patients with mild symptoms [122]. These findings highlight the potential value of exosomes in the early diagnosis of AD, which is very important in sabotaging disease progression but currently difficult to achieve. Studies have also shown that α-synuclein, whose aggregation plays a central role in Parkinson's disease pathology, is released in exosomes in an *in vitro* model system of Parkinson's disease [123]; and prion proteins, biomarkers for transmissible spongiform encephalopathies, are packaged into exosomes released from prion-infected neuronal cells [124]. These exosomal proteins may have great potential in clinical diagnostics and should be further explored.

It is very important to know that in early 2016, the first cancer diagnostic blood test called ExoDx Lung which was developed to detect free-released exosomes became available commercially in the US. This applicable diagnostic tool is based on the exploitation of five different mutations — all of them fusions between the genes encoding anaplastic lymphoma kinase (ALK) and echinoderm microtubule-associated protein-like 4 (EML4) that lead to a form of non-small cell lung cancer (NSCLC). The launch of this 'liquid biopsy' from Exosome Diagnostics of Cambridge, Massachusetts, marked a step forward in the maturity of the fledgling science of exosome biology [125].

1.3.3. DELIVERY SYSTEM

Due to the strong impact of exosomes in cancer pathogenesis and biological compatibilities (i.e. they are able to cross physiological barriers like the BBB), exosomes are strong candidates for advanced therapeutic applications. These biological features include targeting exosomes, re-engineering and modifying them as therapeutic devices.

Drug loading of exosomes can be achieved either endogenously or exogenously. Endogenous, or passive loading is carried out by inducing the overexpression of the RNA molecules of interest in producer cells. This passive loading is accomplished by the native exosomal loading mechanisms of the cell itself and results in exosomes that contain the drug before their isolation. Exogenous, or active loading start with the collection of exosomes and requires co-incubation or electroporation of the exosomes with the drug/molecule of interest [110] like siRNA [126], doxorubicin [4], [127], paclitaxel [128] and curcumin [129] by using different strategies, (Figure 3).

In this concept, many investigators have developed clinical trials studies in order to analyze the use of exosomes as nanocarrires of several drugs and small molecules. In 2005, Escudier et al [130] conducted the first clinical trial with exosomes in which they test the feasibility of exosomes applied to metastatic melanoma vaccination with autologous dendritic cell (DC) derived-exosomes (DEX) pulsed with the melanoma-associated antigen 3 (MAGE 3). Antigens were captured in the peripheral organs then DC incorporated MHC-antigenic peptide complexes into the exosomes with immunostimulating factors. After treatment, released exosomes transfer MHC-antigenic peptide complexes and associated proteins to antigen-naïve DCs in the regional lymph nodes acquiring the ability to stimulate CD4+ and CD8+ T cells [131], [132].

Another phase I study based on exosomes vaccination has carried out by Dai et al., in 2008 [133]. This study is based on the immunotherapy of colorectal cancer (CRC) through ascites-derived exosomes (Aex) in combination with the granulocyte-macrophage colony-stimulating factor (GM-CSF).

The discovery of the anti-inflammatory effect of various molecules as curcumin and after several studies about exosomes as natural carrier, an applied technique was investigated by loading curcumin in exosomes in order to improve the biodistribution, stability, solubility and efficacy of this molecule [129] in which they were used firstly in the treatment of brain inflammatory diseases. The great results found, led to their uses in cancer therapy especially in the treatment of colon cancer [134], [135] in Phase I clinical trial (**NCT01294072**). In which researchers will investigate if plant exosomes are able to improve the delivery of curcumin to both normal colon tissue and colon tumor.

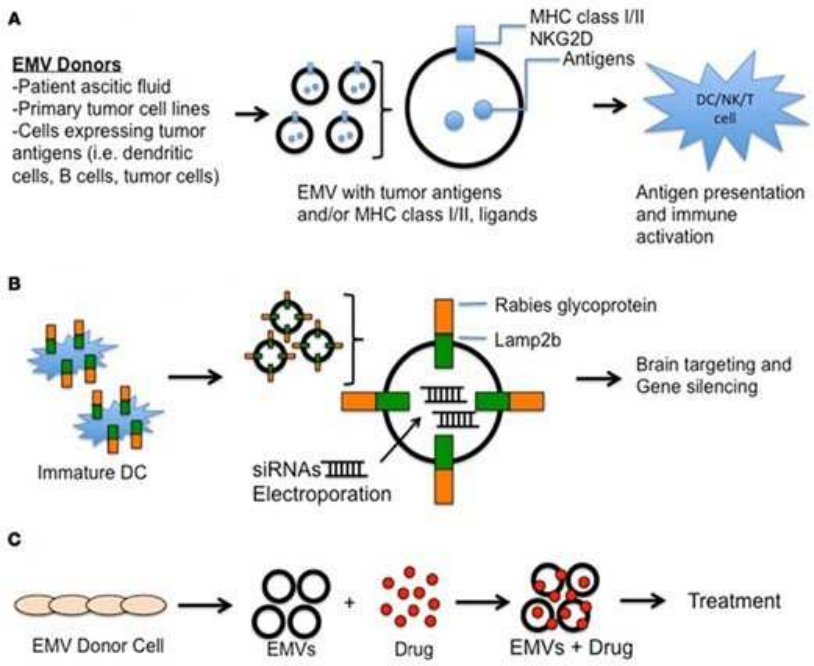

Figure 3. Extracellular membrane vesicles-based therapies. **A)** EMV immunotherapy. **B)** EMV RNAi therapy. **C)** EMV drug therapy.

2. RATIONALE

Cancer patients need better therapeutic opportunities in terms of efficacy and compliance. Most of the chemotherapeutic drugs have a narrow therapeutic window, a range of doses that produces therapeutic response without causing any significant adverse effect in patients [136]. Many variables can influence the therapeutic window and among them, drug formulation, off-target effects, biochemical and genetic characteristics of the patients were thoroughly studied in the last decade [137]. Personalized medicine, a tailored approach to cure individual patients, is the optimal choice to overcome these limitations [138], [139]. From one side, many laboratories and pharmaceutical companies are currently focusing on the genomic and genetic characteristics of the tumors [140], [141]. On the other side, nanomaterials hold great promises for cancer patients but also face major challenges to be translated into clinic [142]–[146]. Organic materials such as liposomes have been a breakthrough in the field of drug delivery but also offer many limits such as reproducibility, organ toxicity and/or immune response, which have limited their application [1], [147], [148]. Nature offers many opportunities for new drug vehicles. Normal and cancerous cells communicate with each other and their environment both locally and at great distance. Among the mechanism of communication, extracellular vesicles have been recognized as an emerging new class of vehicles [149], [150]. Exosomes are a subclass of extracellular vesicles that represent an extraordinary material rich of information for diagnostic applications and therapeutic opportunities already described in section 1.3.2. Moreover, besides being a diagnostic tool, exosomes are ideal drug delivery agents described in section 1.3.3. The size ranging from 30 to 200 nm has been demonstrated to be optimal for long circulating time thereby avoiding fast clearance [2]. They can freely circulate and distribute into biological fluids such as blood, urine, ascites, saliva and cerebrospinal fluid. The membrane composition shares optimal fusogenic properties with cell membranes and in the same instances may exhibit a specific cell tropism [151], [152]. Exosomes derived from patients can avoid immune surveillance better than *in vitro* formulated pegylated liposomes [3], [152], [153]. Interestingly, exosomes have a neutral lipid molar ratio similar to the optimal composition for liposome fusion and stability [151], [154]. Based on those studies, the term ‘exocure’

was created, a DDS that utilizes exosomes to deliver material of interest to cure pathology [155].

What we learned from the pioneering 'nanodrugs' like Doxil was that the alteration of parameters such as pharmacokinetics and biodistribution could shift the equilibrium from toxicity to efficacy [147]. In this concept, it was mandatory to further study how exosomes can help in cancer treatment in term of increasing anticancer efficacy of doxorubicin with low adverse effects, by trying different strategies in both *in vitro* and *in vivo* using different cancer models.

3. AIMS

In this PhD thesis, we aimed to use exosomes as DDS for doxorubicin as many researchers tried to investigate the advantages of drug encapsulation inside these nanovesicles. It was essential to further study other possible pathways leading to improve the utility of these natural nanocarriers. Differently from previously published papers that focused on the efficacy of the doxorubicin encapsulated in exosomes, in this thesis for the first time, we studied if unmodified exosomes loaded with DOX are less toxic than free DOX by altering the biodistribution of the drug.
In this concept, the previously mentioned points were deeply studied following these main goals:

- To test the hypothesis that exosomes could increase the efficacy of doxorubicin by actively targeting tumor cells and decreasing toxicity by altering the biodistribution of the drug.
- To determine whether exosomes could increase the therapeutic index of DOX. By utilizing a breast and a new syngeneic mouse model of ovarian cancer and analyzing the Maximum tolerated dose (MTD) of exoDOX and DOX and the related toxicity *in vivo,* suggesting new therapeutic opportunities for exosomal drug delivery in cancer patients.

4. MATERIALS AND METHODS

4.1. REAGENTS

Cells were purchased from Sigma-Aldrich (Sigma- Aldrich, Switzerland; HCT-116 colorectal cancer cell line), Cell Biolabs (Cell Biolabs, CA, USA; MDA-MB-231 triple negative breast cancer cell line), DLD1 , LOVO(ATCC, USA) and STOSE (mouse ovarian cell line) developed by Dr. B. Vanderhyden's group [156] and grown as indicated. MDA MB-231 CD63-GFP and STOSE CD63-GFP cell lines were prepared by transduction of MDA-MB-231 and STOSE cell lines with lentivirus containing CD63-GFP plasmid purchased from System Biosciences (CA, USA). Antibodies: α-tubulin (TUBA1A; T9026, 1:10,000) from Sigma-Aldrich (MO, USA); Flotillin1 (FLOT1; ab41927, 1:1000) from Abcam (Cambridge, UK); Lamp1 (9091S, 1:1000) from Cell Signaling (MA, USA). Secondary antibodies were from Thermo Fisher Scientific (MA, USA): antirabbit (31464, 1:10,000) and antimouse (31432,1:10,000).

Nude (immunocompromised) and FVB/N (immunocompetent) mice were purchased from Harlan Laboratories (Udine, Italy). The experimental procedures were approved by the Italian Ministry of Health no. 788/2015-PR and performed in accordance with the institutional guidelines. We utilized at least three female mice of 8 weeks of age per data point.

4.2. EXOSOMES LOADING AND CHARACTERIZATION

4.2.1. EXOSOMES EXTRACTION AND DRUG LOADING

To this end, several protocols and commercially reagents have been designed to analyze the physical properties of exosomes in order to purify them from heterogeneous biological samples. Taking as example, differential ultracentrifugation is one of the widely cited isolation method that contains a series of high speed spins (~100,000 x g) for the selective precipitation of exosomes from different solutions [157], the presence of contaminations of protein and cellular debris has been noted using these protocols [158]. Similarly, many commercially available reagents such as the Invitrogen Total Exosome Isolation Kit (Life Technologies, USA), ExoSpin Exosome Purification Kit (Cell Guidance Systems, USA)

and ExoQuick-TC™ kit (System Biosciences, USA) can facilitate exosomes precipitation from solutions with low speed centrifugation (10,000–20,000 x g) by using precipitation of vesicles with poly-ethylene glycol [159]. Finally, exosomes have been isolated also based on their buoyant density in viscous fluids, where samples are layered onto discontinuous sucrose or iodixanol gradients and subjected to high speed centrifugation (100,000 x g, exosomes recovered from the 1.10–1.20 g/mL fraction/s11). The advantage of this method is that it is less prone to capture contaminating cellular debris. Additionally, this method is also highly user intensive and is not suited for high-throughput applications [160].

In our experiments, exosomes from MDA-MB-231, HCT-116, DLD1 , LOVO, STOSE, MDA-MB-231 CD63-GFP and STOSE CD63 GFP cell lines were prepared from exosome-depleted medium conditioned for 48 h and purified with AB CELL CULTURE-Nanovesicles solution according to the instructions (AB ANALITICA, Padova, Italy) as described in (Figure 4). Exosomes quantification was done by the Bradford method.

For DOX loading, a total quantity of 200 μg of exosomes were mixed with 200 μg of DOX in electroporation buffer (1.15 mM potassium phosphate, 25 mM potassium chloride, 21% Optiprep) and electroporated at 150 V, 0.125 × 1000 μF under max capacitance in a 0.4 cm cuvette. Exosomal doxorubicin (exoDOX) were collected by centrifugation and washed three-times with PBS 1X. DOX concentration in exosomes was quantified by measuring the absorbance at 490 nm using Tecan F200 instrument (Tecan, Männedorf, Switzerland).

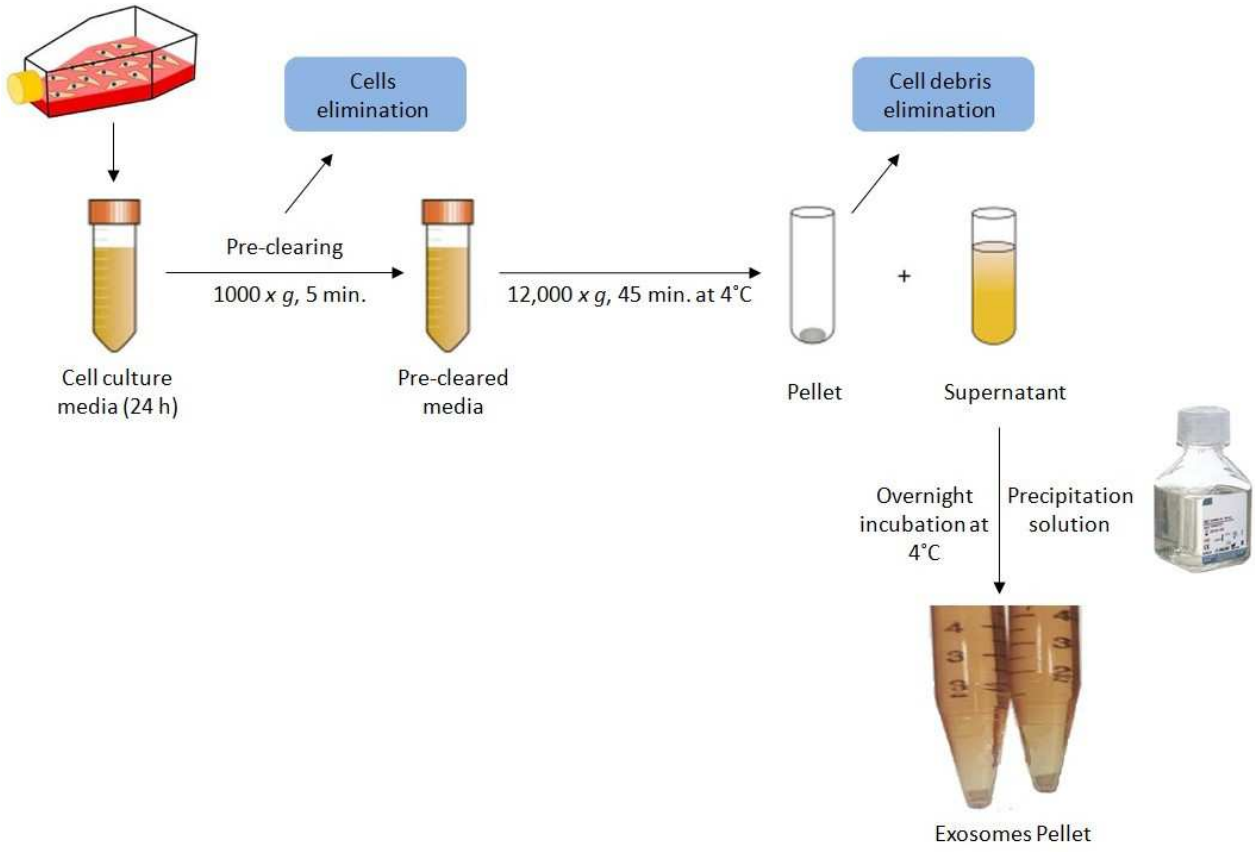

Figure 4. Exosomes isolation protocol. Indicating the different centrifugation steps using precipitation solution.

4.2.2. TRANSMISSION ELECTRON MICROSCOPY

Briefly describing transmission electron microscopy (TEM) that is a microscopy technique in which a beam of electrons is transmitted through an ultra-thin specimen, interacting with the specimen as it passes through it. An image is formed from the interaction of the electrons transmitted through the specimen; the image is magnified and focused onto an imaging device, such as a fluorescent screen, on a layer of photographic film, or to be detected by a sensor such as a charge-coupled device (Figure 5).

In our characterizations using TEM, exosomes were resuspended in PBS 2% glutaraldehyde (30 min) and deposited on formvar/carbon-coated electron microscopy (EM) grids. Two percent of uranyl acetate was added to the exosome-coated grids for 10 min and washed three-times with water. After drying in air, exosomes were imaged with a transmission electron microscope (EM 208, Philips,

Eindhoven, The Netherlands). Micrographs were taken with a Quemesa Camera (Olympus Soft Imaging Solutions, Munster, Germany).

4.2.3. SCANNING ELECTRON MICROSCOPY

Instead, scanning electron microscopy works with different theory in which a beam of electrons is propelled by magnetic rings through a tall chamber column pumped down to a vacuum, with the beam becoming more focused as it passes through progressively stronger magnets. The electrons bounce off some tiny sample, and the intensity of electrons bouncing off the shape of the sample are interpreted as pixel numbers, corresponding to shades of black & gray, forming an image (Figure 5).

To perform scanning electron microscopy (SEM) analyses, exosomes were dehydrated in a graded 30–100% ethanol series, dried in a CO_2 apparatus at a critical point (Bal-Tec; EM Technology and Application, Liechtenstein), sputter coated with gold in an Edwards S150A apparatus (Edwards High Vacuum, UK), and examined with a Leica Stereoscan 430i scanning electron microscope (Leica Cambridge Ltd, UK).

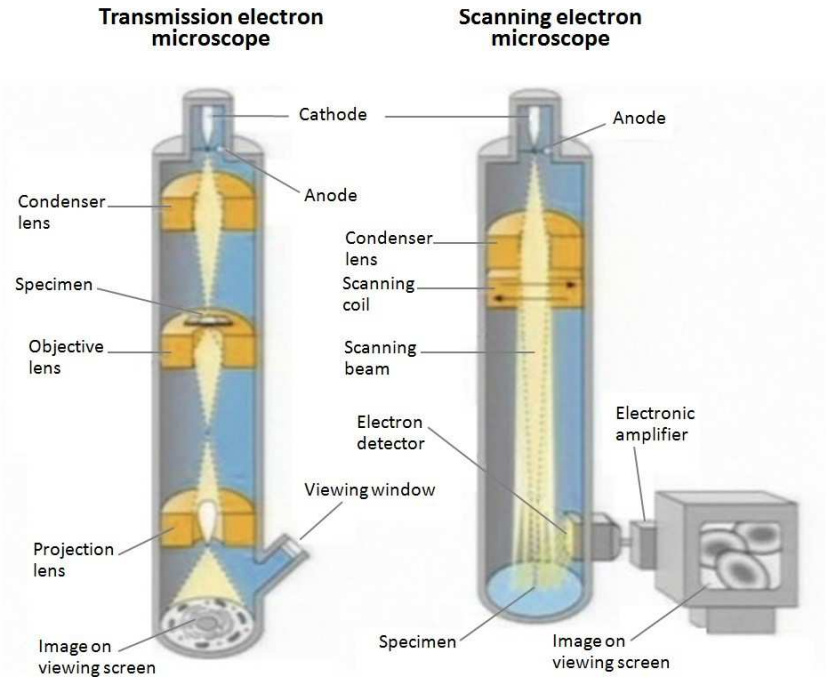

Figure 5. Schematic of the transmission and scanning electron microscopes

4.2.4. NANOPARTICLES TRACKING ANALYSIS

Nanoparticles tracking analysis is a useful technique to evaluate particles dimensions in addition to the approximate determination of concentration in nanoparticles/ml. This technique is based on the use of a laser beam that passes through the sample chamber and the particles in suspension in the path of the beam scatter the light in such a manner that they can be easily visualized via a long working distance, 20x magnification microscope onto which is mounted a video camera. The camera captures a video file of the particles moving under Brownian motion. The NTA software tracks many particles individually and using the Stokes Einstein equation calculates their hydrodynamic diameters. The NanoSight range of instruments provides high resolution particle size, concentration and aggregation measurements while a fluorescence mode provides specific results for labelled particles. The range provides real time monitoring of the subtle changes in the characteristics of particle populations with all of these analyses confirmed by visual validation indicated in (Figure 6).

For the characterization in our experiments, the size of exosomes was determined by NTA with a NanoSight LM10 instrument (Malvern Instruments, UK) in a PBS 1X buffer by diluting the samples at a concentration of about 10–20 µg/ml by measuring the exosomal proteins by Bradford quantification assay.

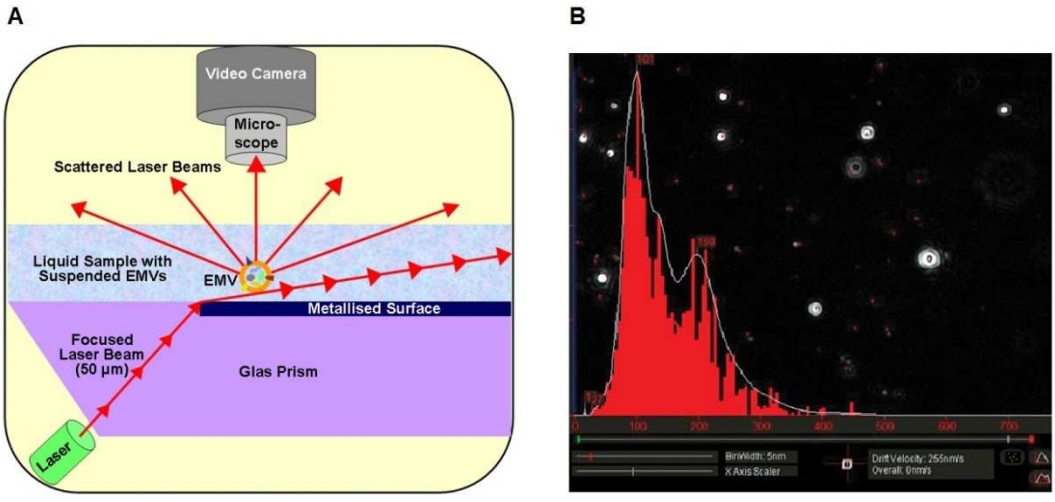

Figure 6. Nanoparticles tracking analysis. A) Principal configuration of the instrumentation (NanoSight) for NTA of extracellular microvesicles (EMV). **B)** Size distribution plot.

4.2.5. WESTERN BLOT

The cell pellets and exosomes (from 1.5 x 10^7 cells) were resuspended into radioimmunoprecipitation assay buffer supplemented with a protease inhibitor mixture (Complete-EDTA, Roche, Switzerland) for protein extraction and 50 μg of proteins were run in 8% denaturating polyacrylamide gel. After electrophoresis, the proteins were transferred on nitrocellulose membrane (Whatman International Ltd, UK). The membranes were blocked with 5% (w/v) skim milk in Tris-buffered saline Tween-20 solution (TBS-T) and incubated overnight with primary antibodies (Lamp1, FLOT1 and α-tubulin). After washing, the membranes were incubated for 1 h with secondary antibodies in 5% milk TBS-T at RT. The membranes were developed with ECL solution (Euroclone, Italy) and visualized with ChemiDoc Imager instrument (Bio-Rad Laboratories, CA, USA).

4.3. *IN VITRO* EXPERIMENTS

4.3.1. DRUG RELEASE TEST

The release of DOX and exoDOX were evaluated with a dialysis membrane of 20.000 Molecular weight cut-off (MWCO) that had been dipped into 50% fetal bovine serum in PBS 1X, at pH 7.4, indicated in (Figure 7). The cumulative release of DOX was evaluated by measuring the fluorescence intensity *(I)* at Ex 465/Em 595 nm of DOX inside the dialysis membrane at different time points (0, 0.5, 1, 2, 3, 6, 8, 12, 18 and 24 h). The percentage of cumulative release was calculated using this equation below:

$$R = \frac{I_0 - I_t}{I_0} \times 100\%$$

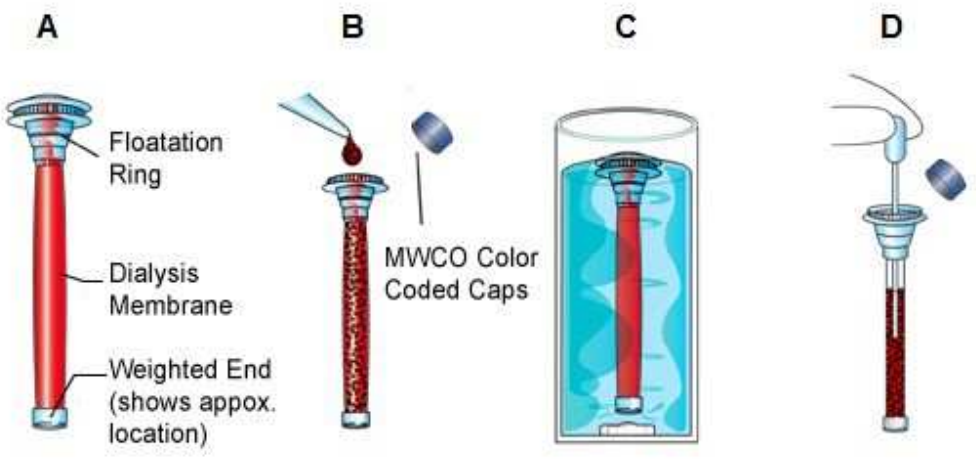

Figure 7. Schematic picture of dialysis membrane of 20.000 MWCO, indicating the different steps for **A)** Membrane buffer equilibration. **B)** Loading with analyzed solution. **C)** Incubation in 50% FBS + 50% PBS and **D)** Sample collection.

4.3.2. THE HALF MAXIMAL INHIBITORY CONCENTRATION & CELL VIABILITY ASSAY

The CellTiter-Glo® Luminescent Cell Viability Assay is a homogeneous method to determine the number of viable cells in culture based on quantification of the ATP, which signals the presence of metabolically active cells. The CellTiter-Glo® Assay is designed for use with multiwell-plate formats, making it ideal for automated high-throughput screening (HTS) and cell proliferation and cytotoxicity assays. The homogeneous assay procedure (Figure 8) utilize a single reagent (CellTiter-Glo® Reagent) added directly to the cells cultured in serum-supplemented medium. Cell washing, removal of medium or multiple pipetting steps are not required. The homogeneous "add-mix-measure" format results in cell lysis and generation of a luminescent signal proportional to the amount of ATP present. The amount of ATP is directly proportional to the number of cells present in culture in agreement with previous reports [161].

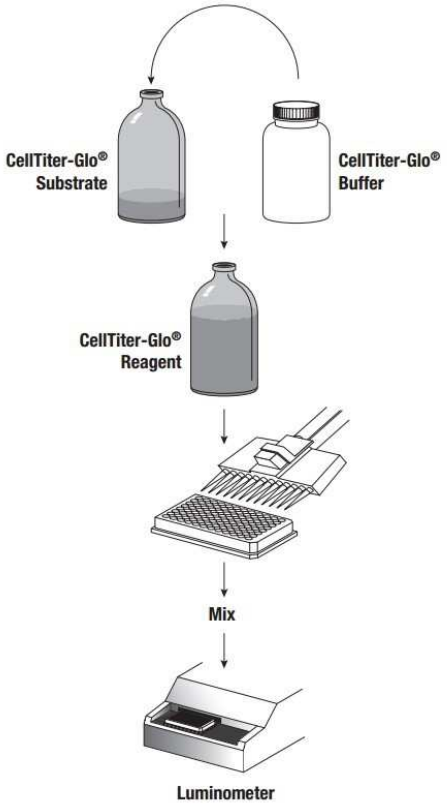

Figure 8. Flow diagram showing preparation and use of CellTiter-Glo® Reagent.

The CellTiter-Glo® Assay relies on the properties of a proprietary thermostable luciferase (Ultra-Glo™ Recombinant Luciferase), which generates a stable "glow-type" luminescent signal and improves the performance across a wide range of assay conditions. The luciferase reaction for this assay is shown in (Figure 9).

Figure 9. The luciferase reaction. Mono-oxygenation of luciferin is catalyzed by luciferase in the presence of Mg^{2+}, ATP and molecular oxygen.

In order to evaluate the half maximal inhibitory concentration (IC_{50}) of DOX, cells were plated with a density of 10^3 cells/well in a 96-wells plate (Becton Dickinson, NJ, USA) and incubated for 24 h to allow the attachment of cells. The next day, cells were treated with DOX starting with a concentration of 1 μg/ml followed by five 1:10 serial dilutions. After 96 h, the cell viability was evaluated by CellTiter-Glo® Luminescence assay (Promega, WI, USA) with the Infinite 200 PRO instrument (Tecan) and IC50 was calculated using the GraphPad program (Prism, CA, USA).

In order to evaluate the cytotoxicity, 10^3 cells/well were plated in 96-well culture plates and the day after seeding, were treated with DOX or exoDOX at a concentration that depend on the IC_{50} each cell line. Cell viability was measured after 96 h, according to the supplier (Promega, WI, USA; G7571), with a Tecan F200 instrument (Tecan, Switzerland). Averages and standard errors were obtained from three different experiments.

4.3.3. CELLULAR INTERNALIZATION

MDA-MB-231 cells were seeded in 24-multiwell plates at a density of 10^5 cells/well. The following day, the cells were treated with DOX or exoDOX at a concentration of 100 ng/ml and incubated for (1, 6 and 24 h) in comparison with untreated cells. The cells were imaged with a Leica fluorescence microscope at 20X magnification.

4.3.4. HUMAN CARDIAC MICROVASCULAR ENDOTHELIAL CELLS TRANSWELL ASSAY

To study the ability of exoDOX to an cross endothelial cell barrier, a transwell system was carried out as indicated in (Figure 10). Human cardiac microvascular endothelial cells (PromoCell, Germany) were plated at the density of 105 cells on cell culture insert with pore size of 8 μm (Becton Dickinson, NJ, USA) pretreated with 5 μg/cm2 of fibronectin (Sigma-Aldrich, MO, USA). The next day, two concentrations of 10 μg/ml and 50 μg/ml of both exoDOX and DOX were added on the top of cell-culture insert in phenol red free medium and the concentration of DOX was read

from the bottom by measuring the absorbance at 490 nm at different time points (0, 0.5, 2, 4, 7, 16 and 28 h).

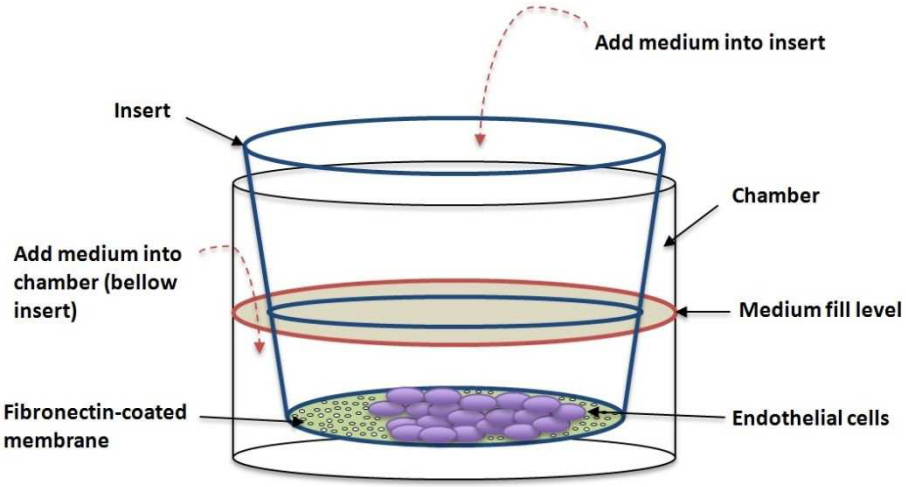

Figure 10. Schematic picture of transwell describing the ability of DOX and exoDOX to cross a reconstructed myocardial endothelial monolayer

4.3.5. CD63-GFP VIRUS PRODUCTION AND TRANSDUCTION

To produce lentivirus, 7 × 10^5 HEK293T packaging cells/well were seeded in a 6 multiwell plate, 1 day before transfection. For each well, 2 µg of custom CD63-GFP plasmid from System Biosciences (CA, USA), 0.5 µg of pMD2G (VSV-G envelope expressing plasmid), 1 µg of psPAX2 (lentiviral packaging plasmid) were diluted in 100 µl of plain DMEM plus 16 µl of transfection agent (FuGENE® HD, Promega) and incubated 20 min at RT. The cells were incubated for 24 h at 37 °C, after which the medium was refreshed. Lentivirus-containing supernatants were collected at 48 and 72 hours post-transfection with 20% of FBS (Figure 11). The two collections of lentiviral particles were pooled, filtered through a 0.45 µm membrane (Sartorius Stedim/PVDF) and stored at −80 °C.

MDA-MB-231 and STOSE cell lines were transduced with lentiviral supernatants supplemented with 8 µg/ml hexabromide (Sigma). At 48 h post-infection, medium was replaced and cells were selected with 2 µg/ml of puromycin or 5 ug/ml blasticidin (Gibco). Antibiotic selection was stopped as soon as no surviving cells remained in the non transduction control plate [162], [163].

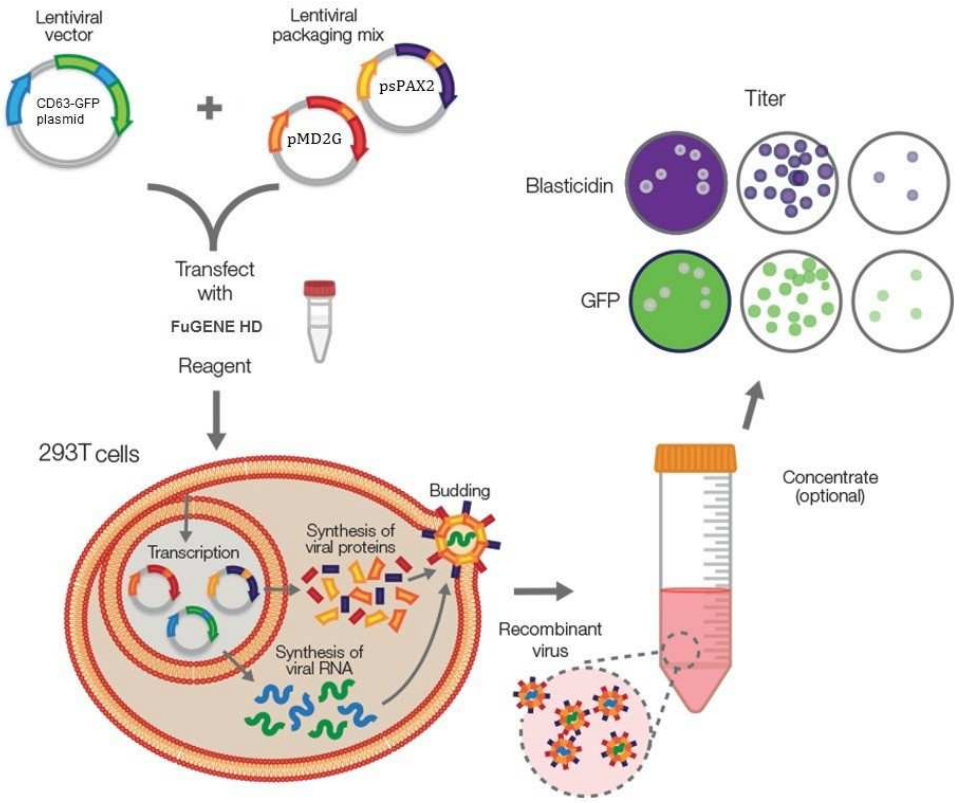

Figure 11. Lentiviral production. A lentiviral construct containing the CD63-GFP along with lentiviral packaging mix is cotransfected into 293T cells using FuGENE® HD reagent. Following incubation of cells, supernatant containing lentivirus is harvested and cellular debris is removed by centrifugation. Depending on the lentiviral construct, viral titer is determined either by puromycin or blasticidin selection or analyzing the percentage of GFP-positive cells.

4.3.6. FLUORESCENCE IMAGING OF CELLS/EXO (CD63-GFP)

MDA-MB-231 CD63-GFP and STOSE CD63-GFP cells were incubated in exosome free medium for 48 h. The medium was then collected and exosomes were extracted using AB CELL CULTURE-Nanovesicles solution according to the instructions (AB ANALITICA, Padova, Italy). The exosomes were diluted 1:100 in PBS 1X and a drop was laid on cover slip, analyzed together with the cells of origins with a fluorescence microscope using a filter set with Ex 490/Em 520 nm wavelengths.

4.4. *IN VIVO* EXPERIMENTS

4.4.1. MOUSE XENOGRAFTS

In xenograft tumor assays, in order to test exoDOX and DOX efficacy using the treatment dose, 4×10^6 MDA-MB-231 cells were mixed with 30% of Matrigel (BD Bioscience, CA, USA) and implanted subcutaneously into the flanks of 8-week-old female nude mice. Once tumors reached measurable size (>50 mm^3), mice were treated intravenously (iv.) with indicated drugs two-times per week for seven treatments.

Instead, to test the ability of exoDOX to increase the therapeutic index of DOX, 3×10^6 MDA-MB-231 cells were mixed with 30% of Matrigel (BD Bioscience, CA, USA) and implanted subcutaneously into 8-week-old female nude mice. 5×10^6 STOSE cells were mixed with 30% of Matrigel (BD Bioscience) and implanted subcutaneously into the flanks of 8-week-old female FVB/N mice when tumors reached a measurable size (>50 mm^3), mice were treated intraperitoneally (ip.) with DOX, Doxil and exoDOX two-times per week for a total of five treatments.

For all *in vivo* experiments, tumor volumes were measured with a caliper and calculated using the formula: $(\text{length} \times \text{width}^2)/2$.

4.4.2. HISTOPATHOLOGY

Histopathology was performed in order to evaluate the toxicity of exoDOX in different tissues, after the end of the treatment. Organs of mice were collected and fixed in phosphatebuffered 10% formalin, embedded in paraffin, sectioned at a thickness of 3 μm and stained with hematoxylin and eosin (H&E). The tissues were analyzed with light microscopy using different magnifications. Morphological details were analyzed at 40X objective.

4.4.3. BIODISTRIBUTION AND PHARMACOKINETICS (PK)

For the biodistribution evaluation of exoDOX compared with DOX, tissues and tumors were washed with 10 ml of cold PBS/heparin before collection. Blood was collected from the left ventricle of the heart under anesthesia. The organs were diluted in 500 ul of PBS/BSA 4% and homogenized with Qiagen TissueRuptor for 20 sec at power 4 in ice.

In the pharmacokinetic (PK) experiments, mice were treated with 3 mg/kg (ip.) and the blood was collected after 0.08, 0.25, 0.5, 1, 3, 18, 36 and 72 h. Samples were stored at -80°C.

The concentrations of DOX in serum, tissues and tumors were measured by liquid chromatography tandem mass spectrometry (LC-MS/MS). The proteins were precipitated with two volumes of cold acetonitrile containing 20 ng/ml daunorubicin as an internal standard. The cleared supernatant was diluted with two volumes of 0.2% formic acid and 10 ul were injected on LC-MS/MS system. The chromatographic separation was performed on Accucore-150 30 × 2.1 mm 2.6 um C18 column (Thermo Scientific, MA, USA) equilibrated with a 0.7 ml/min of 0.2% formic/acetonitrile (95:5) and maintained at 50°C. An elution gradient B from 5 to 80% of acetonitrile over 5 min was applied and 3 min of equilibration A 4000 QTRAP MS/MS system equipped with Turbo ESI source (AB Sciex, MA, USA) was applied in positive-ion mode. The transitions of DOX and daunorubicin were monitored in multireaction monitoring mode at m/z 544.1→397.2 and 528.2→321.1, respectively. The spray voltage was set at 5000 V with the source temperature at 400°C. The curtain gas, nebulizer gas (gas1) and auxiliary gas (gas 2) were set at 20, 50 and 50 arbitrary units, respectively.

4.4.4. MAXIMUM TOLERATED DOSE

In order to evaluate the *in vivo* maximum tolerated dose (MTD) of exoDOX and free in comparison with the commercially used drug formulation known as Doxil® (liposomal DOX) , nude mice were treated with different concentrations of exoDOX, Doxil or free DOX as indicated in (Figure 12). The drugs were injected i.p. (3, 5, 7 and 15 mg/kg), two-times per week for a total of five injections. As objective scale, we measured the body weight (BW) of mice.

For the same reason and in order to validate the results in immunocompetent mouse model. The tolerability of exoDOX was tested in isogenic FVB/N mice. The mice were treated with DOX and exoDOX at 3 and 6 mg/kg, two times per week for a total of five treatments.

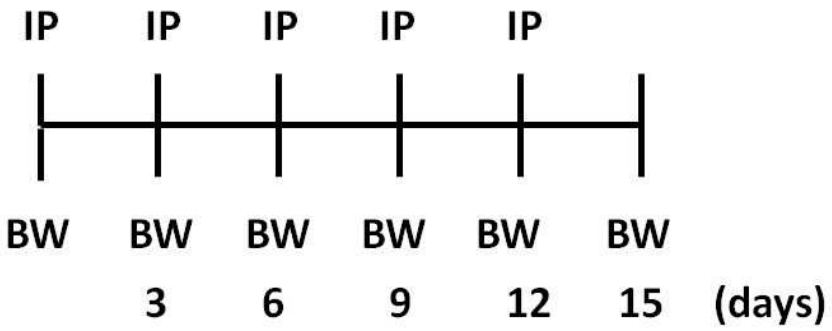

Figure 12. Schematic design for the injection protocol during MTD experiments. **IP** (intraperitoneal injection), **BW** (Body weight).

4.4.5. STATISTICAL ANALYSIS

The statistical significance was determined using the t-test. A *p*-value less than 0.05 was considered significant for all comparisons made.

5. RESULTS AND DISCUSSION

5.1. CHARACTERIZATION OF EXOSOMAL DOXORUBICIN

Exosomes were isolated from cancer cells since it has been hypothesized that they have an intrinsic property to target the tumor microenvironment [164]–[169]. To enrich the fraction of exosomes from the supernatant culture of MDA-MB-231, HCT-116 and STOSE cell lines, AB CELL CULTURE-Nanovesicles solution from (AB ANALITICA, Padova, Italy) was utilized. The hydrodynamic dimension of vesicles was characterized by nanoparticle tracking analysis [170]. The mean and standard deviation values were 155 ± 55 nm, 156 ± 55 nm and 101 ± 50 nm in MDA-MB-231, HCT-116 and STOSE cell lines, respectively, (Figure 13).

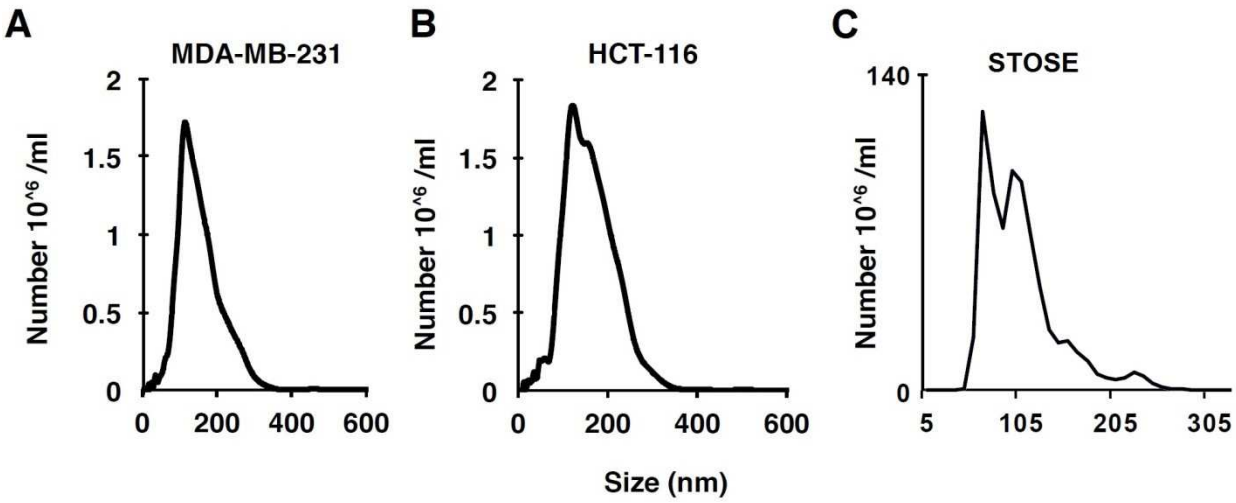

Figure 13. Nanoparticles tracking analysis of (**A**) MDA-MB-231, (**B**) HCT-116 and (**C**) STOSE exoso

mes, showing the sizes and concentrations of the extracted vesicles.

Exosomes were also characterized by scanning (SEM) and transmission electron microscope (TEM). The (Figure 14) depict a regular size with a spherical shape [171].

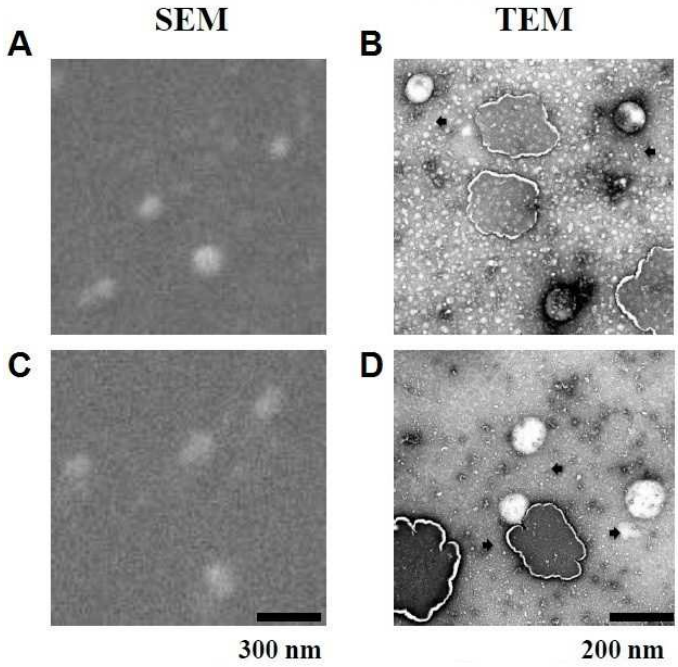

Figure 14. Scanning (**A, C**) and Transmission (**B, D**) electron microscope images of MDA-MB-231 and HCT-116 exosomes respectively demonstrate their shapes and dimensions

Isolated exosomes and their cells of origin were next analyzed by Western blotting with antibodies specific to Lamp1 (Lysosomal Associated Membrane Protein 1) and Flotillin 1 (caveolae-associated, integral membrane protein 1) exosomal markers [123], [172]. In addition to α-tubulin as negative and positive internal control.

Results in (Figure 15), showed that Human Lamp1 was detected in MDA-MB-231 exosomes but not in mouse STOSE exosomes as expected. Human/mouse Flotilin 1 was detected in both exosomes from MDA-MB-231 and STOSE cells. α-tubulin was present in the cell extracts but not in exosomes as expected. Confirming that exosomes extracted using the mentioned isolation protocol. These results demonstrate that our method isolate clean exosome populations, in addition it

should be known that this protocol is less time consuming compared to ultracentrifugation protocols.

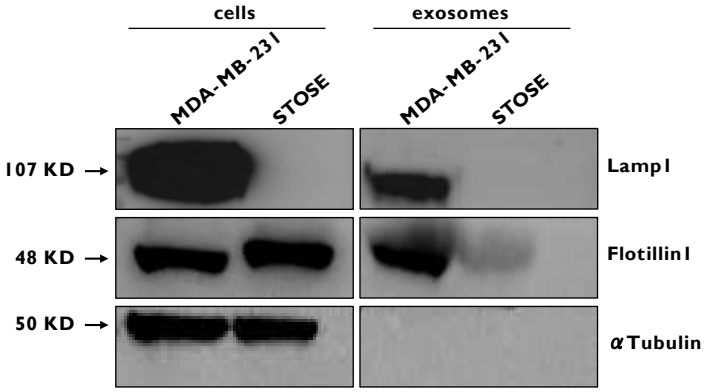

Figure 15. Western blot analysis of exosomes purified from MDA-MB-231 and STOSE cells. Human Lamp1 was detected in MDA-MB-231 exosomes but not in mouse STOSE exosomes as expected. Human/mouse Flotilin 1 was detected in both exosomes from MDA-MB-231 and STOSE cells.

To further confirm exosomes purification, cells were infected with CD63-GFP fusion protein (exosomal marker) and the isolated exosomes were analyzed under microscope. Fluorescence analysis of MDA-MB-231 CD63-GFP and STOSE CD63-GFP exosomes showed a dotted appearance as expected for vesicular accumulation (Figure 16).

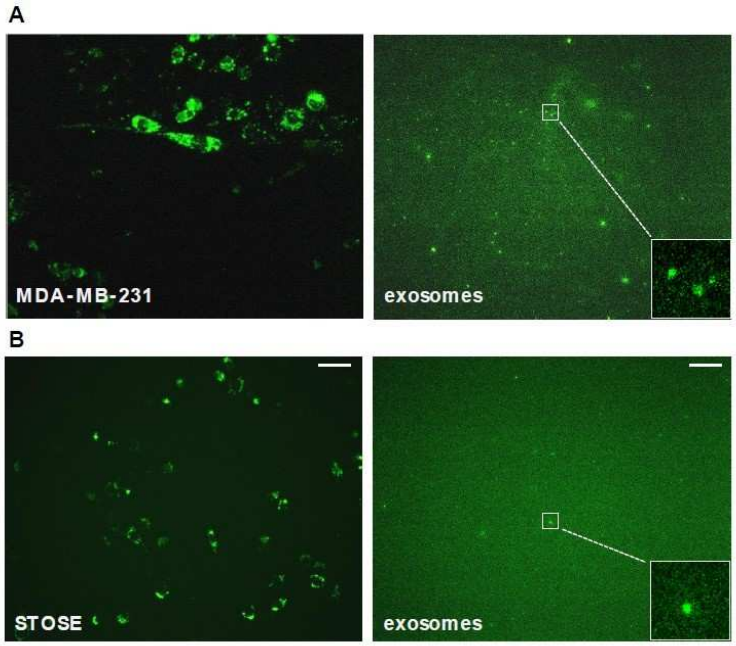

Figure 16. (**A**) MDA-MB-231 and (**B**) STOSE CD63-GFP cell lines and the related exosomes. Cells were acquired at 20X and exosomes at 40X magnification under fluorescence microscope. Exosomes appear as green dot in the box. Scale bar, 25 μm.

The vesicles were then loaded through electroporation [126], [173] and the loading of DOX was confirmed by measuring by NTA the dimension of the loaded exosomes, which increased to 176 ± 53 nm and 209 ± 54 nm in MDA-MB-231 and HCT-116 cell lines, respectively. Compared with free diffusion, electroporation increases the DOX loading efficiency of about three-times with a yield of 2.56 ± 0.57% (encapsulated/total), (Figure 17). Additionally, to load 1 µg of DOX, 22.5 ± 6.64 µg of exosomes were utilized measured by Bradford method.

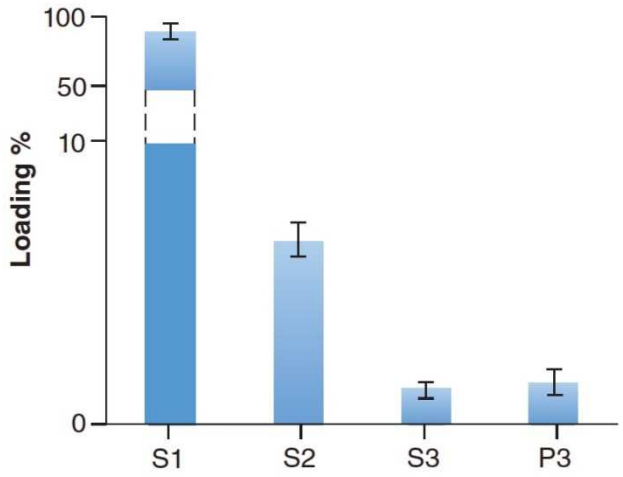

Figure 17. Loading efficiency of exosomal doxorubicin. After loading, the exosomes were washed three-times and the quantity of drug released in the supernatant or entrapped in the pellet was measured. P: Pellet; P3: Pellet (exosomes) after three washes; S: Supernatant; S1, S2 and S3: Supernatant after one, two and three washes, respectively.

5.2. EXODOX STABILITY AND CELLULAR INTERNAZLIZATION

It is important to determine the stability of exoDOX in serum before *in vivo* application. A time point analysis of exosomes loaded with DOX was performed in 50% serum utilizing a semipermeable membrane (Figure 18). A two-phase kinetic of release was observed. In the first 2 h, the release of exoDOX was similar to free DOX. Later, the release of DOX from exosomes was slow and never reached 100% over a period of 24 h. This difference in release could be explained by the interaction of DOX with different biological content of exosomes such as DNA, RNA and membranes.

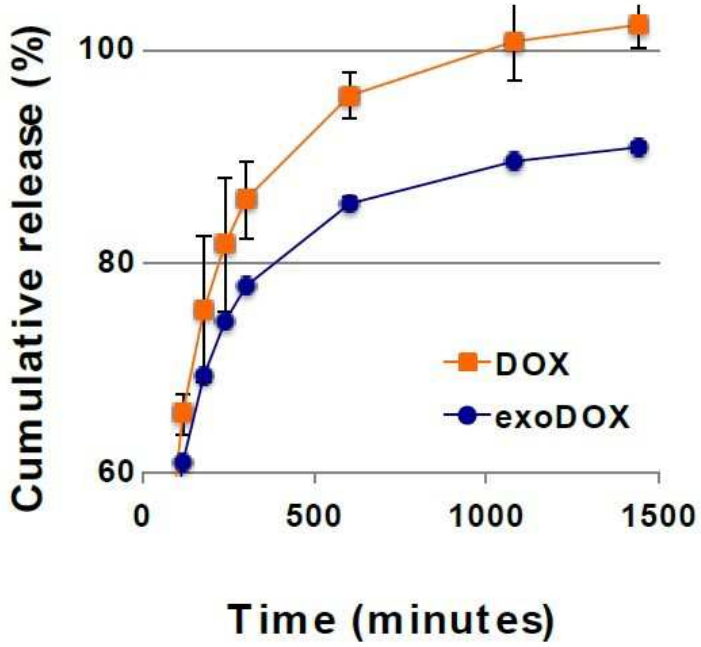

Figure 18. Release of DOX from exosomes. The cumulative release of DOX was evaluated by measuring the fluorescence of DOX inside the dialysis membrane at different time points, pH 7.4.

The interaction and internalization of exosomes with cells has been the subject of many research papers. Exosomes can deliver different biological messengers such as RNA, miRNA, proteins, etc., utilizing 'native' mechanisms, which can also be utilized to deliver exogenous materials such as drugs. Different mechanisms of interaction with cells have been postulated: receptor- or lipid raft-mediated endocytosis, macropinocytosis or direct fusion with cell membranes. It appears from those studies that the content of the exosomes is efficiently released in the cytoplasm [3], [174]–[177]. Time course analysis of DOX and exoDOX internalization in MDA-MB-231 cells showed a similar pattern of drug accumulation in the nucleus (Figure 19). These data suggest that exosomes could efficiently release the DOX to exert its cytotoxic effect.

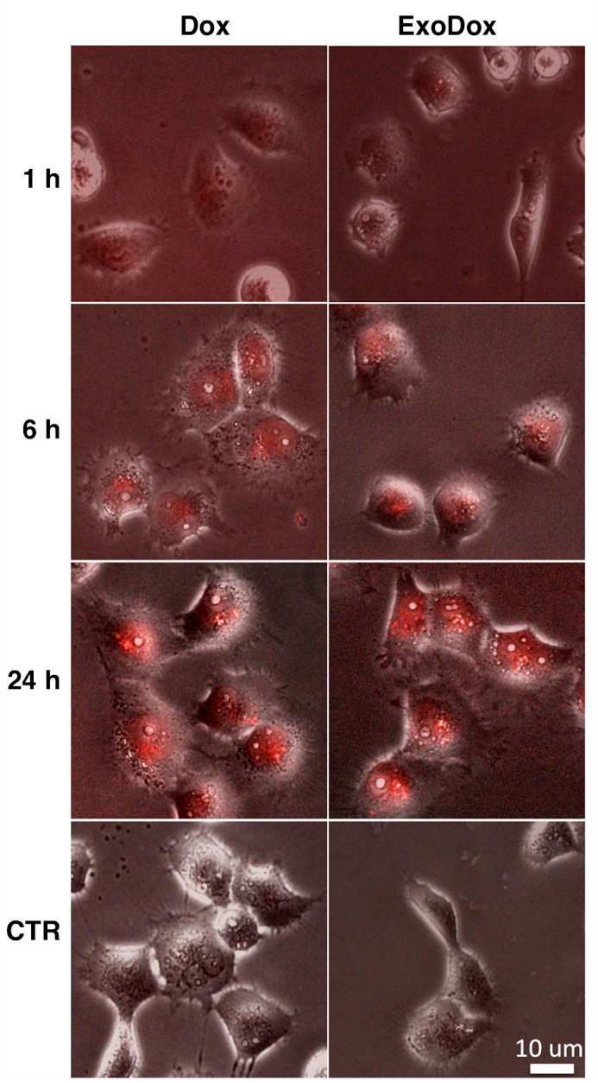

Figure 19. Fluorescence analysis of DOX and exoDOX in MDA-MB-231 cells. Time point analysis of 1, 6 and 24 hours of DOX autofluorescence showed increase accumulation in the nucleus. CTR: untreated cells.

5.3. EXODOX HAS A FEWER APTITUDE TO CROSS MYOCARDIAL ENDOTHELIAL CELLS THAN FREE DOX

Endothelial myocardial cells were plated into transwell membrane inserts (pore size 8 μm) coated with fibronectin. DOX and exoDOX (10 and 50 μg) were added into the insert chamber and the absorbance was read from the bottom. A time point analysis showed that at both concentrations, exoDOX has a lower ability to cross myocardial endothelia cells than free DOX (Figure 20). Although the experiment was performed under static conditions, it was demonstrated the aptitude of exosomes to avoid extravasation in normal heart tissue.

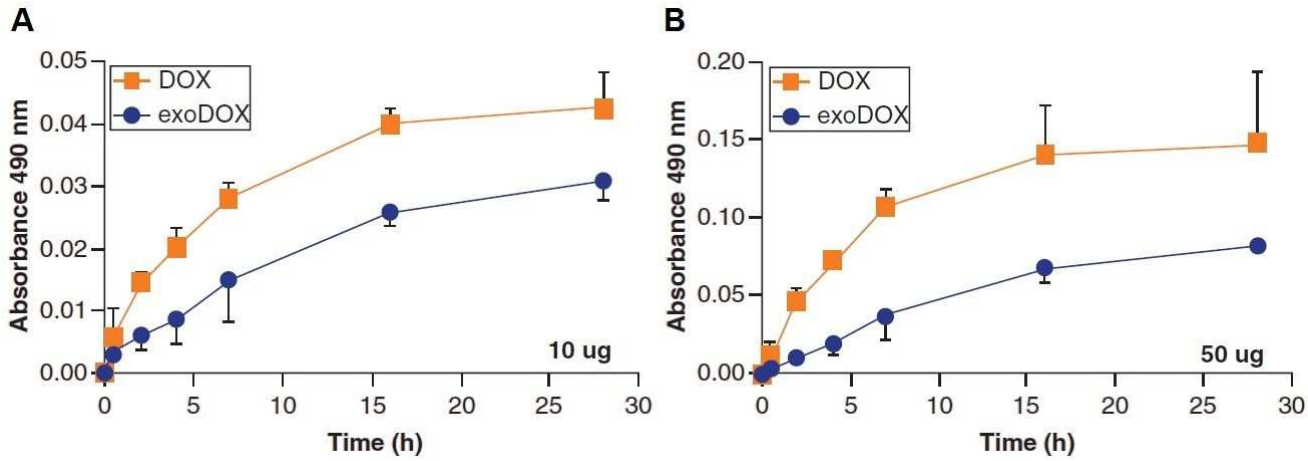

Figure 20. **Myocardial endothelial cells transwell assay**. Absorbance of (**A**) 10 μg and (**B**) 50 μg of DOX and exoDOX in the lower chamber at seven time points (0, 0.5, 2, 4, 7, 16 and 28 h). Experiments were run in duplicates. Mean and standard deviation are reported.

5.4. ANTI-TUMOR EFFICACY OF EXODOX AND DOX

5.4.1. *IN VITRO* EFFICACY

After exosome isolation and characterization, cells were treated with three different concentrations of DOX (100 ng/ml, 50 ng/ml and 25 ng/ml) and exoDOX from MDA-MB-231 and HCT-116 cell lines. The exoDOX were crossed on both cell lines in order to test if there was cell lineage specificity. The cell viability was measured at different time points as reported in Figure 21 (A & B). Similar to data reported in other published papers [127], [178], we observed that exoDOX killed cancer cells at the same extent as free DOX. The same effect was also observed in two others colon cancer cell lines; LOVO and DLD-1 (Figure 22).

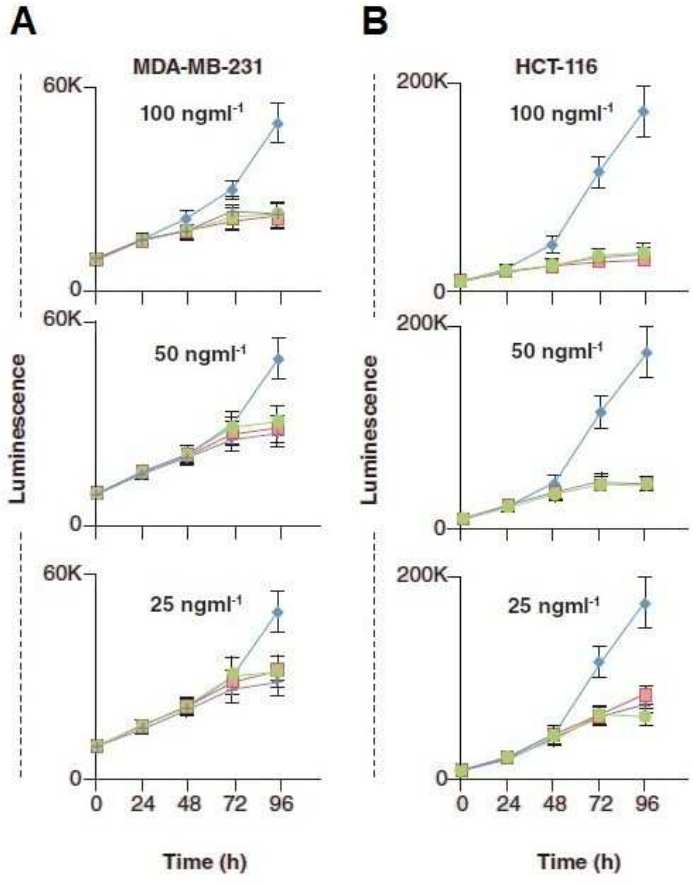

Figure 21. Cell viability assays showed no difference among treated cells. (**A**) MDA-MB-231 and (**B**) HCT-116 cells were treated with different concentrations of DOX (■), exo231DOX (•), exoHCTDOX (▭) and control (♦). Y-axis: luminescence refers to count per second.

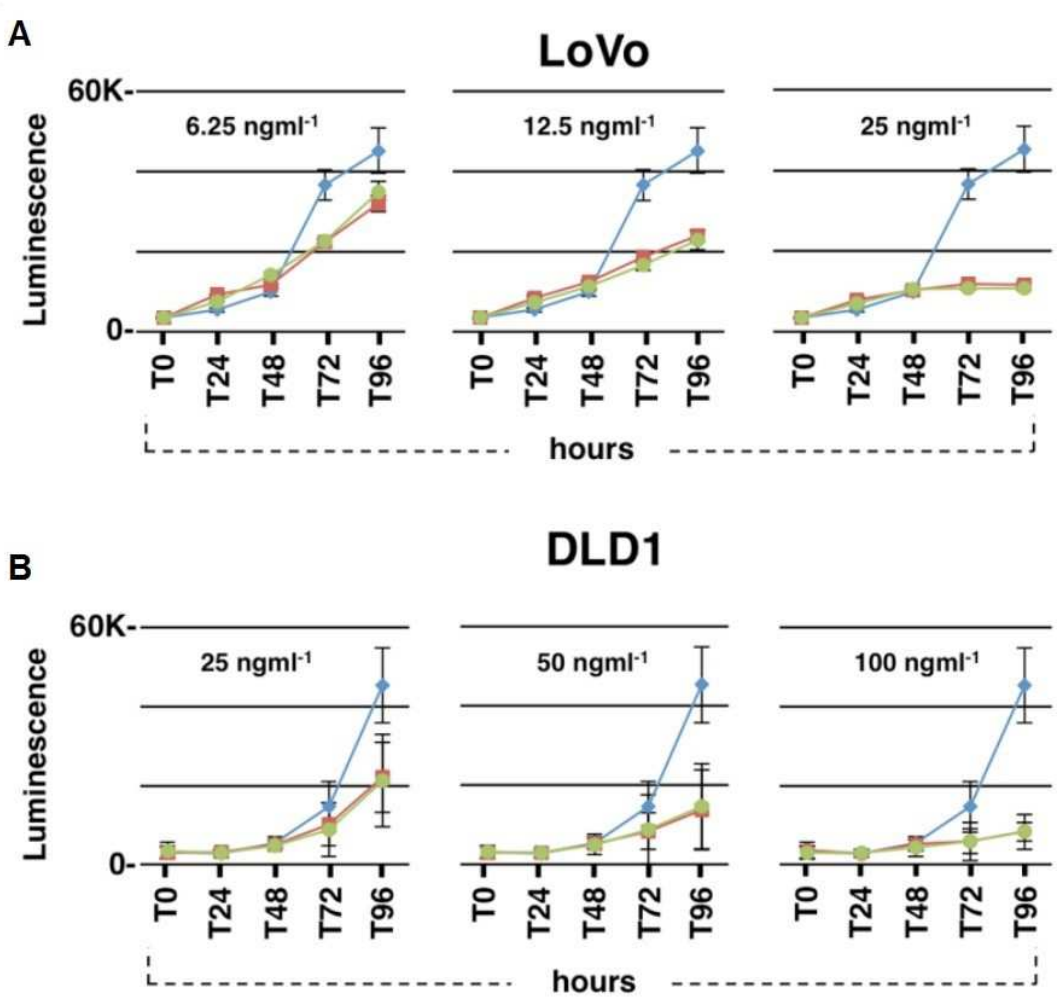

Figure 22. **Cell viability assay showed no difference among treated cells.** (**A**) LOVO and (**B**) DLD1 cell lines were treated with different concentrations (as indicated) of DOX (■), exoDOX (•), and control (♦). Y axis: Luminescence refers to count per second (K=1000).

Ovarian cancer is a lethal disease. Scientists have worked for years to establish a representative mouse model. Recently, Dr. Barbara Vanderhyden's group has developed a spontaneously transformed mouse ovarian surface epithelial cell line (STOSE), which closely recapitulates the characteristics of human high-grade serous ovarian cancer (HGSOC) [156].

Since STOSE cells closely recapitulate HGSOC, it was decided to validate the data obtained with MDA-MB-231 breast cancer cells. First, we calculated the IC_{50} of DOX on both cell lines. IC_{50} analysis of DOX demonstrated a similar sensitivity of STOSE and MDA-MB- 231 cell lines. The average of IC50 was 18.78 ± 1.25 and 13.85 ± 1.22 ng/ml for STOSE and MDA-MB-231 cell lines, respectively (Figure 23).

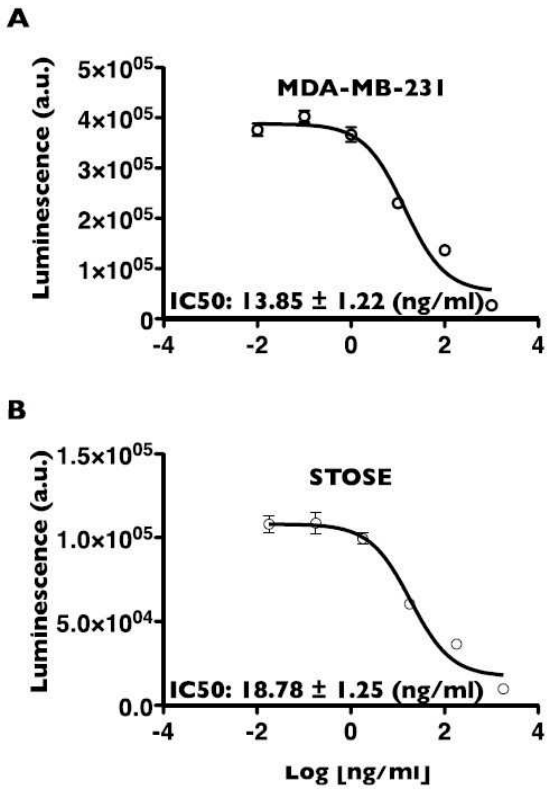

Figure 23. IC_{50} of DOX in (**A**) MDA-MB-231 and (**B**) STOSE cell lines by using 1:10 dilution scale starting from 1 µg/ml. Cell viability was evaluated after 96 hours. Experiments were run in triplicates. Mean and error standard are reported.

Treatment of STOSE cells with different concentrations of DOX and exoDOX showed the same effect on cell viability (Figure 24) as previously demonstrated with MDA-MB-231 cell lines.

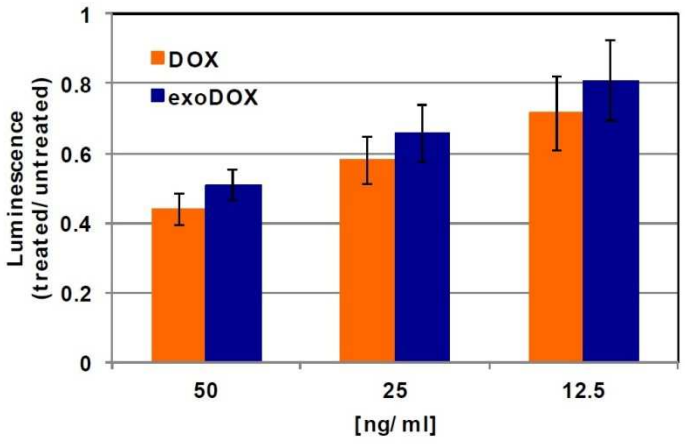

Figure 24. ExoDOX has the same effect of doxorubicin *in vitro*. Cell viability assays showed no difference among treated cells. STOSE cells were treated with three different concentrations of DOX (orange) and exoDOX (Blue). Experiments were run in triplicates. Mean and standard deviation are reported.

5.4.2. *IN VIVO* EFFICACY

In vitro analyses in static conditions have several limitations and it is more appropriate to use an *in vivo* model to mimic physiologic conditions. In addition, pegylated liposomal doxorubicin was two times less effective compared with free DOX in *in vitro* cell viability assay but more effective *in vivo* [179]. In this setting, the MDA-MB-231 cancer cells were injected as a subcutaneous xenograft and treated with free DOX or exoDOX prepared from MDA-MB-231 or HCT-116 cell lines. At a dose in which DOX did not produce any significant toxic side effect in mice (1.5 mg/kg, Figure 25A) [180], the efficacy of exoDOX was comparable to that of free DOX. The volume of the tumors was inhibited by about 30% compared with untreated mice (Figure 25B).

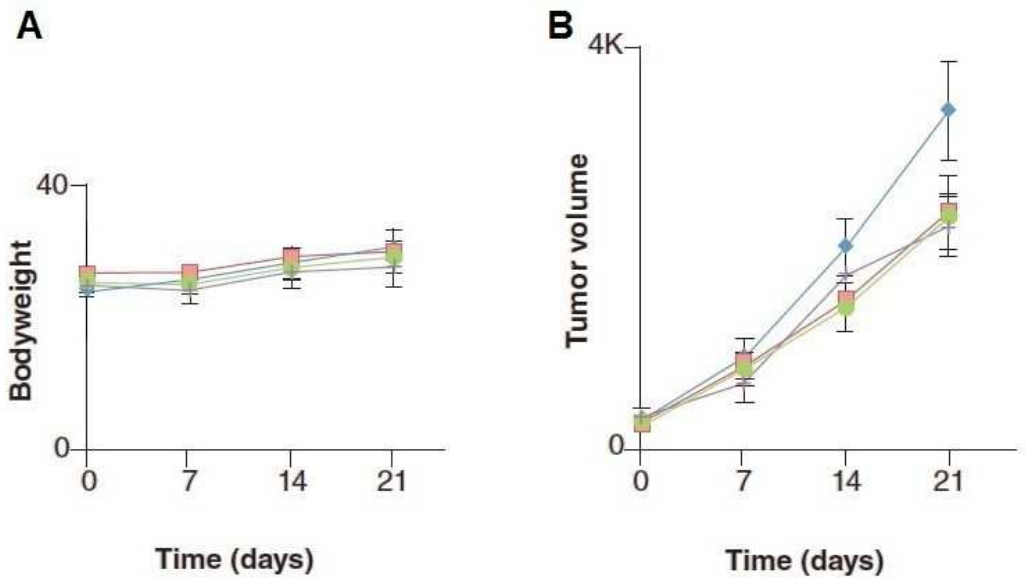

Figure 25. Exosomal doxorubicin has the same effect of doxorubicin *in vivo.* MDA-MB-231 cells were implanted in the flank of nude mice. The animals were treated by intravenous injection (1.5 mg/kg) with DOX (■), exo231DOX (•), exoHCTDOX (▭) and control (♦). (**A**) The bodyweight of treated mice was normal suggesting no evidence of toxicity with treatments. (K: 1000). (**B**) The tumor volume was monitored for 21 days every week. No difference was observed between treatments.

5.5. DIFFERENCE IN ACUTE TOXICITY *IN VIVO*

5.5.1. *IN VIVO* TOXICITY ANALYSES OF EXODOX & DOX

The clinical benefit of liposomal DOX is due to the reduced cardiac toxicity compared with free DOX [147]. In order to test the toxic side effects of exoDOX, the mice were treated at the acute toxic dose of 15 mg/kg of DOX [181], [182]. After a period of 9 days, controls and exoDOX-treated mice exhibited normal behavior and clinical appearance; however, DOX-treated mice showed lack of grooming, limited movement (hunched posture, ruffled hair coat, naso-ocular discharge) and were carefully sacrificed. As objective scale, we measured the bodyweight of mice, which is recognized a universal parameter to follow the health of the mice during the experiments. The animals treated with DOX lost more than 25% of their total bodyweight (Figure 26). The bodyweight of exoDOX-treated mice decreased by an average of 10%, indicating less toxicity. The same mice were also analyzed by histopathology (see below).

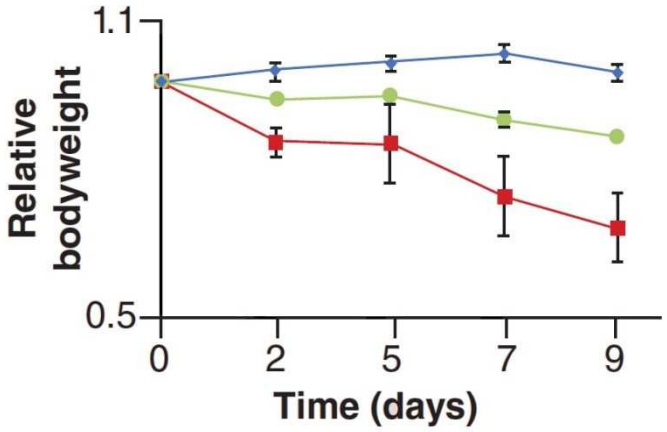

Figure 26. Doxorubicin is more toxic than exosomal doxorubicin in mice. Mice treated by intraperitoneal injection with high levels (15 mg/kg) of DOX (■), exoHCTDOX (•) and controls (♦). Bodyweight was monitored at the indicated time points for 9 days.

5.5.2. HISTOPATHOLOGY AND BIODISTRIBUTION ANALYSES

We hypothesized that the different observed toxicity was due to a distinctive biodistribution of DOX in the heart. The mice were injected with 15 mg/kg of DOX or exoDOX and after 3 h, the biodistribution of the drug was evaluated in the serum and heart. It was found that the concentration of DOX in the serum was comparable to exoDOX. This result suggested that the exoDOX preparations could diffuse in the body similar to free drug (Figure 27).

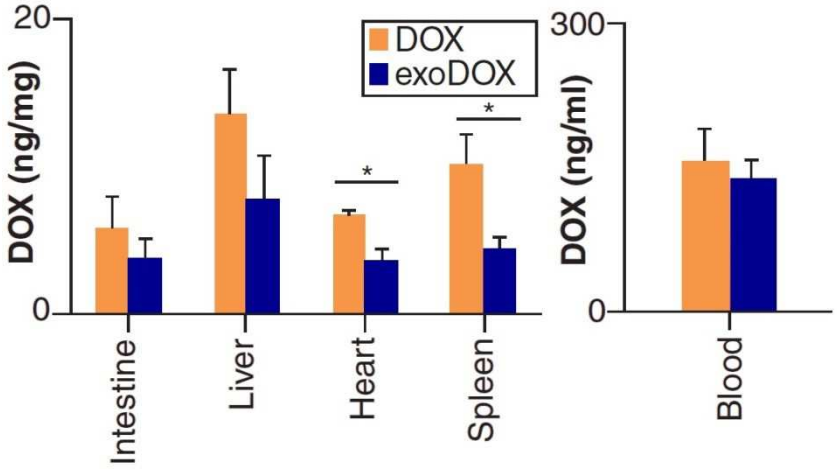

Figure 27. Mice were treated by ip. injection with high levels (15 mg/kg) of DOX and exoHCTDOX. The tissues were collected after 3 h. Although the level of DOX in the blood was equal, the heart tissue accumulated less exoDOX. * $p < 0.05$.

Differently from DOX, the accumulation of exoDOX in the heart was reduced by about 40% ($p < 0.05$). To better understand if the different biodistribution was due to an altered PK profile, DOX and exoDOX were evaluated in the serum at different time points. (Figure 28) showed that DOX and exo DOX have the same PK profile. A paper recently published showed that exosomes accumulated less in muscle and heart tissues [183]. In the heart, the myocardium is supplied by vessels with tight junctions and the well-developed lymphatic system reduced the accumulation of membrane-based nanovectors such as liposomes [184]. Since a major problem of DOX is the cardiac toxicity, our results support exoDOX as an innovative and safe system to deliver DOX in cancer patients [130].

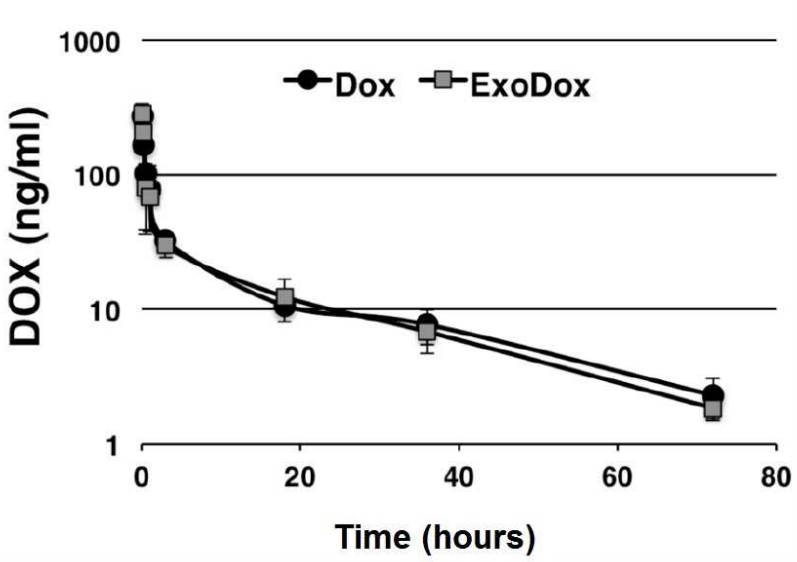

Figure 28. Mice were treated by ip. injection with high levels (15 mg/kg) of DOX and exoHCT DOX. The tissues were collected after 3 h. Although the level of DOX in the blood was equal, the heart tissue accumulated less exoDOX. * $p < 0.05$.

To support our observations, we analyzed the heart tissue by histopathology. The heart of mice treated with exoDOX or untreated appeared normal (Figure 29A & B). In accordance with the literature [185], mice treated with DOX showed vacuolization and hypereosinophilia of the cytoplasm compared with untreated mice (Figure 29C & D). Moderate disarrangement of cardiomyocytes was also evident in some sections.

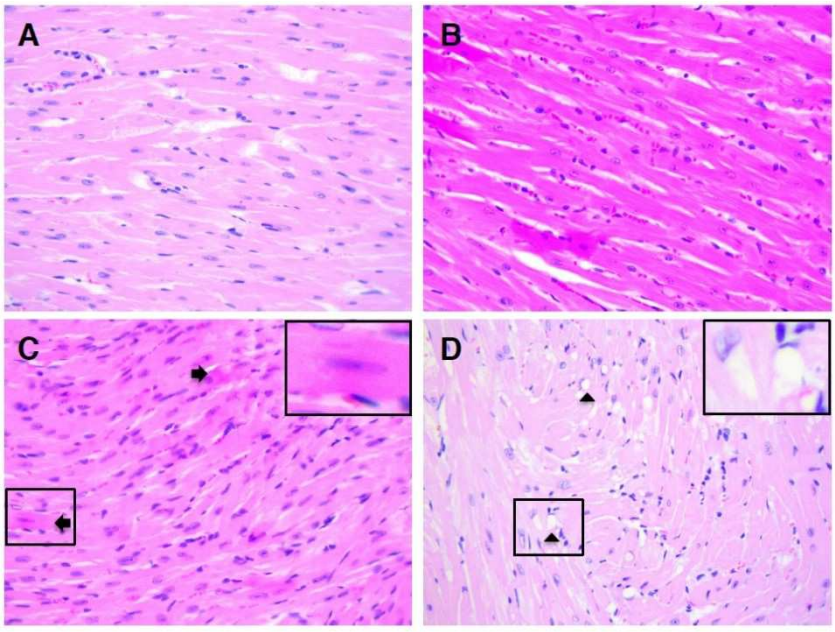

Figure 29. Exosomal doxorubicin-treated mice have normal cardiac tissue. DOX toxicity is well documented and that four mice were analyzed. In untreated (**A**) and exoDOX (**B**) treated mice, myocardial fibers showed the regular organized pattern of cytoplasmic striations with central located nuclei. The mice treated with DOX (**C & D**) exhibited scattered cytoplasmic paranuclear vacuoles (arrowheads) and focal intense eosinophilic (pink) cytoplasm, devoid of their transversal striations (arrows). The images in the boxes were enlarged (3×) in the top right corner. H&E staining, original magnification 40X.

Other tissues such as intestine, liver, kidney, spleen, lung and brain did not reveal evident or significant toxicity (Figure 30).

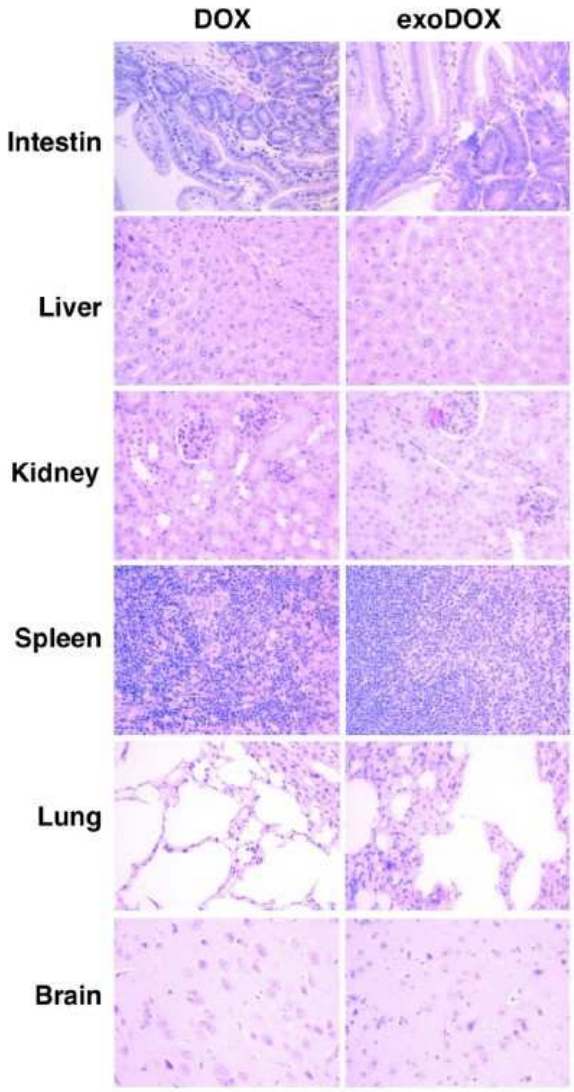

Figure 30. Histopathologic analysis of DOX and exoDOX treated mice (i.p.; 15mg/kg) after 9 days of treatment. The intestine, liver, kidney, spleen, lung and brain did not reveal evident or significant toxicity.

5.6. EXOSOMES INCREASE TOLERABILITY OF DOX IN MOUSE

Subsequently, nude mice were treated with different concentrations of exoDOX, Doxil (liposomal DOX) or free DOX as indicated in (Figure 31). The drug was injected intraperitoneally, two-times per week for a total of five injections. As objective scale of wellness, we measured the body weight of mice: up to 3 mg/kg, there was no difference between treatments and no adverse effects were observed (Figure 31A & B). At 5 and 7 mg/kg, the mice treated with DOX started to lose weight after 10 days and finally they were sacrificed. ExoDOX and Doxil-treated mice were healthy at all tested concentrations (Figure 31C & D).

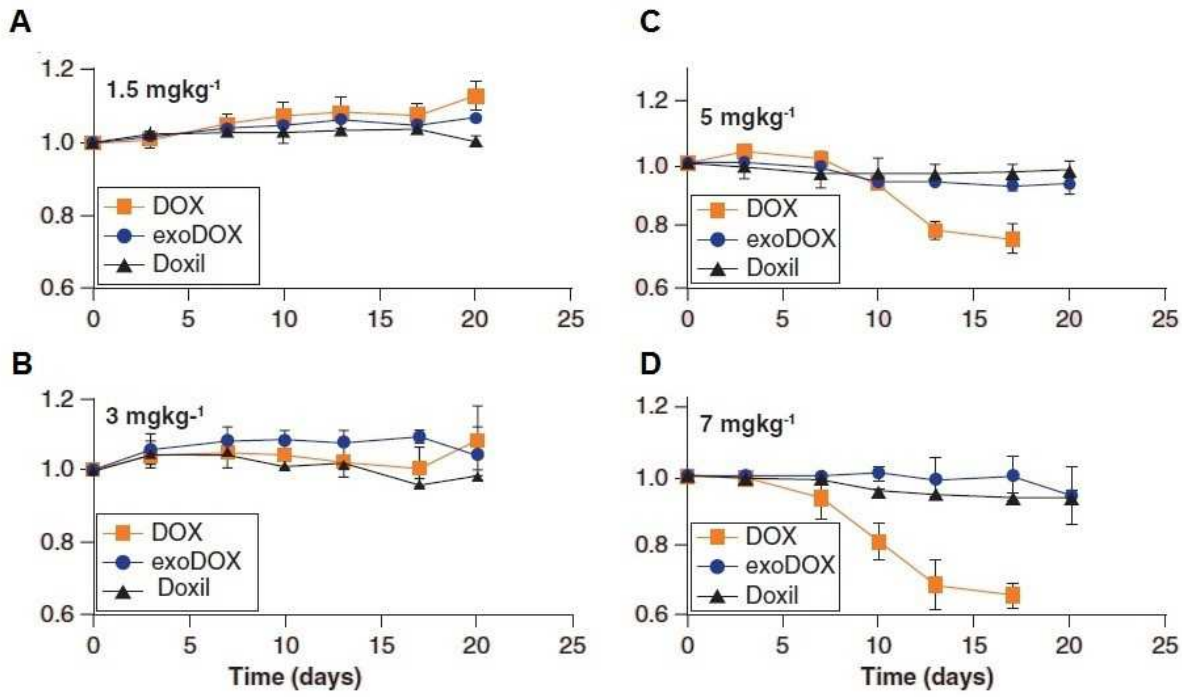

Figure 31. Maximum tolerated dose experiment in nude mice utilizing four doses of DOX, Doxil and exoDOX. (**A**) 1.5 mg/kg, (**B**) 3 mg/kg, (**C**) 5 mg/kg and (**D**) 7 mg/kg; body weight was monitored at the indicated time points for 20 days.

The tolerability of exoDOX was tested in isogenic FVB/N mice. The mice were treated with DOX and exoDOX at 3 and 6 mg/kg, two times per week for a total of five treatments (Figure 32A & B). Similarly to nude mice, at 6 mg/kg, the DOX-treated mice lost almost 20% of their body weight although the effect was less evident than in nude mice.

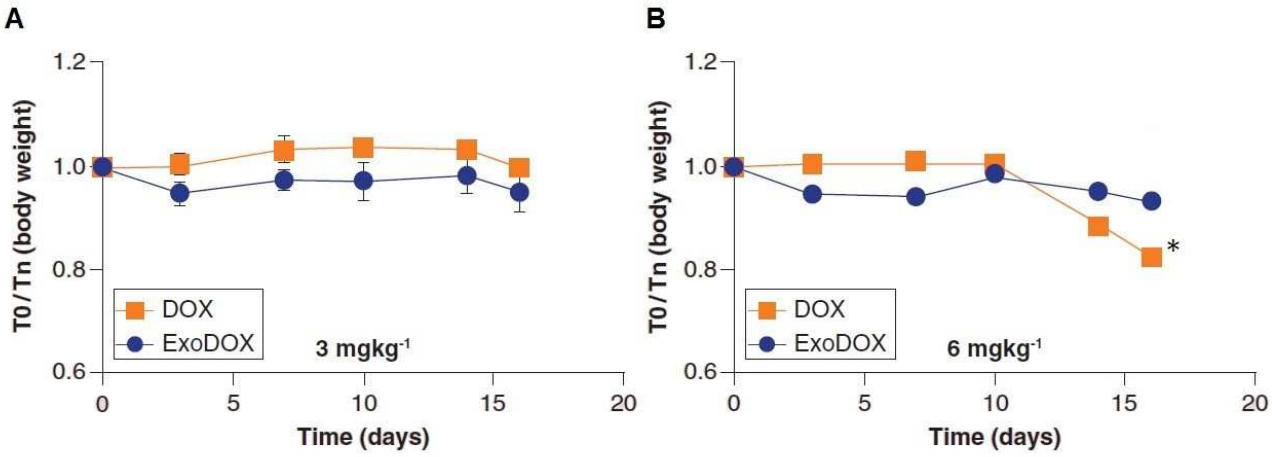

Figure 32. MTD experiment in FVB/N mice using 2 doses of DOX and exoDOX, (**A**) 3 mg/kg, (**B**) 6 mg/kg. Body weight was monitored at the indicated time points for 16 days. MTD: Maximum tolerated dose.

Histopathological analyses demonstrated that the hearts of DOX-treated mice were normal at 3 mg/kg but showed vacuoles and moderate myofibrils disorganization at 6 mg/kg (Figure 33A & B). In exoDOX-treated mice, the heart appears normal as untreated control (Figure 33C & D).

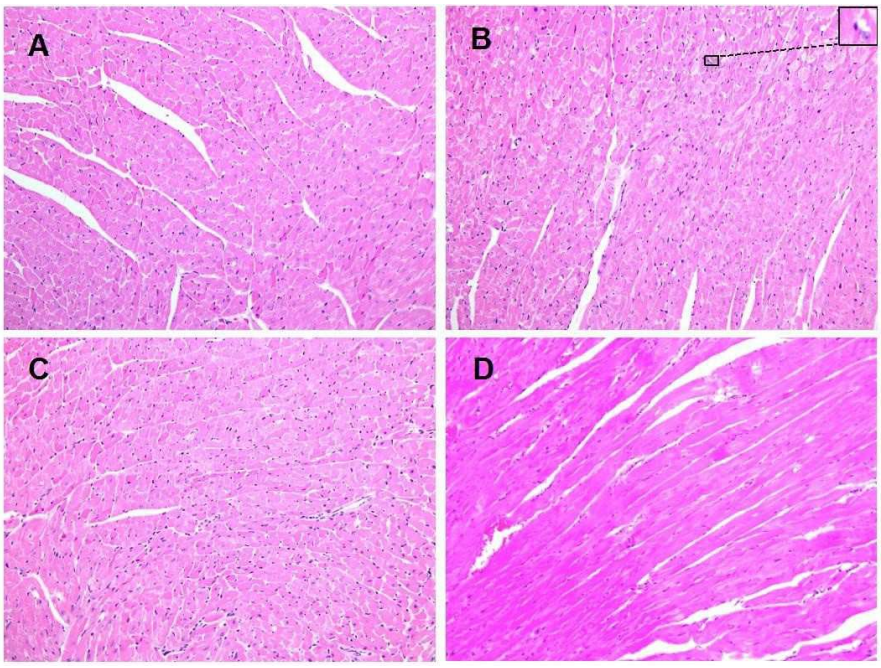

Figure 33. ExoDOX-treated mice have normal cardiac tissue after maximum tolerated dose. FVB/N mice were treated at (**A**) 3 mg/kg, (**B**) 6 mg/kg of DOX, (**C**) 6 mg/kg of exoDOX or (**D**) control. In (**B**) scattered cytoplasmic paranuclear vacuoles are zoomed in H&E staining. Original magnification, 40X. MTD: Maximum tolerated dose.

All other tissues were apparently normal (Figure 34).

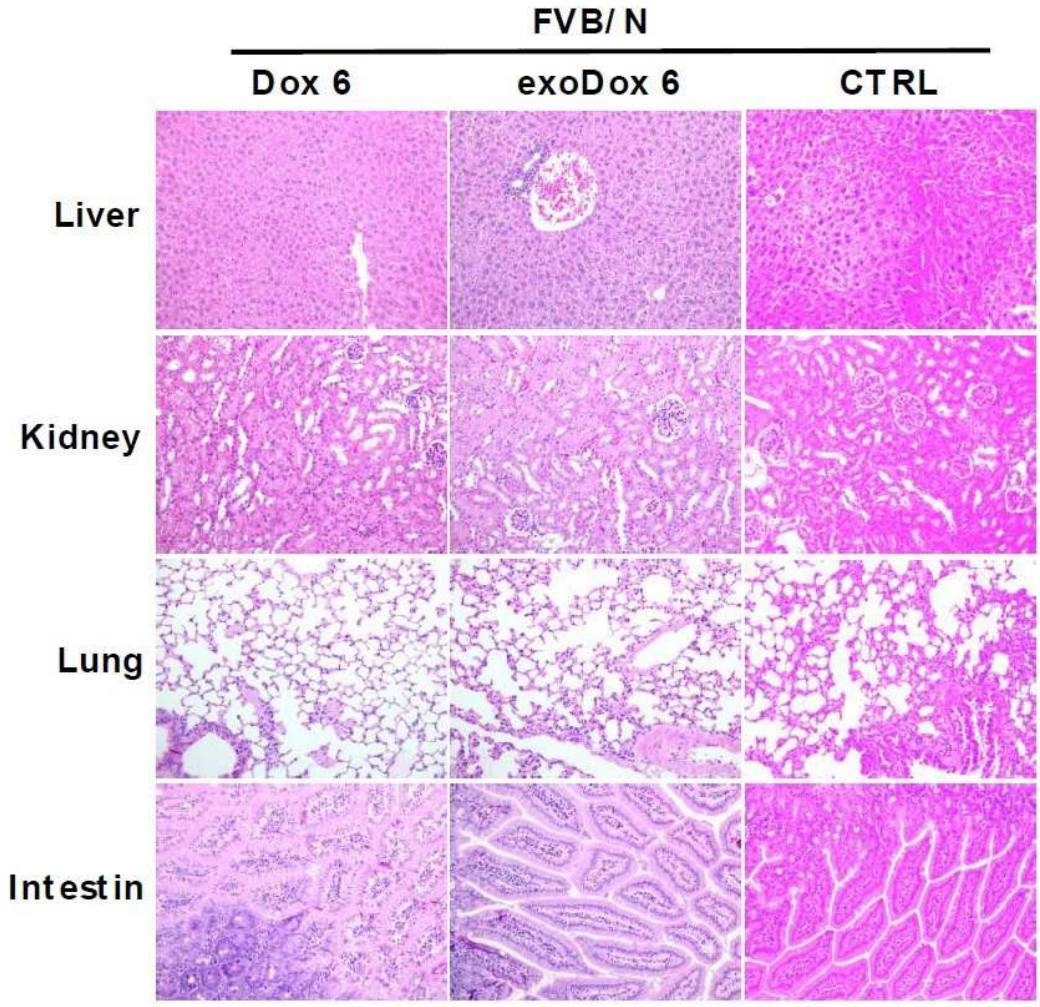

Figure 34. FVB/N mice were treated with 6 mg/kg of DOX or exoDOX and analyzed after 16 days. No obvious toxicity was observed. H&E staining, original magnification 40X.

5.7. EXOSOMES INCREASE DOX EFFICACY IN A MOUSE MODEL OF BREAST CANCER

Following the experiments of toxicity, it was decided to treat the mice with a double concentration of exoDOX compared with free DOX. MDA-MB-231 cell lines were injected subcutaneously in nude mice and when the tumors reached an average size >50 mm^3, exoDOX (6 mg/kg), Doxil (6 mg/kg) and DOX (3 mg/kg) were injected intraperitoneally two-times per week for a total of five treatments. The tumors treated with exoDOX and Doxil clearly had not grown compared with the DOX treated mice (Figure 35A). At the end of the experiment, DOX in the tumor was quantified by MS. (Figure 35B)shows that the concentration of exoDOX in the tumor had doubled compared with DOX concentration (p-value < 0.05).

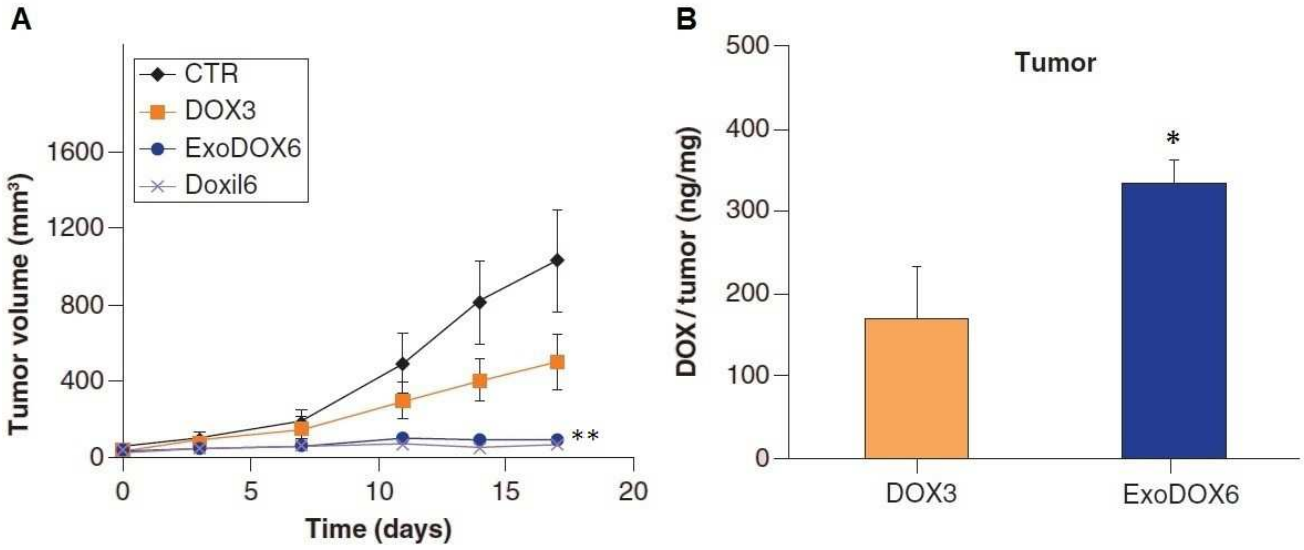

Figure 35. ExoDOX efficacy on MDA-MB-231 tumor growth. (**A**) Tumor volume in nude mice treated by ip. injection with (3 mg/kg) DOX (▭), (6 mg/kg) exoDOX (•), (6 mg/kg) Doxil (×) and controls (♦). (**B**) In the tumors (3 h), exoDOX accumulated more compared with the DOX-treated mice. Y axis: concentration of DOX per gram of tissue. *p < 0.05. ip.: Intraperitoneally.

5.8. EXOSOMES INCREASE DOX EFFICACY IN AN IMMUNOCOMPETENT MOUSE MODEL OF HIGHGRADE SEROUS OVARIAN CANCER

STOSE cell lines were inoculated subcutaneously in FVB/N mice to demonstrate the efficacy of exoDOX. After the tumor reached a size >50 mm^3, mice were treated with 3 mg/kg of DOX and 3 or 6 mg/kg of exoDOX (Figure 36A). At higher concentration, the exoDOX was more effective than free DOX, similar to MDA-MB-231 breast cancer model. Tumors analysis showed that at 6 mg/kg, exoDOX accumulated about two-times more than free DOX (Figure 36B; p-value <0.05).

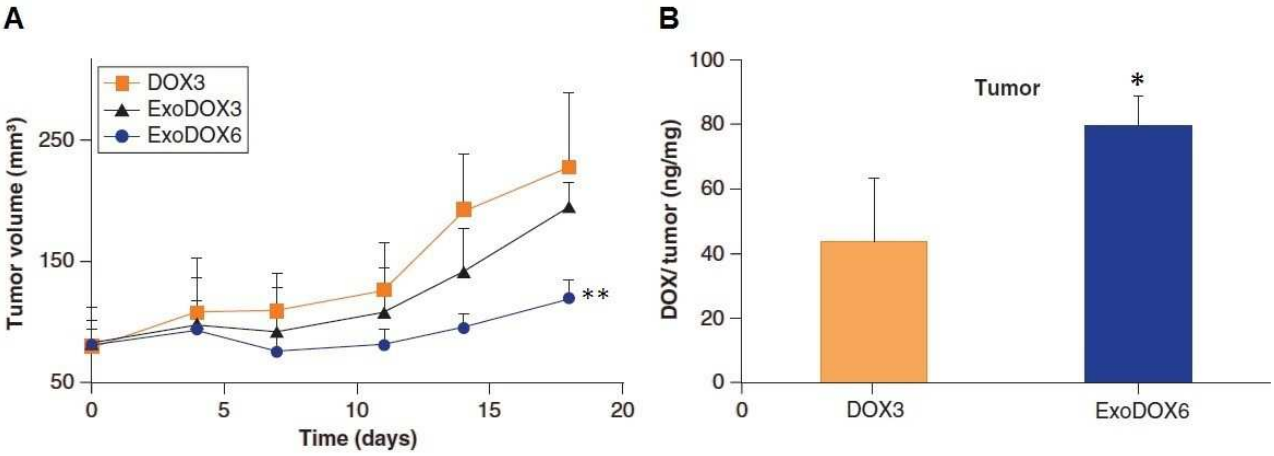

Figure 36. ExoDOX efficacy on STOSE tumor growth. (**A**) Tumor volume in FVB/N mice treated by ip. injection with (3 mg/kg) (□) of DOX, (3 mg/kg) (△) of exoDOX and (•) (6 mg/kg) of exoDOX. (**B**) In the tumors (3 h), exoDOX accumulated more compared with the DOX-treated mice. Y axis: concentration of DOX per gram of tissue. *p < 0.05. ip.: Intraperitoneally.

6. CONCLUSIONS

The success of newly formulated drugs such as Doxil is primarily due to the reduced toxicity more than an increase in its efficacy. Specifically for DOX, the cardiac toxicity is a limiting factor during therapy. A different biodistribution of liposomal DOX limits the cardiac toxicity compared with DOX [147]. In this thesis, we tested the hypothesis that DOX encapsulated in exosomes has a different therapeutic activity compared with free DOX. Although tumor exosomes loaded with DOX could decrease the growth of cancer cells *in vitro* and *in vivo*, the efficacy was similar to free DOX. This result is supported by data from other publications in which exosomes were modified to perform active targeting [126]. In addition, we tested if exoDOX is less toxic than free DOX. The results were evident by visual inspection of the mice tissues. After 9 days of treatment, the DOX-treated mice lacked grooming, had hunched posture and lost significant body weight. The exoDOX-treated mice appeared healthy and the histopathologic analysis confirmed that the cardiac tissue in exoDOX-treated mice was normal. Biodistribution analyses showed a similar quantity of DOX and exoDOX in the serum but a reduced accumulation in the heart of exoDOX-treated mice compared with DOX.

Additionally, in this thesis we demonstrate the utility of exosomes to deliver DOX in highly devastating female cancers. We carried out *in vitro* and *in vivo* experiments to provide conclusive evidences, which revealed that: similar to liposomes, myocardial endothelial cells limit exoDOX crossing, avoiding accumulation of drug in the heart. The kinetics of myocardial endothelial extravasation are slower in exoDOX compared with DOX; the maximum tolerated dose in immunodeficient and immunocompetent mice of exoDOX is higher than in free drug, thus limiting the cardiac toxicity without affecting other organs; concluding that exosomes increase the therapeutic index of DOX in breast and ovarian cancer mouse models (Figure 37).

Taken together, the results of this thesis suggest that exosomes could be used to reduce the toxicity of DOX by altering the biodistribution. It could be of interest, to test other chemotherapeutic drugs to understand if exosomes are a valid drug delivery system for broad application. In this concept, many investigators are focusing on the use of Paclitaxel encapsulation in exosomes for better delivery and efficacy [128], [186], [187].

Finally, it should be known that clinical trials have demonstrated that exosomes are a biocompatible material that could be safely used in humans. Phase I studies showed no severe adverse effects and set up new clinical grade protocols for the preparation of exosomes [133], [188]. Based on literature and our data during this thesis, we can envisage an easy application of exosomes as drug delivery system in humans especially for lethal diseases such as cancer.

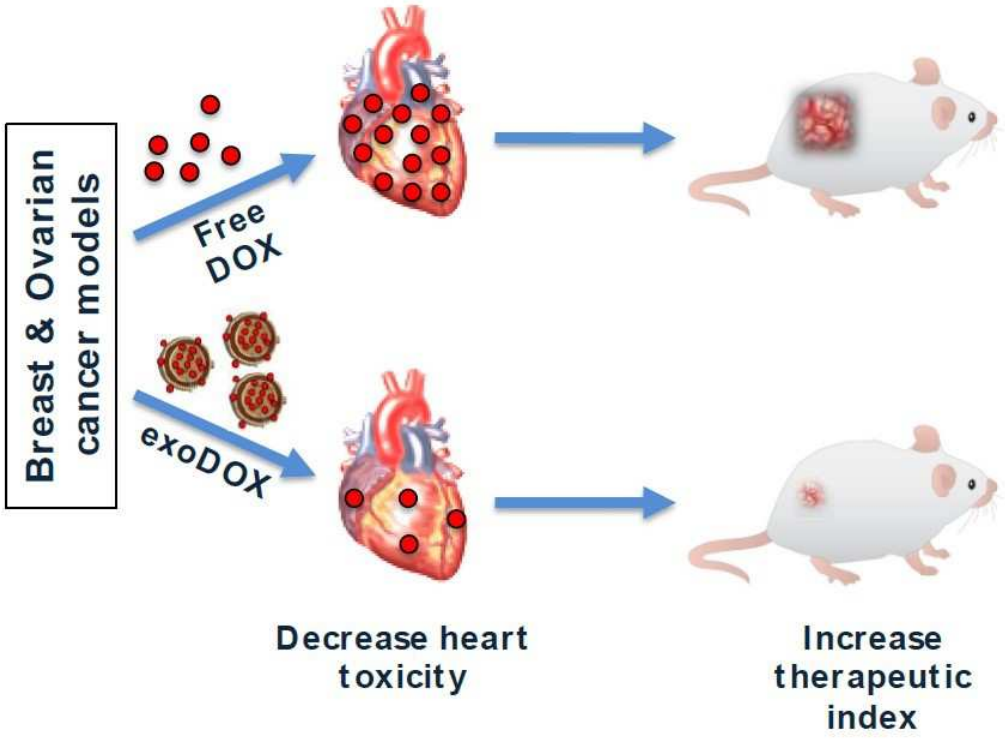

Figure 37. Working model on the benefit of exosomes as drug delivery system for doxorubicin.

7. BIBLIOGRAPHY

[1] Y. Barenholz, "Doxil®--the first FDA-approved nano-drug: lessons learned.," *J. Control. Release*, vol. 160, no. 2, pp. 117–34, Jun. 2012.

[2] J.-W. Yoo, D. J. Irvine, D. E. Discher, and S. Mitragotri, "Bio-inspired, bioengineered and biomimetic drug delivery carriers.," *Nat. Rev. Drug Discov.*, vol. 10, no. 7, pp. 521–35, Jul. 2011.

[3] M. E. Marcus and J. N. Leonard, "FedExosomes: Engineering Therapeutic Biological Nanoparticles that Truly Deliver.," *Pharmaceuticals (Basel).*, vol. 6, no. 5, pp. 659–80, 2013.

[4] G. Toffoli, M. Hadla, G. Corona, I. Caligiuri, S. Palazzolo, S. Semeraro, A. Gamini, V. Canzonieri, and F. Rizzolio, "Exosomal doxorubicin reduces the cardiac toxicity of doxorubicin.," *Nanomedicine (Lond).*, vol. 10, pp. 2963–2971, 2015.

[5] M. Hadla, S. Palazzolo, G. Corona, I. Caligiuri, V. Canzonieri, G. Toffoli, and F. Rizzolio, "Exosomes increase the therapeutic index of doxorubicin in breast and ovarian cancer mouse models.," *Nanomedicine (Lond).*, vol. 11, no. 18, pp. 2431–41, Sep. 2016.

[6] G. Birrenbach and P. P. Speiser, "Polymerized micelles and their use as adjuvants in immunology.," *J. Pharm. Sci.*, vol. 65, no. 12, pp. 1763–6, Dec. 1976.

[7] J. Kreuter, "Nanoparticles and nanocapsules--new dosage forms in the nanometer size range.," *Pharm. Acta Helv.*, vol. 53, no. 2, pp. 33–9, 1978.

[8] U. Scheffel, B. A. Rhodes, T. K. Natarajan, and H. N. Wagner, "Albumin microspheres for study of the reticuloendothelial system.," *J. Nucl. Med.*, vol. 13, no. 7, pp. 498–503, Jul. 1972.

[9] K. Sugibayashi, Y. Morimoto, T. Nadai, and Y. Kato, "Drug-carrier property of albumin microspheres in chemotherapy. I. Tissue distribution of microsphere-entrapped 5-fluorouracil in mice.," *Chem. Pharm. Bull. (Tokyo).*, vol. 25, no. 12, pp. 3433–4, Dec. 1977.

[10] A. D. Bangham, M. M. Standish, and J. C. Watkins, "Diffusion of univalent ions across the lamellae of swollen phospholipids.," *J. Mol. Biol.*, vol. 13, no. 1, pp. 238–52, Aug. 1965.

[11] G. Gregoriadis and B. E. Ryman, "Liposomes as carriers of enzymes or drugs: a

new approach to the treatment of storage diseases.," *Biochem. J.*, vol. 124, no. 5, p. 58P, Oct. 1971.

[12] "Contents pages," *Trans. Faraday Soc.*, vol. 9, p. P001, 1913.

[13] Z. Tuzar and P. Kratochvíl, "Block and graft copolymer micelles in solution," *Adv. Colloid Interface Sci.*, vol. 6, no. 3, pp. 201–232, Oct. 1976.

[14] H. Bader, H. Ringsdorf, and B. Schmidt, "No Title," *Angew. Makromol. Chemie*, vol. 123, no. 1, pp. 457–485, Aug. 1984.

[15] A. V Kabanov, V. P. Chekhonin, Alakhov VYu, E. V Batrakova, A. S. Lebedev, N. S. Melik-Nubarov, S. A. Arzhakov, A. V Levashov, G. V Morozov, and E. S. Severin, "The neuroleptic activity of haloperidol increases after its solubilization in surfactant micelles. Micelles as microcontainers for drug targeting.," *FEBS Lett.*, vol. 258, no. 2, pp. 343–5, Dec. 1989.

[16] M. Yokoyama, T. Okano, Y. Sakurai, H. Ekimoto, C. Shibazaki, and K. Kataoka, "Toxicity and antitumor activity against solid tumors of micelle-forming polymeric anticancer drug and its extremely long circulation in blood.," *Cancer Res.*, vol. 51, no. 12, pp. 3229–36, Jun. 1991.

[17] P. J. Flory, "Molecular Size Distribution in Three Dimensional Polymers. I. Gelation 1," *J. Am. Chem. Soc.*, vol. 63, no. 11, pp. 3083–3090, Nov. 1941.

[18] E. BUHLEIER, W. WEHNER, and F. VÖGTLE, "'Cascade'- and 'Nonskid-Chain-like' Syntheses of Molecular Cavity Topologies," *Synthesis (Stuttg).*, vol. 1978, no. 2, pp. 155–158, 1978.

[19] D. A. Tomalia, H. Baker, J. Dewald, M. Hall, G. Kallos, S. Martin, J. Roeck, J. Ryder, and P. Smith, "A New Class of Polymers: Starburst-Dendritic Macromolecules," *Polym. J.*, vol. 17, no. 1, pp. 117–132, Jan. 1985.

[20] R. B. Kolhatkar, P. Swaan, and H. Ghandehari, "Potential oral delivery of 7-ethyl-10-hydroxy-camptothecin (SN-38) using poly(amidoamine) dendrimers.," *Pharm. Res.*, vol. 25, no. 7, pp. 1723–9, Jul. 2008.

[21] M. Najlah, S. Freeman, D. Attwood, and A. D'Emanuele, "In vitro evaluation of dendrimer prodrugs for oral drug delivery.," *Int. J. Pharm.*, vol. 336, no. 1, pp. 183–90, May 2007.

[22] D. A. Tomalia, "Starburst/Cascade Dendrimers: Fundamental building blocks for a new nanoscopic chemistry set," *Adv. Mater.*, vol. 6, no. 7–8, pp. 529–539, Jul. 1994.

[23] P. W. K. Rothemund, “Folding DNA to create nanoscale shapes and patterns.,” *Nature*, vol. 440, no. 7082, pp. 297–302, Mar. 2006.

[24] N. C. Seeman, “Nucleic acid junctions and lattices.,” *J. Theor. Biol.*, vol. 99, no. 2, pp. 237–47, Nov. 1982.

[25] T. J. Fu and N. C. Seeman, “DNA double-crossover molecules.,” *Biochemistry*, vol. 32, no. 13, pp. 3211–20, Apr. 1993.

[26] T. J. Webster, “Nanomedicine: what’s in a definition?,” *Int. J. Nanomedicine*, vol. 1, no. 2, pp. 115–6, 2006.

[27] V. Wagner, A. Dullaart, A.-K. Bock, and A. Zweck, “The emerging nanomedicine landscape.,” *Nat. Biotechnol.*, vol. 24, no. 10, pp. 1211–7, Oct. 2006.

[28] D. J. Bharali, M. Khalil, M. Gurbuz, T. M. Simone, and S. A. Mousa, “Nanoparticles and cancer therapy: a concise review with emphasis on dendrimers.,” *Int. J. Nanomedicine*, vol. 4, pp. 1–7, 2009.

[29] S. Svenson, “Clinical translation of nanomedicines,” *Curr. Opin. Solid State Mater. Sci.*, vol. 16, no. 6, pp. 287–294, Dec. 2012.

[30] C. Dianzani, G. P. Zara, G. Maina, P. Pettazzoni, S. Pizzimenti, F. Rossi, C. L. Gigliotti, E. S. Ciamporcero, M. Daga, and G. Barrera, “Drug delivery nanoparticles in skin cancers.,” *Biomed Res. Int.*, vol. 2014, p. 895986, 2014.

[31] K. Greish, “Enhanced permeability and retention (EPR) effect for anticancer nanomedicine drug targeting.,” *Methods Mol. Biol.*, vol. 624, pp. 25–37, 2010.

[32] R. Duncan and R. Gaspar, “Nanomedicine(s) under the microscope.,” *Mol. Pharm.*, vol. 8, no. 6, pp. 2101–41, Dec. 2011.

[33] Y. Li, J. Wang, M. G. Wientjes, and J. L.-S. Au, “Delivery of nanomedicines to extracellular and intracellular compartments of a solid tumor.,” *Adv. Drug Deliv. Rev.*, vol. 64, no. 1, pp. 29–39, Jan. 2012.

[34] L. Brannon-Peppas and J. O. Blanchette, “Nanoparticle and targeted systems for cancer therapy.,” *Adv. Drug Deliv. Rev.*, vol. 56, no. 11, pp. 1649–59, Sep. 2004.

[35] M. Ferrari, “Frontiers in cancer nanomedicine: directing mass transport through biological barriers.,” *Trends Biotechnol.*, vol. 28, no. 4, pp. 181–8, Apr. 2010.

[36] E. Tasciotti, X. Liu, R. Bhavane, K. Plant, A. D. Leonard, B. K. Price, M. M.-C. Cheng, P. Decuzzi, J. M. Tour, F. Robertson, and M. Ferrari, “Mesoporous silicon

particles as a multistage delivery system for imaging and therapeutic applications," *Nat. Nanotechnol.*, vol. 3, no. 3, pp. 151–157, Mar. 2008.

[37] T. Tanaka, P. Decuzzi, M. Cristofanilli, J. H. Sakamoto, E. Tasciotti, F. M. Robertson, and M. Ferrari, "Nanotechnology for breast cancer therapy.," *Biomed. Microdevices*, vol. 11, no. 1, pp. 49–63, Feb. 2009.

[38] M. L. Etheridge, S. A. Campbell, A. G. Erdman, C. L. Haynes, S. M. Wolf, and J. McCullough, "The big picture on nanomedicine: the state of investigational and approved nanomedicine products.," *Nanomedicine*, vol. 9, no. 1, pp. 1–14, Jan. 2013.

[39] M. Hay, D. W. Thomas, J. L. Craighead, C. Economides, and J. Rosenthal, "Clinical development success rates for investigational drugs.," *Nat. Biotechnol.*, vol. 32, no. 1, pp. 40–51, Jan. 2014.

[40] I. Brook, "Approval of zidovudine (AZT) for acquired immunodeficiency syndrome. A challenge to the medical and pharmaceutical communities.," *JAMA*, vol. 258, no. 11, p. 1517, Sep. 1987.

[41] T. M. Allen, W. W. K. Cheng, J. I. Hare, and K. M. Laginha, "Pharmacokinetics and pharmacodynamics of lipidic nano-particles in cancer.," *Anticancer. Agents Med. Chem.*, vol. 6, no. 6, pp. 513–23, Nov. 2006.

[42] V. Kumar, S. Bayda, M. Hadla, I. Caligiuri, C. Russo Spena, S. Palazzolo, S. Kempter, G. Corona, G. Toffoli, and F. Rizzolio, "Enhanced Chemotherapeutic Behavior of Open-Caged DNA@Doxorubicin Nanostructures for Cancer Cells.," *J. Cell. Physiol.*, vol. 231, no. 1, pp. 106–10, Jan. 2016.

[43] Y. Min, J. M. Caster, M. J. Eblan, and A. Z. Wang, "Clinical Translation of Nanomedicine.," *Chem. Rev.*, vol. 115, no. 19, pp. 11147–90, Oct. 2015.

[44] K. Chatterjee, J. Zhang, N. Honbo, and J. S. Karliner, "Doxorubicin cardiomyopathy.," *Cardiology*, vol. 115, no. 2, pp. 155–62, 2010.

[45] A. Gabizon, R. Catane, B. Uziely, B. Kaufman, T. Safra, R. Cohen, F. Martin, A. Huang, and Y. Barenholz, "Prolonged circulation time and enhanced accumulation in malignant exudates of doxorubicin encapsulated in polyethylene-glycol coated liposomes.," *Cancer Res.*, vol. 54, no. 4, pp. 987–92, Feb. 1994.

[46] S. Wang, W. Fan, G. Kim, H. J. Hah, Y.-E. K. Lee, R. Kopelman, M. Ethirajan, A. Gupta, L. N. Goswami, P. Pera, J. Morgan, and R. K. Pandey, "Novel methods to

incorporate photosensitizers into nanocarriers for cancer treatment by photodynamic therapy," *Lasers Surg. Med.*, vol. 43, no. 7, pp. 686–695, Sep. 2011.

[47] A. O. Elzoghby, W. M. Samy, and N. A. Elgindy, "Albumin-based nanoparticles as potential controlled release drug delivery systems.," *J. Control. Release*, vol. 157, no. 2, pp. 168–82, Jan. 2012.

[48] K. Y. Choi, H. Chung, K. H. Min, H. Y. Yoon, K. Kim, J. H. Park, I. C. Kwon, and S. Y. Jeong, "Self-assembled hyaluronic acid nanoparticles for active tumor targeting.," *Biomaterials*, vol. 31, no. 1, pp. 106–14, Jan. 2010.

[49] S. A. Agnihotri, N. N. Mallikarjuna, and T. M. Aminabhavi, "Recent advances on chitosan-based micro- and nanoparticles in drug delivery.," *J. Control. Release*, vol. 100, no. 1, pp. 5–28, Nov. 2004.

[50] J. Panyam and V. Labhasetwar, "Biodegradable nanoparticles for drug and gene delivery to cells and tissue.," *Adv. Drug Deliv. Rev.*, vol. 55, no. 3, pp. 329–47, Feb. 2003.

[51] C. Vauthier and K. Bouchemal, "Methods for the preparation and manufacture of polymeric nanoparticles.," *Pharm. Res.*, vol. 26, no. 5, pp. 1025–58, May 2009.

[52] R. A. Jain, "The manufacturing techniques of various drug loaded biodegradable poly(lactide-co-glycolide) (PLGA) devices.," *Biomaterials*, vol. 21, no. 23, pp. 2475–90, Dec. 2000.

[53] A. Kumari, S. K. Yadav, and S. C. Yadav, "Biodegradable polymeric nanoparticles based drug delivery systems.," *Colloids Surf. B. Biointerfaces*, vol. 75, no. 1, pp. 1–18, Jan. 2010.

[54] E. Allémann, J. C. Leroux, R. Gurny, and E. Doelker, "In vitro extended-release properties of drug-loaded poly(DL-lactic acid) nanoparticles produced by a salting-out procedure.," *Pharm. Res.*, vol. 10, no. 12, pp. 1732–7, Dec. 1993.

[55] L. S. Nair and C. T. Laurencin, "Biodegradable polymers as biomaterials," *Prog. Polym. Sci.*, vol. 32, no. 8–9, pp. 762–798, Aug. 2007.

[56] M. Fasano, S. Curry, E. Terreno, M. Galliano, G. Fanali, P. Narciso, S. Notari, and P. Ascenzi, "The extraordinary ligand binding properties of human serum albumin.," *IUBMB Life*, vol. 57, no. 12, pp. 787–96, Dec. 2005.

[57] J. Gong, M. Huo, J. Zhou, Y. Zhang, X. Peng, D. Yu, H. Zhang, and J. Li, "Synthesis,

characterization, drug-loading capacity and safety of novel octyl modified serum albumin micelles.," *Int. J. Pharm.*, vol. 376, no. 1–2, pp. 161–8, Jul. 2009.

[58] P. K. Ghosh, "Hydrophilic polymeric nanoparticles as drug carriers," *IJBB Vol.37(5) [October 2000]*, 2000.

[59] N. Kamaly, Z. Xiao, P. M. Valencia, A. F. Radovic-Moreno, and O. C. Farokhzad, "Targeted polymeric therapeutic nanoparticles: design, development and clinical translation.," *Chem. Soc. Rev.*, vol. 41, no. 7, pp. 2971–3010, Apr. 2012.

[60] M. C. Wani, H. L. Taylor, M. E. Wall, P. Coggon, and A. T. McPhail, "Plant antitumor agents. VI. Isolation and structure of taxol, a novel antileukemic and antitumor agent from Taxus brevifolia," *J. Am. Chem. Soc.*, vol. 93, no. 9, pp. 2325–2327, May 1971.

[61] E. K. Rowinsky and R. C. Donehower, "Paclitaxel (taxol)," *N. Engl. J. Med.*, vol. 332, no. 15, pp. 1004–14, Apr. 1995.

[62] H. Gelderblom, J. Verweij, K. Nooter, and A. Sparreboom, "Cremophor EL: the drawbacks and advantages of vehicle selection for drug formulation.," *Eur. J. Cancer*, vol. 37, no. 13, pp. 1590–8, Sep. 2001.

[63] K. Paál, J. Müller, and L. Hegedûs, "High affinity binding of paclitaxel to human serum albumin.," *Eur. J. Biochem.*, vol. 268, no. 7, pp. 2187–91, Apr. 2001.

[64] M. J. Hawkins, P. Soon-Shiong, and N. Desai, "Protein nanoparticles as drug carriers in clinical medicine.," *Adv. Drug Deliv. Rev.*, vol. 60, no. 8, pp. 876–85, May 2008.

[65] M. Purcell, J. F. Neault, and H. A. Tajmir-Riahi, "Interaction of taxol with human serum albumin," *Biochim. Biophys. Acta - Protein Struct. Mol. Enzymol.*, vol. 1478, no. 1, pp. 61–68, Mar. 2000.

[66] T. A. John, S. M. Vogel, C. Tiruppathi, A. B. Malik, and R. D. Minshall, "Quantitative analysis of albumin uptake and transport in the rat microvessel endothelial monolayer.," *Am. J. Physiol. Lung Cell. Mol. Physiol.*, vol. 284, no. 1, pp. L187-96, Jan. 2003.

[67] N. Desai, V. Trieu, Z. Yao, L. Louie, S. Ci, A. Yang, C. Tao, T. De, B. Beals, D. Dykes, P. Noker, R. Yao, E. Labao, M. Hawkins, and P. Soon-Shiong, "Increased antitumor activity, intratumor paclitaxel concentrations, and endothelial cell transport of cremophor-free, albumin-bound paclitaxel, ABI-007, compared with cremophor-based paclitaxel.," *Clin. Cancer Res.*, vol. 12, no. 4, pp. 1317–

24, Feb. 2006.

[68] N. K. Ibrahim, N. Desai, S. Legha, P. Soon-Shiong, R. L. Theriault, E. Rivera, B. Esmaeli, S. E. Ring, A. Bedikian, G. N. Hortobagyi, and J. A. Ellerhorst, "Phase I and pharmacokinetic study of ABI-007, a Cremophor-free, protein-stabilized, nanoparticle formulation of paclitaxel.," *Clin. Cancer Res.*, vol. 8, no. 5, pp. 1038–44, May 2002.

[69] N. K. Ibrahim, B. Samuels, R. Page, D. Doval, K. M. Patel, S. C. Rao, M. K. Nair, P. Bhar, N. Desai, and G. N. Hortobagyi, "Multicenter phase II trial of ABI-007, an albumin-bound paclitaxel, in women with metastatic breast cancer.," *J. Clin. Oncol.*, vol. 23, no. 25, pp. 6019–26, Sep. 2005.

[70] W. J. Gradishar, S. Tjulandin, N. Davidson, H. Shaw, N. Desai, P. Bhar, M. Hawkins, and J. O'Shaughnessy, "Phase III trial of nanoparticle albumin-bound paclitaxel compared with polyethylated castor oil-based paclitaxel in women with breast cancer.," *J. Clin. Oncol.*, vol. 23, no. 31, pp. 7794–803, Nov. 2005.

[71] M. R. Green, G. M. Manikhas, S. Orlov, B. Afanasyev, A. M. Makhson, P. Bhar, and M. J. Hawkins, "Abraxane, a novel Cremophor-free, albumin-bound particle form of paclitaxel for the treatment of advanced non-small-cell lung cancer.," *Ann. Oncol.*, vol. 17, no. 8, pp. 1263–8, Aug. 2006.

[72] D. D. Von Hoff, R. K. Ramanathan, M. J. Borad, D. A. Laheru, L. S. Smith, T. E. Wood, R. L. Korn, N. Desai, V. Trieu, J. L. Iglesias, H. Zhang, P. Soon-Shiong, T. Shi, N. V Rajeshkumar, A. Maitra, and M. Hidalgo, "Gemcitabine plus nab-paclitaxel is an active regimen in patients with advanced pancreatic cancer: a phase I/II trial.," *J. Clin. Oncol.*, vol. 29, no. 34, pp. 4548–54, Dec. 2011.

[73] M. J. Moore, D. Goldstein, J. Hamm, A. Figer, J. R. Hecht, S. Gallinger, H. J. Au, P. Murawa, D. Walde, R. A. Wolff, D. Campos, R. Lim, K. Ding, G. Clark, T. Voskoglou-Nomikos, M. Ptasynski, W. Parulekar, and National Cancer Institute of Canada Clinical Trials Group, "Erlotinib plus gemcitabine compared with gemcitabine alone in patients with advanced pancreatic cancer: a phase III trial of the National Cancer Institute of Canada Clinical Trials Group.," *J. Clin. Oncol.*, vol. 25, no. 15, pp. 1960–6, May 2007.

[74] V. Heinemann, S. Boeck, A. Hinke, R. Labianca, and C. Louvet, "Meta-analysis of randomized trials: evaluation of benefit from gemcitabine-based combination chemotherapy applied in advanced pancreatic cancer.," *BMC Cancer*, vol. 8, p.

82, 2008.

[75] C. Louvet, R. Labianca, P. Hammel, G. Lledo, M. G. Zampino, T. André, A. Zaniboni, M. Ducreux, E. Aitini, J. Taïeb, R. Faroux, C. Lepere, A. de Gramont, GERCOR, and GISCAD, "Gemcitabine in combination with oxaliplatin compared with gemcitabine alone in locally advanced or metastatic pancreatic cancer: results of a GERCOR and GISCAD phase III trial.," *J. Clin. Oncol.*, vol. 23, no. 15, pp. 3509–16, May 2005.

[76] V. Heinemann, D. Quietzsch, F. Gieseler, M. Gonnermann, H. Schönekäs, A. Rost, H. Neuhaus, C. Haag, M. Clemens, B. Heinrich, U. Vehling-Kaiser, M. Fuchs, D. Fleckenstein, W. Gesierich, D. Uthgenannt, H. Einsele, A. Holstege, A. Hinke, A. Schalhorn, and R. Wilkowski, "Randomized phase III trial of gemcitabine plus cisplatin compared with gemcitabine alone in advanced pancreatic cancer.," *J. Clin. Oncol.*, vol. 24, no. 24, pp. 3946–52, Aug. 2006.

[77] G. Colucci, F. Giuliani, V. Gebbia, M. Biglietto, P. Rabitti, G. Uomo, S. Cigolari, A. Testa, E. Maiello, and M. Lopez, "Gemcitabine alone or with cisplatin for the treatment of patients with locally advanced and/or metastatic pancreatic carcinoma: a prospective, randomized phase III study of the Gruppo Oncologia dell'Italia Meridionale.," *Cancer*, vol. 94, no. 4, pp. 902–10, Feb. 2002.

[78] S. M. Moghimi, "Recent developments in polymeric nanoparticle engineering and their applications in experimental and clinical oncology.," *Anticancer. Agents Med. Chem.*, vol. 6, no. 6, pp. 553–561, Nov. 2006.

[79] R. Srikar, A. Upendran, and R. Kannan, "Polymeric nanoparticles for molecular imaging.," *Wiley Interdiscip. Rev. Nanomed. Nanobiotechnol.*, vol. 6, no. 3, pp. 245–67.

[80] J. L. Boyer, "Bile formation and secretion.," *Compr. Physiol.*, vol. 3, no. 3, pp. 1035–78, Jul. 2013.

[81] J. Iqbal and M. M. Hussain, "Intestinal lipid absorption.," *Am. J. Physiol. Endocrinol. Metab.*, vol. 296, no. 6, pp. E1183-94, Jun. 2009.

[82] X. Chen, Y. An, D. Zhao, Z. He, Y. Zhang, J. Cheng, and L. Shi, "Core-shell-corona au-micelle composites with a tunable smart hybrid shell.," *Langmuir*, vol. 24, no. 15, pp. 8198–204, Aug. 2008.

[83] M. L. Adams, A. Lavasanifar, and G. S. Kwon, "Amphiphilic block copolymers for drug delivery," *J. Pharm. Sci.*, vol. 92, no. 7, pp. 1343–1355, Jul. 2003.

[84] A. Rösler, G. W. Vandermeulen, and H. A. Klok, “Advanced drug delivery devices via self-assembly of amphiphilic block copolymers.,” *Adv. Drug Deliv. Rev.*, vol. 53, no. 1, pp. 95–108, Dec. 2001.

[85] M. Ishiguro and L. K. Koopal, “Surfactant adsorption to soil components and soils.,” *Adv. Colloid Interface Sci.*, vol. 231, pp. 59–102, May 2016.

[86] F. M. Veronese, O. Schiavon, G. Pasut, R. Mendichi, L. Andersson, A. Tsirk, J. Ford, G. Wu, S. Kneller, J. Davies, and R. Duncan, “PEG-doxorubicin conjugates: influence of polymer structure on drug release, in vitro cytotoxicity, biodistribution, and antitumor activity.,” *Bioconjug. Chem.*, vol. 16, no. 4, pp. 775–84.

[87] A. Lalatsa, A. G. Schätzlein, M. Mazza, T. B. H. Le, and I. F. Uchegbu, “Amphiphilic poly(L-amino acids) - new materials for drug delivery.,” *J. Control. Release*, vol. 161, no. 2, pp. 523–36, Jul. 2012.

[88] S. Acharya and S. K. Sahoo, “PLGA nanoparticles containing various anticancer agents and tumour delivery by EPR effect.,” *Adv. Drug Deliv. Rev.*, vol. 63, no. 3, pp. 170–83, Mar. 2011.

[89] E.-K. Lim, Y.-M. Huh, J. Yang, K. Lee, J.-S. Suh, and S. Haam, “pH-triggered drug-releasing magnetic nanoparticles for cancer therapy guided by molecular imaging by MRI.,” *Adv. Mater.*, vol. 23, no. 21, pp. 2436–42, Jun. 2011.

[90] S. C. Kim, D. W. Kim, Y. H. Shim, J. S. Bang, H. S. Oh, S. Wan Kim, and M. H. Seo, “In vivo evaluation of polymeric micellar paclitaxel formulation: toxicity and efficacy.,” *J. Control. Release*, vol. 72, no. 1–3, pp. 191–202, May 2001.

[91] V. P. Torchilin, “Polymeric contrast agents for medical imaging.,” *Curr. Pharm. Biotechnol.*, vol. 1, no. 2, pp. 183–215, Sep. 2000.

[92] H. Yang, H. Mao, Z. Wan, A. Zhu, M. Guo, Y. Li, X. Li, J. Wan, X. Yang, X. Shuai, and H. Chen, “Micelles assembled with carbocyanine dyes for theranostic near-infrared fluorescent cancer imaging and photothermal therapy.,” *Biomaterials*, vol. 34, no. 36, pp. 9124–33, Dec. 2013.

[93] R. R. Patil, J. Yu, S. R. Banerjee, Y. Ren, D. Leong, X. Jiang, M. Pomper, B. Tsui, D. L. Kraitchman, and H.-Q. Mao, “Probing in vivo trafficking of polymer/DNA micellar nanoparticles using SPECT/CT imaging.,” *Mol. Ther.*, vol. 19, no. 9, pp. 1626–35, Sep. 2011.

[94] E. CHARGAFF and R. WEST, “The biological significance of the thromboplastic

protein of blood.," *J. Biol. Chem.*, vol. 166, no. 1, pp. 189–97, Nov. 1946.

[95] P. Wolf, "The nature and significance of platelet products in human plasma.," *Br. J. Haematol.*, vol. 13, no. 3, pp. 269–88, May 1967.

[96] A. J. Dalton, "Microvesicles and vesicles of multivesicular bodies versus "virus-like" particles.," *J. Natl. Cancer Inst.*, vol. 54, no. 5, pp. 1137–48, May 1975.

[97] B. T. Pan, K. Teng, C. Wu, M. Adam, and R. M. Johnstone, "Electron microscopic evidence for externalization of the transferrin receptor in vesicular form in sheep reticulocytes.," *J. Cell Biol.*, vol. 101, no. 3, pp. 942–8, Sep. 1985.

[98] J. Huotari and A. Helenius, "Endosome maturation.," *EMBO J.*, vol. 30, no. 17, pp. 3481–500, Aug. 2011.

[99] V. Van Giau and S. S. A. An, "Emergence of exosomal miRNAs as a diagnostic biomarker for Alzheimer's disease.," *J. Neurol. Sci.*, vol. 360, pp. 141–52, Jan. 2016.

[100] M. Simons and G. Raposo, "Exosomes--vesicular carriers for intercellular communication.," *Curr. Opin. Cell Biol.*, vol. 21, no. 4, pp. 575–81, Aug. 2009.

[101] R. Nieuwland and A. Sturk, "Why do cells release vesicles?," *Thromb. Res.*, pp. S49-51, Apr. 2010.

[102] Q. Zhou, M. Li, X. Wang, Q. Li, T. Wang, Q. Zhu, X. Zhou, X. Wang, X. Gao, and X. Li, "Immune-related microRNAs are abundant in breast milk exosomes.," *Int. J. Biol. Sci.*, vol. 8, no. 1, pp. 118–23, 2012.

[103] J. M. Street, P. E. Barran, C. L. Mackay, S. Weidt, C. Balmforth, T. S. Walsh, R. T. A. Chalmers, D. J. Webb, and J. W. Dear, "Identification and proteomic profiling of exosomes in human cerebrospinal fluid.," *J. Transl. Med.*, vol. 10, p. 5, 2012.

[104] K. R. Qazi, P. Torregrosa Paredes, B. Dahlberg, J. Grunewald, A. Eklund, and S. Gabrielsson, "Proinflammatory exosomes in bronchoalveolar lavage fluid of patients with sarcoidosis.," *Thorax*, vol. 65, no. 11, pp. 1016–24, Nov. 2010.

[105] C. Lässer, V. S. Alikhani, K. Ekström, M. Eldh, P. T. Paredes, A. Bossios, M. Sjöstrand, S. Gabrielsson, J. Lötvall, and H. Valadi, "Human saliva, plasma and breast milk exosomes contain RNA: uptake by macrophages.," *J. Transl. Med.*, vol. 9, p. 9, 2011.

[106] S. Keller, J. Ridinger, A.-K. Rupp, J. W. G. Janssen, and P. Altevogt, "Body fluid derived exosomes as a novel template for clinical diagnostics.," *J. Transl. Med.*,

vol. 9, p. 86, 2011.

[107] A. Gallo, M. Tandon, I. Alevizos, and G. G. Illei, “The majority of microRNAs detectable in serum and saliva is concentrated in exosomes.,” *PLoS One*, vol. 7, no. 3, p. e30679, 2012.

[108] I. Dimov, L. Jankovic Velickovic, and V. Stefanovic, “Urinary exosomes.,” *ScientificWorldJournal.*, vol. 9, pp. 1107–18, 2009.

[109] M. P. Bard, J. P. Hegmans, A. Hemmes, T. M. Luider, R. Willemsen, L.-A. A. Severijnen, J. P. van Meerbeeck, S. A. Burgers, H. C. Hoogsteden, and B. N. Lambrecht, “Proteomic analysis of exosomes isolated from human malignant pleural effusions.,” *Am. J. Respir. Cell Mol. Biol.*, vol. 31, no. 1, pp. 114–21, Jul. 2004.

[110] S. EL Andaloussi, I. Mäger, X. O. Breakefield, and M. J. A. Wood, “Extracellular vesicles: biology and emerging therapeutic opportunities.,” *Nat. Rev. Drug Discov.*, vol. 12, no. 5, pp. 347–57, May 2013.

[111] R. E. Lane, D. Korbie, W. Anderson, R. Vaidyanathan, and M. Trau, “Analysis of exosome purification methods using a model liposome system and tunable-resistive pulse sensing.,” *Sci. Rep.*, vol. 5, p. 7639, 2015.

[112] A. Benito-Martin, A. Di Giannatale, S. Ceder, and H. Peinado, “The new deal: a potential role for secreted vesicles in innate immunity and tumor progression.,” *Front. Immunol.*, vol. 6, p. 66, 2015.

[113] H. Shao, J. Chung, and D. Issadore, “Diagnostic technologies for circulating tumour cells and exosomes.,” *Biosci. Rep.*, vol. 36, no. 1, p. e00292, 2016.

[114] S. Kreimer, A. M. Belov, I. Ghiran, S. K. Murthy, D. A. Frank, and A. R. Ivanov, “Mass-spectrometry-based molecular characterization of extracellular vesicles: lipidomics and proteomics.,” *J. Proteome Res.*, vol. 14, no. 6, pp. 2367–84, Jun. 2015.

[115] N. Zarovni, A. Corrado, P. Guazzi, D. Zocco, E. Lari, G. Radano, J. Muhhina, C. Fondelli, J. Gavrilova, and A. Chiesi, “Integrated isolation and quantitative analysis of exosome shuttled proteins and nucleic acids using immunocapture approaches.,” *Methods*, vol. 87, pp. 46–58, Oct. 2015.

[116] M. Logozzi, A. De Milito, L. Lugini, M. Borghi, L. Calabrò, M. Spada, M. Perdicchio, M. L. Marino, C. Federici, E. Iessi, D. Brambilla, G. Venturi, F. Lozupone, M. Santinami, V. Huber, M. Maio, L. Rivoltini, and S. Fais, “High

levels of exosomes expressing CD63 and caveolin-1 in plasma of melanoma patients.," *PLoS One*, vol. 4, no. 4, p. e5219, 2009.

[117] Y. Yoshioka, Y. Konishi, N. Kosaka, T. Katsuda, T. Kato, and T. Ochiya, "Comparative marker analysis of extracellular vesicles in different human cancer types.," *J. Extracell. vesicles*, vol. 2, 2013.

[118] M.-W. Welker, D. Reichert, S. Susser, C. Sarrazin, Y. Martinez, E. Herrmann, S. Zeuzem, A. Piiper, and B. Kronenberger, "Soluble serum CD81 is elevated in patients with chronic hepatitis C and correlates with alanine aminotransferase serum activity.," *PLoS One*, vol. 7, no. 2, p. e30796, 2012.

[119] J. Skog, T. Würdinger, S. van Rijn, D. H. Meijer, L. Gainche, M. Sena-Esteves, W. T. Curry, B. S. Carter, A. M. Krichevsky, and X. O. Breakefield, "Glioblastoma microvesicles transport RNA and proteins that promote tumour growth and provide diagnostic biomarkers.," *Nat. Cell Biol.*, vol. 10, no. 12, pp. 1470–6, Dec. 2008.

[120] M. W. Graner, O. Alzate, A. M. Dechkovskaia, J. D. Keene, J. H. Sampson, D. A. Mitchell, and D. D. Bigner, "Proteomic and immunologic analyses of brain tumor exosomes.," *FASEB J.*, vol. 23, no. 5, pp. 1541–57, May 2009.

[121] L. Rajendran, M. Honsho, T. R. Zahn, P. Keller, K. D. Geiger, P. Verkade, and K. Simons, "Alzheimer's disease beta-amyloid peptides are released in association with exosomes.," *Proc. Natl. Acad. Sci. U. S. A.*, vol. 103, no. 30, pp. 11172–7, Jul. 2006.

[122] S. Saman, W. Kim, M. Raya, Y. Visnick, S. Miro, S. Saman, B. Jackson, A. C. McKee, V. E. Alvarez, N. C. Y. Lee, and G. F. Hall, "Exosome-associated tau is secreted in tauopathy models and is selectively phosphorylated in cerebrospinal fluid in early Alzheimer disease.," *J. Biol. Chem.*, vol. 287, no. 6, pp. 3842–9, Feb. 2012.

[123] L. Alvarez-Erviti, Y. Seow, A. H. Schapira, C. Gardiner, I. L. Sargent, M. J. A. Wood, and J. M. Cooper, "Lysosomal dysfunction increases exosome-mediated alpha-synuclein release and transmission," *Neurobiol. Dis.*, vol. 42, no. 3, p. 360, 2011.

[124] L. J. Vella, R. A. Sharples, V. A. Lawson, C. L. Masters, R. Cappai, and A. F. Hill, "Packaging of prions into exosomes is associated with a novel pathway of PrP processing.," *J. Pathol.*, vol. 211, no. 5, pp. 582–90, Apr. 2007.

[125] C. Sheridan, “Exosome cancer diagnostic reaches market.,” *Nat. Biotechnol.*, vol. 34, no. 4, pp. 359–60, Apr. 2016.

[126] L. Alvarez-Erviti, Y. Seow, H. Yin, C. Betts, S. Lakhal, and M. J. A. Wood, “Delivery of siRNA to the mouse brain by systemic injection of targeted exosomes,” *Nat. Biotechnol.*, vol. 29, no. 4, pp. 341–345, Apr. 2011.

[127] Y. Tian, S. Li, J. Song, T. Ji, M. Zhu, G. J. Anderson, J. Wei, and G. Nie, “A doxorubicin delivery platform using engineered natural membrane vesicle exosomes for targeted tumor therapy.,” *Biomaterials*, vol. 35, no. 7, pp. 2383–90, Feb. 2014.

[128] H. Saari, E. Lázaro-Ibáñez, T. Viitala, E. Vuorimaa-Laukkanen, P. Siljander, and M. Yliperttula, “Microvesicle- and exosome-mediated drug delivery enhances the cytotoxicity of Paclitaxel in autologous prostate cancer cells.,” *J. Control. Release*, vol. 220, no. Pt B, pp. 727–37, Dec. 2015.

[129] X. Zhuang, X. Xiang, W. Grizzle, D. Sun, S. Zhang, R. C. Axtell, S. Ju, J. Mu, L. Zhang, L. Steinman, D. Miller, and H.-G. Zhang, “Treatment of brain inflammatory diseases by delivering exosome encapsulated anti-inflammatory drugs from the nasal region to the brain.,” *Mol. Ther.*, vol. 19, no. 10, pp. 1769–79, Oct. 2011.

[130] M. A. Morse, J. Garst, T. Osada, S. Khan, A. Hobeika, T. M. Clay, N. Valente, R. Shreeniwas, M. A. Sutton, A. Delcayre, D.-H. Hsu, J.-B. Le Pecq, and H. K. Lyerly, “A phase I study of dexosome immunotherapy in patients with advanced non-small cell lung cancer.,” *J. Transl. Med.*, vol. 3, no. 1, p. 9, Feb. 2005.

[131] C. Théry, L. Zitvogel, and S. Amigorena, “Exosomes: composition, biogenesis and function.,” *Nat. Rev. Immunol.*, vol. 2, no. 8, pp. 569–79, Aug. 2002.

[132] F. André, N. Chaput, N. E. C. Schartz, C. Flament, N. Aubert, J. Bernard, F. Lemonnier, G. Raposo, B. Escudier, D.-H. Hsu, T. Tursz, S. Amigorena, E. Angevin, and L. Zitvogel, “Exosomes as potent cell-free peptide-based vaccine. I. Dendritic cell-derived exosomes transfer functional MHC class I/peptide complexes to dendritic cells.,” *J. Immunol.*, vol. 172, no. 4, pp. 2126–36, Feb. 2004.

[133] S. Dai, D. Wei, Z. Wu, X. Zhou, X. Wei, H. Huang, and G. Li, “Phase I clinical trial of autologous ascites-derived exosomes combined with GM-CSF for colorectal cancer.,” *Mol. Ther.*, vol. 16, no. 4, pp. 782–90, Apr. 2008.

[134] Q. Wang, X. Zhuang, J. Mu, Z.-B. Deng, H. Jiang, L. Zhang, X. Xiang, B. Wang, J. Yan, D. Miller, and H.-G. Zhang, "Delivery of therapeutic agents by nanoparticles made of grapefruit-derived lipids.," *Nat. Commun.*, vol. 4, p. 1867, 2013.

[135] J. Mu, X. Zhuang, Q. Wang, H. Jiang, Z.-B. Deng, B. Wang, L. Zhang, S. Kakar, Y. Jun, D. Miller, and H.-G. Zhang, "Interspecies communication between plant and mouse gut host cells through edible plant derived exosome-like nanoparticles.," *Mol. Nutr. Food Res.*, vol. 58, no. 7, pp. 1561–73, Jul. 2014.

[136] G. Minotti, P. Menna, E. Salvatorelli, G. Cairo, and L. Gianni, "Anthracyclines: molecular advances and pharmacologic developments in antitumor activity and cardiotoxicity.," *Pharmacol. Rev.*, vol. 56, no. 2, pp. 185–229, Jun. 2004.

[137] P. Y. Muller and M. N. Milton, "The determination and interpretation of the therapeutic index in drug development.," *Nat. Rev. Drug Discov.*, vol. 11, no. 10, pp. 751–61, Oct. 2012.

[138] M. A. Hamburg and F. S. Collins, "The path to personalized medicine.," *N. Engl. J. Med.*, vol. 363, no. 4, pp. 301–4, Jul. 2010.

[139] S. Kunjachan, J. Ehling, G. Storm, F. Kiessling, and T. Lammers, "Noninvasive Imaging of Nanomedicines and Nanotheranostics: Principles, Progress, and Prospects.," *Chem. Rev.*, vol. 115, no. 19, pp. 10907–37, Oct. 2015.

[140] M. Gerlinger, A. J. Rowan, S. Horswell, J. Larkin, D. Endesfelder, E. Gronroos, P. Martinez, N. Matthews, A. Stewart, P. Tarpey, I. Varela, B. Phillimore, S. Begum, N. Q. McDonald, A. Butler, D. Jones, K. Raine, C. Latimer, C. R. Santos, M. Nohadani, A. C. Eklund, B. Spencer-Dene, G. Clark, L. Pickering, G. Stamp, M. Gore, Z. Szallasi, J. Downward, P. A. Futreal, and C. Swanton, "Intratumor heterogeneity and branched evolution revealed by multiregion sequencing.," *N. Engl. J. Med.*, vol. 366, no. 10, pp. 883–92, Mar. 2012.

[141] F. Rizzolio, L. Esposito, D. Muresu, R. Fratamico, R. Jaraha, G. V. Caprioli, and A. Giordano, "RB gene family: genome-wide ChIP approaches could open undiscovered roads.," *J. Cell. Biochem.*, vol. 109, no. 5, pp. 839–43, Apr. 2010.

[142] E. Blanco, H. Shen, and M. Ferrari, "Principles of nanoparticle design for overcoming biological barriers to drug delivery.," *Nat. Biotechnol.*, vol. 33, no. 9, pp. 941–51, Sep. 2015.

[143] J. Wolfram, H. Shen, and M. Ferrari, "Multistage vector (MSV) therapeutics.," *J.*

Control. Release, vol. 219, pp. 406–15, Dec. 2015.

[144] T. Ojha, L. Rizzo, G. Storm, F. Kiessling, and T. Lammers, "Image-guided drug delivery: preclinical applications and clinical translation.," *Expert Opin. Drug Deliv.*, vol. 12, no. 8, pp. 1203–7, Aug. 2015.

[145] V. Kumar, S. Palazzolo, S. Bayda, G. Corona, G. Toffoli, and F. Rizzolio, "DNA Nanotechnology for Cancer Therapy.," *Theranostics*, vol. 6, no. 5, pp. 710–25, 2016.

[146] O. L. Gobbo, K. Sjaastad, M. W. Radomski, Y. Volkov, and A. Prina-Mello, "Magnetic Nanoparticles in Cancer Theranostics.," *Theranostics*, vol. 5, no. 11, pp. 1249–63, 2015.

[147] A. Gabizon, H. Shmeeda, and Y. Barenholz, "Pharmacokinetics of pegylated liposomal Doxorubicin: review of animal and human studies.," *Clin. Pharmacokinet.*, vol. 42, no. 5, pp. 419–36, 2003.

[148] P. Guo, J. Yang, D. Jia, M. A. Moses, and D. T. Auguste, "ICAM-1-Targeted, Lcn2 siRNA-Encapsulating Liposomes are Potent Anti-angiogenic Agents for Triple Negative Breast Cancer.," *Theranostics*, vol. 6, no. 1, pp. 1–13, 2016.

[149] G. Raposo and W. Stoorvogel, "Extracellular vesicles: exosomes, microvesicles, and friends.," *J. Cell Biol.*, vol. 200, no. 4, pp. 373–83, Feb. 2013.

[150] S. Mathivanan, H. Ji, and R. J. Simpson, "Exosomes: extracellular organelles important in intercellular communication.," *J. Proteomics*, vol. 73, no. 10, pp. 1907–20, Sep. 2010.

[151] M. E. Haque, T. J. McIntosh, and B. R. Lentz, "Influence of lipid composition on physical properties and peg-mediated fusion of curved and uncurved model membrane vesicles: "nature's own" fusogenic lipid bilayer.," *Biochemistry*, vol. 40, no. 14, pp. 4340–8, Apr. 2001.

[152] S. A. A. Kooijmans, P. Vader, S. M. van Dommelen, W. W. van Solinge, and R. M. Schiffelers, "Exosome mimetics: a novel class of drug delivery systems.," *Int. J. Nanomedicine*, vol. 7, pp. 1525–41, 2012.

[153] D. Landesman-Milo and D. Peer, "Altering the immune response with lipid-based nanoparticles.," *J. Control. Release*, vol. 161, no. 2, pp. 600–8, Jul. 2012.

[154] T. J. Smyth, J. S. Redzic, M. W. Graner, and T. J. Anchordoquy, "Examination of the specificity of tumor cell derived exosomes with tumor cells in vitro.," *Biochim. Biophys. Acta*, vol. 1838, no. 11, pp. 2954–65, Nov. 2014.

[155] N. Kosaka, F. Takeshita, Y. Yoshioka, K. Hagiwara, T. Katsuda, M. Ono, and T. Ochiya, “Exosomal tumor-suppressive microRNAs as novel cancer therapy: "exocure" is another choice for cancer treatment.,” *Adv. Drug Deliv. Rev.*, vol. 65, no. 3, pp. 376–82, Mar. 2013.

[156] C. W. McCloskey, R. L. Goldberg, L. E. Carter, L. F. Gamwell, E. M. Al-Hujaily, O. Collins, E. A. Macdonald, K. Garson, M. Daneshmand, E. Carmona, and B. C. Vanderhyden, “A New Spontaneously Transformed Syngeneic Model of High-Grade Serous Ovarian Cancer with a Tumor-Initiating Cell Population,” *Front. Oncol.*, vol. 4, 2014.

[157] C. Théry, S. Amigorena, G. Raposo, and A. Clayton, “Isolation and characterization of exosomes from cell culture supernatants and biological fluids.,” *Curr. Protoc. Cell Biol.*, vol. Chapter 3, p. Unit 3.22, Apr. 2006.

[158] B. J. Tauro, D. W. Greening, R. A. Mathias, H. Ji, S. Mathivanan, A. M. Scott, and R. J. Simpson, “Comparison of ultracentrifugation, density gradient separation, and immunoaffinity capture methods for isolating human colon cancer cell line LIM1863-derived exosomes.,” *Methods*, vol. 56, no. 2, pp. 293–304, Feb. 2012.

[159] E. van der Pol, F. A. W. Coumans, A. E. Grootemaat, C. Gardiner, I. L. Sargent, P. Harrison, A. Sturk, T. G. van Leeuwen, and R. Nieuwland, “Particle size distribution of exosomes and microvesicles determined by transmission electron microscopy, flow cytometry, nanoparticle tracking analysis, and resistive pulse sensing.,” *J. Thromb. Haemost.*, vol. 12, no. 7, pp. 1182–92, Jul. 2014.

[160] H. Kalra, C. G. Adda, M. Liem, C.-S. Ang, A. Mechler, R. J. Simpson, M. D. Hulett, and S. Mathivanan, “Comparative proteomics evaluation of plasma exosome isolation techniques and assessment of the stability of exosomes in normal human blood plasma.,” *Proteomics*, vol. 13, no. 22, pp. 3354–64, Nov. 2013.

[161] S. P. Crouch, R. Kozlowski, K. J. Slater, and J. Fletcher, “The use of ATP bioluminescence as a measure of cell proliferation and cytotoxicity.,” *J. Immunol. Methods*, vol. 160, no. 1, pp. 81–8, Mar. 1993.

[162] M. Maioli, S. Santaniello, A. Montella, P. Bandiera, S. Cantoni, C. Cavallini, F. Bianchi, V. Lionetti, F. Rizzolio, I. Marchesi, L. Bagella, and C. Ventura, “Hyaluronan esters drive Smad gene expression and signaling enhancing

cardiogenesis in mouse embryonic and human mesenchymal stem cells.," *PLoS One*, vol. 5, no. 11, p. e15151, 2010.

[163] I. Marchesi, F. P. Fiorentino, F. Rizzolio, A. Giordano, and L. Bagella, "The ablation of EZH2 uncovers its crucial role in rhabdomyosarcoma formation.," *Cell Cycle*, vol. 11, no. 20, pp. 3828–36, Oct. 2012.

[164] A. Suetsugu, K. Honma, S. Saji, H. Moriwaki, T. Ochiya, and R. M. Hoffman, "Imaging exosome transfer from breast cancer cells to stroma at metastatic sites in orthotopic nude-mouse models.," *Adv. Drug Deliv. Rev.*, vol. 65, no. 3, pp. 383–90, Mar. 2013.

[165] R. M. Hoffman, "Stromal-cell and cancer-cell exosomes leading the metastatic exodus for the promised niche," *Breast Cancer Res.*, vol. 15, no. 3, p. 310, 2013.

[166] S. Rana, K. Malinowska, and M. Zöller, "Exosomal Tumor MicroRNA Modulates Premetastatic Organ Cells," *Neoplasia*, vol. 15, no. 3, p. 281, 2013.

[167] J. L. Hood, R. S. San, and S. A. Wickline, "Exosomes released by melanoma cells prepare sentinel lymph nodes for tumor metastasis.," *Cancer Res.*, vol. 71, no. 11, pp. 3792–801, Jun. 2011.

[168] H. Peinado, M. Alečković, S. Lavotshkin, I. Matei, B. Costa-Silva, G. Moreno-Bueno, M. Hergueta-Redondo, C. Williams, G. García-Santos, A. Nitadori-Hoshino, C. Hoffman, K. Badal, B. A. Garcia, M. K. Callahan, J. Yuan, V. R. Martins, J. Skog, R. N. Kaplan, M. S. Brady, J. D. Wolchok, P. B. Chapman, Y. Kang, J. Bromberg, and D. Lyden, "Melanoma exosomes educate bone marrow progenitor cells toward a pro-metastatic phenotype through MET," *Nat. Med.*, vol. 18, no. 6, p. 883, 2012.

[169] I. Parolini, C. Federici, C. Raggi, L. Lugini, S. Palleschi, A. De Milito, C. Coscia, E. Iessi, M. Logozzi, A. Molinari, M. Colone, M. Tatti, M. Sargiacomo, and S. Fais, "Microenvironmental pH Is a Key Factor for Exosome Traffic in Tumor Cells," *J. Biol. Chem.*, vol. 284, no. 49, p. 34211, 2009.

[170] R. A. Dragovic, C. Gardiner, A. S. Brooks, D. S. Tannetta, D. J. P. Ferguson, P. Hole, B. Carr, C. W. G. Redman, A. L. Harris, P. J. Dobson, P. Harrison, and I. L. Sargent, "Sizing and phenotyping of cellular vesicles using Nanoparticle Tracking Analysis," *Nanomedicine*, vol. 7, no. 6, p. 780, 2011.

[171] V. Sokolova, A.-K. Ludwig, S. Hornung, O. Rotan, P. A. Horn, M. Epple, and B. Giebel, "Characterisation of exosomes derived from human cells by

nanoparticle tracking analysis and scanning electron microscopy.," *Colloids Surf. B. Biointerfaces*, vol. 87, no. 1, pp. 146–50, Oct. 2011.

[172] K. Strauss, C. Goebel, H. Runz, W. Möbius, S. Weiss, I. Feussner, M. Simons, and A. Schneider, "Exosome Secretion Ameliorates Lysosomal Storage of Cholesterol in Niemann-Pick Type C Disease," *J. Biol. Chem.*, vol. 285, no. 34, p. 26279, 2010.

[173] J. L. Hood, M. J. Scott, and S. A. Wickline, "Maximizing Exosome Colloidal Stability Following Electroporation," *Anal. Biochem.*, vol. 448, p. 41, 2014.

[174] D. Fitzner, M. Schnaars, D. van Rossum, G. Krishnamoorthy, P. Dibaj, M. Bakhti, T. Regen, U.-K. Hanisch, and M. Simons, "Selective transfer of exosomes from oligodendrocytes to microglia by macropinocytosis.," *J. Cell Sci.*, vol. 124, no. Pt 3, pp. 447–58, Feb. 2011.

[175] C. Escrevente, S. Keller, P. Altevogt, and J. Costa, "Interaction and uptake of exosomes by ovarian cancer cells.," *BMC Cancer*, vol. 11, p. 108, 2011.

[176] A. E. Morelli, A. T. Larregina, W. J. Shufesky, M. L. G. Sullivan, D. B. Stolz, G. D. Papworth, A. F. Zahorchak, A. J. Logar, Z. Wang, S. C. Watkins, L. D. Falo, and A. W. Thomson, "Endocytosis, intracellular sorting, and processing of exosomes by dendritic cells.," *Blood*, vol. 104, no. 10, pp. 3257–66, Nov. 2004.

[177] A. Montecalvo, A. T. Larregina, W. J. Shufesky, D. B. Stolz, M. L. G. Sullivan, J. M. Karlsson, C. J. Baty, G. A. Gibson, G. Erdos, Z. Wang, J. Milosevic, O. A. Tkacheva, S. J. Divito, R. Jordan, J. Lyons-Weiler, S. C. Watkins, and A. E. Morelli, "Mechanism of transfer of functional microRNAs between mouse dendritic cells via exosomes.," *Blood*, vol. 119, no. 3, pp. 756–66, Jan. 2012.

[178] S. C. Jang, O. Y. Kim, C. M. Yoon, D.-S. Choi, T.-Y. Roh, J. Park, J. Nilsson, J. Lötvall, Y.-K. Kim, and Y. S. Gho, "Bioinspired exosome-mimetic nanovesicles for targeted delivery of chemotherapeutics to malignant tumors.," *ACS Nano*, vol. 7, no. 9, pp. 7698–710, Sep. 2013.

[179] A. T. Horowitz, Y. Barenholz, and A. A. Gabizon, "In vitro cytotoxicity of liposome-encapsulated doxorubicin: dependence on liposome composition and drug release.," *Biochim. Biophys. Acta*, vol. 1109, no. 2, pp. 203–9, Aug. 1992.

[180] M. B. Chougule, A. R. Patel, T. Jackson, and M. Singh, "Antitumor activity of Noscapine in combination with Doxorubicin in triple negative breast cancer.,"

PLoS One, vol. 6, no. 3, p. e17733, 2011.

[181] A. Riad, S. Bien, D. Westermann, P. M. Becher, K. Loya, U. Landmesser, H. K. Kroemer, H. P. Schultheiss, and C. Tschöpe, "Pretreatment with statin attenuates the cardiotoxicity of Doxorubicin in mice.," *Cancer Res.*, vol. 69, no. 2, pp. 695–9, Jan. 2009.

[182] X. Marechal, D. Montaigne, C. Marciniak, P. Marchetti, S. M. Hassoun, J. C. Beauvillain, S. Lancel, and R. Neviere, "Doxorubicin-induced cardiac dysfunction is attenuated by ciclosporin treatment in mice through improvements in mitochondrial bioenergetics.," *Clin. Sci. (Lond).*, vol. 121, no. 9, pp. 405–13, Nov. 2011.

[183] C. P. Lai, O. Mardini, M. Ericsson, S. Prabhakar, C. A. Maguire, J. W. Chen, B. A. Tannous, and X. O. Breakefield, "Dynamic biodistribution of extracellular vesicles in vivo using a multimodal imaging reporter.," *ACS Nano*, vol. 8, no. 1, pp. 483–94, Jan. 2014.

[184] A. M. Rahman, S. W. Yusuf, and M. S. Ewer, "Anthracycline-induced cardiotoxicity and the cardiac-sparing effect of liposomal formulation.," *Int. J. Nanomedicine*, vol. 2, no. 4, pp. 567–83, 2007.

[185] L. E. Olson, D. Bedja, S. J. Alvey, A. J. Cardounel, K. L. Gabrielson, and R. H. Reeves, "Protection from doxorubicin-induced cardiac toxicity in mice with a null allele of carbonyl reductase 1.," *Cancer Res.*, vol. 63, no. 20, pp. 6602–6, Oct. 2003.

[186] L. Pascucci, V. Coccè, A. Bonomi, D. Ami, P. Ceccarelli, E. Ciusani, L. Viganò, A. Locatelli, F. Sisto, S. M. Doglia, E. Parati, M. E. Bernardo, M. Muraca, G. Alessandri, G. Bondiolotti, and A. Pessina, "Paclitaxel is incorporated by mesenchymal stromal cells and released in exosomes that inhibit in vitro tumor growth: a new approach for drug delivery.," *J. Control. Release*, vol. 192, pp. 262–70, Oct. 2014.

[187] M. S. Kim, M. J. Haney, Y. Zhao, V. Mahajan, I. Deygen, N. L. Klyachko, E. Inskoe, A. Piroyan, M. Sokolsky, O. Okolie, S. D. Hingtgen, A. V Kabanov, and E. V Batrakova, "Development of exosome-encapsulated paclitaxel to overcome MDR in cancer cells.," *Nanomedicine*, vol. 12, no. 3, pp. 655–64, Apr. 2016.

[188] B. Escudier, T. Dorval, N. Chaput, F. André, M.-P. Caby, S. Novault, C. Flament, C. Leboulaire, C. Borg, S. Amigorena, C. Boccaccio, C. Bonnerot, O. Dhellin, M.

Movassagh, S. Piperno, C. Robert, V. Serra, N. Valente, J.-B. Le Pecq, A. Spatz, O. Lantz, T. Tursz, E. Angevin, and L. Zitvogel, “No Title,” *J. Transl. Med.*, vol. 3, no. 1, p. 10, 2005.

ACKNOWLEDGEMENT

I thank all the staff of the National Tumor Institute (CRO-Aviano). They provided a good educational environment that makes the integration of students easy. First of them Dr. Giuseppe Toffoli, the director of the Clinical and Experimental Pharmacology division that opened the opportunity for me to be a member in this research unit. I especially thank my PhD tutor Dr. Flavio Rizzolio, Pricinpal Investigator of the Nanomedicine Lab for his helpful and useful advices and supervision during the different parts of my thesis and PhD period.

Additionally, I want to dedicate a special acknowledgement to Prof. Pietro Giusti, previous director of the Doctoral School for Pharmacological Sciences in the University of Padova, for his supervision during the PhD period that I appreciate a lot.

How I cannot thank all the friends in the FSC unit and especially in the Nanomedicine Lab (Stefano, Concetta, Lucia, Barbara and Samer) with whom I shared more closely these 3 years of intense research and experimental work but also of pleasant time; they can understand my satisfaction more than anyone else.

Finally, I thank my father, my mother, my family and especially my wife Duaa, they had always supported me and believed in my efforts. I hope to make them satisfied and repaid for their continuous sacrifices made.

November 2016
Mohamad Hadla